Comparative Study of Different Methods of Vibration Control of Rotor Bearing Systems

by

Neaz Ahmed

A Thesis Presented to the

FACULTY OF THE COLLEGE OF GRADUATE STUDIES

KING FAHD UNIVERSITY OF PETROLEUM & MINERALS

DHAHRAN, SAUDI ARABIA

In Partial Fulfillment of the
Requirements for the Degree of

MASTER OF SCIENCE

In

MECHANICAL ENGINEERING

May, 1993

Comparative study of different methods of vibration control of rotor bearing systems

Ahmed, Neaz, M.S.

King Fahd University of Petroleum and Minerals (Saudi Arabia), 1993

U·M·I
300 N. Zeeb Rd.
Ann Arbor, MI 48106

COMPARATIVE STUDY OF DIFFERENT METHODS OF VIBRATION CONTROL OF ROTOR BEARING SYSTEMS

BY

NEAZ AHMED

A Thesis Presented to the

FACULTY OF THE COLLEGE OF GRADUATE STUDIES

KING FAHD UNIVERSITY OF PETROLEUM & MINERALS

DHAHRAN, SAUDI ARABIA

In Partial Fulfillment of the
Requirements for the Degree of

MASTER OF SCIENCE

In

MECHANICAL ENGINEERING

MAY 1993

Comparative Study of Different Methods of Vibration Control of Rotor-Bearing Systems

Neaz Ahmed

Mechanical Engineering

May 1993

KING FAHD UNIVERSITY OF PETROLEUM AND MINERALS

DHAHRAN, SAUDI ARABIA

This thesis, written by

Neaz Ahmed

under the direction of his Thesis Advisor, and approved by his Thesis committee, has been presented to and accepted by the Dean, College of Graduate Studies, in partial fulfillment of the requirements for the degree of

MASTER OF SCIENCE IN MECHANICAL ENGINEERING

Thesis Committee:

R.R.Guntur July 5, 93
Chairman (Dr. Rao R. Guntur)

7/6/93
Member (Dr. Y. A. R. Khulief)

Ravi S. Rao July 6, 93
Member (Dr. Ravi S. Rao)

July 6, 93
Member (Dr. K. A. F. Moustafa)

Department Chairman

Dean, College of Graduate Studies

Date : 18-7-93

كلية الدراسات العليا
COLLEGE OF GRADUATE STUDIES

123

Dedicated to

My Parents and Wife

Acknowledgment

"In the name of Allah, Most Gracious, Most Merciful. Read in the name of thy Lord and Cherisher, Who created. Created man from a [*leech-like*] clot. Read and thy Lord is Most Bountiful. He Who taught [*the use of*] the pen. Taught man that which he knew not. Nay, but man doth transgress all bounds. In that he looketh upon himself as self-sufficient. verily, to thy Lord is the return [*of all*]".

(The Holy Quran, Surah 96)

All praise and glory to Almighty Allah without whose help no work can be accomplished. Acknowledgement is due to King Fahd University of Petroleum and Minerals for providing support to this research.

My deep appreciation goes to my major thesis advisor Dr. Rao R. Guntur, for his constant help, guidance and the countless hours of attention he devoted throughout the course of this work. It was his insight and knowledge of the subject matter that made this task easier.

Thanks are also due to my thesis committee members Dr. Yahya A. Raouf Khulief, Dr. Ravi S. Rao and Dr. Kamal A. F. Moustafa for their interest, cooperation, advice and constructive criticism.

Special thanks are due to my colleagues and friends for their encouragement and various help that they had provided throughout my graduate studies at KFUPM.

My heartfelt thanks and gratefulness also go to my parents who had the foresight to provide support and encouragement for my education. I am thankful to my wife without whose patience and moral support this work would have been impossible.

Finally the cooperation of the department chairman Dr. Muhammad O. Budair is gratefully appreciated.

Contents

List of Tables

List of Figures

Thesis Abstract

Name : Neaz Ahmed

Title :Comparative Study of Different Methods of Vibration Control of Rotor-Bearing Systems

Major Field :Mechanical Engineering

Date of Degree :May 1993

The performance of three different feedback control systems has been studied in controlling the vibration of a rotor-bearing system. Two Different mathematical models of the rotor-bearing system have been presented. One model is developed by considering the rotor-bearing system on rigid supports and another model is developed by considering the system on flexible supports. The control techniques applied on these models are: the State variable feedback , Integral plus state variable feedback and Linear quadratic servo. The response of the deflection of the rotor has been simulated on a digital computer. The results of the simulation are presented. These control techniques have been compared on the basis of time-response specifications. The relative suitability of controllers is discussed. The effect of the flexibility of the supports, on the response of the rotor-deflection has been studied. The results obtained for different support stiffnesses are discussed.

Master of Science Degree

King Fahd University of Petroleum and Minerals

Dhahran, Saudi Arabia

May 1993

خلاصة الرسالة

الاسم : نياز أحمد

عنوان الرسالة : **مقارنة بين عدة نظريات للتحكم بالاهتزازات في الأنظمة الدوارة المرتكزه على محملات**

التخصيص : **هندسة ميكانيكية**

تاريخ الشهادة : **مايو ١٩٩٣م**

في هذا البحث تمت دراسة أداء ثلاثة نظريات في نظم التحكم ذات التغذية المرتدة للتحكم في الاهتزازات الناتجة في الأنظمة الدوارة المرتكزة علي محملات. لقد تم تقديم نموذجين رياضيين يقومان بمحاكاة الأنظمة الدوارة المرتكزه علي محملات. أحد هذه النماذج يقوم على اعتبار أن المحملات مرتكزه على قاعدة صلبه، بينما يقوم الثاني باعتبار أن القاعدة التي يرتكز عليها المحمل مرنة. نظم التحكم التي تم تطبيقها على النماذج هي : التغذية المرتدة لمتغير الحالة، التكامل مع التغذية المرتدة لمتغير الحالة والتحكم الموازر الخطي في الدرجة الثانية. تمت محاكاة استجابة الدوران الانحنائية باستعمال الحاسوب. يتم تقديم نتائج التمثيل في الرسالة. يتم مقارنة طرق التحكم على أساس محددات الاستجابة الزمنية، الملائمة النسبية لأنظمة التحكم يتم مناقشها. تأثير مرورنة القواعد على استجابة الانحناء الدوارني يتم دراستها. يتم مناقشة نتائج استخدام عدة عوامل مرونة مختلفة لقواعد الأنظمة الدوارة المرتكزه على محملات.

درجة الماجستير في العلوم
جامعة الملك فهد للبترول والمعادن
الظهران - المملكة العربية السعودية
مايو ١٩٩٣م

Chapter 1

Introduction

The vibration of a rotor-bearing system not only perturb the normal operation of a machine, but may also cause serious damage to the machine and even to the entire plant. For this reason, the problem of reducing rotor vibration has been investigated for many years. Previous studies were mainly concentrated on the techniques of balancing of flexible rotors and shafts so that amplitude of rotor vibration would be minimized [1]. However, it is not possible to achieve the desired low levels of vibration by balancing alone. Besides, rotor assemblies which are balanced well initially, degrade with continued operation.

The introduction of passive vibration control devices(such as squeeze film dampers (SFD)) [2, 3, 4] help to reduce rotor vibration and improve stability but these suffer normal limitations associated with passive devices. Since the parameters of an SFD

can not be changed, one which is applicable to a given set of operating conditions may not be universally applicable, especially when several modes of vibration are excited. This limitation led to an evolving interest on active control of rotor vibrations. Several techniques have been adopted by researchers for active control of vibration [5, 6, 7]. Modern control theory may be employed to develop control systems to reduce or eliminate the vibration of rotor-bearing systems [8].

Modern control theory provides different approaches of optimal control of a system [9]. In the present study, three different controllers conceived by using modern control theory are implemented in the rotor-bearing system and their relative suitability in vibration control is studied. The controllers applied in the rotor-bearing system are:

- State variable feedback(SVFB)
- Integral plus state variable feedback(ISVFB)
- Linear quadratic servo(LQS)

Two different models of a rotor-bearing system as shown in Fig. 1.1 are considered:

- The model shown in Fig. 1.1(a) comprises of a rotor modeled as three lumped masses and connected by mass-less flexible shaft, and symmetrically supported on two oil-film journal bearings with rigid supports (model I).

- The model shown in Fig. 1.1(b) is the same as shown in Fig. 1.1(a) except that the bearing supports are flexible (model II). This model is the same as the one in reference [8].

In this study dynamic equations of the models are derived using Newton's law. The system's dynamic equations thus obtained are transformed into state variable form, so that the controllers based on modern control theory can be applied. The performance of each of the controllers is simulated on a digital computer and the suitability of the controllers in vibration control is discussed. The organization of this study is as follows:

Chapter 1 includes a short description of different approaches used in the vibration control of a rotor-bearing system. A literature review of rotor-bearing systems, their vibration control is presented. A review of modern control theory is also presented. A description of the scope of present work is also included. In chapter 2 details of the dynamic models of the considered rotor-bearing system are presented. Controllability and observability of a system are discussed in chapter 3. In chapter 4 a detailed description of the three controllers (SVFB, ISVFB and LQS) is presented. The response of the system described by model I (with and without controllers) is also discussed. Similarly in chapter 5, the response of the system described by model II is discussed. The effect of the stiffness of the supports on the response of the system is also presented in chapter 5. Finally, conclusions about the suitability of the controllers employed to control the vibration is presented in chapter 6. Suggestions

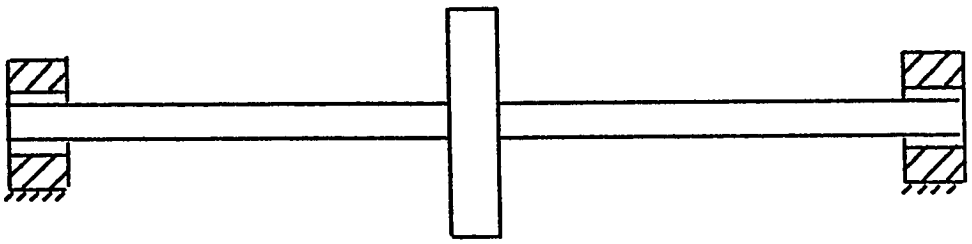

(a)

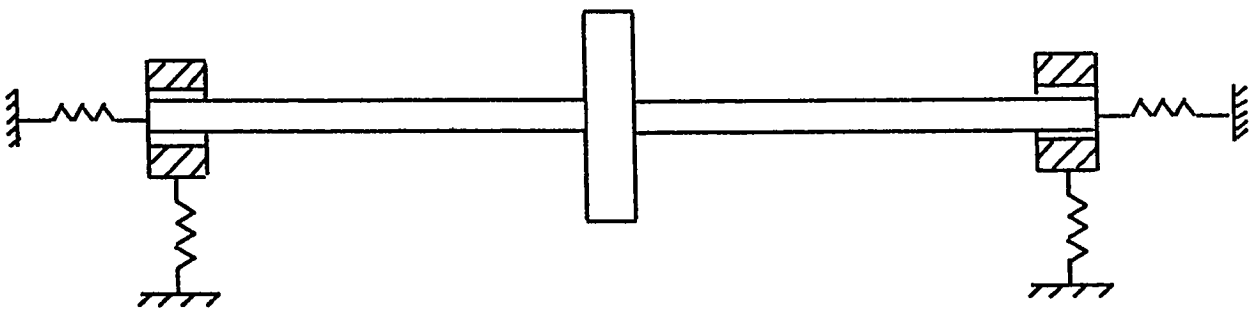

(b)

Figure 1.1: (a) Flexible rotor on flexible bearings mounted on rigid supports. (b) Flexible rotor on flexible bearings mounted on flexible supports.

for further work are also included in this chapter.

1.1 Literature Review

In the study of vibration control of a rotor-bearing system, one of the important problems that stirred the minds of experimentalists and analysts alike is the optimization of control forces [10]. Many investigators have contributed to the knowledge of dynamical parameters which have great influence on the vibrational behavior of rotor-bearing systems [11, 12, 13, 14, 15, 16]. In the recent years much attention has been focused on optimal control systems.

1.1.1 Rotor-Bearing System

In order to develop a dynamic model of a rotor-bearing system and to obtain a suitable set of oil-film bearing coefficients, the relevant literature has been reviewed. The bearings which support a rotor significantly influence its dynamic behavior. For many years rotating shafts and bearings were not considered to interact with one another [11] . In the early years of the twentieth century with the development of high speed machines where rotors were required to operate at high speeds, the influence of bearings and foundations on the dynamic behavior of the system was realized.

A study of the relevant literature reveals that a considerable attention had been

focussed on determination of stiffness and damping coefficients of fluid-film journal bearings for use in linearized lateral rotor vibration analysis [12, 13, 14]. Parallel advancements in computer based algorithms, measurement devices and equipment accelerated both theoretical and experimental approaches to tackle the problems of rotor-bearing systems. Morton[14] compared the experimental values of bearing coefficients with those predicted on the basis of the theory. He found that the theory underestimated the damping and overestimated the stiffness of the bearings.

Studies have been conducted to provide a means of selecting values of oil-film bearing parameters such that the fit between the measured and computed values can be optimized [15, 16, 17]. Investigations have been carried out to observe the behavior of rotor-bearing system with squeeze-film dampers and without dampers [3, 18, 19]. It is found that experimental values of the stiffness and damping coefficients obtained by using the squeeze-film dampers are in good agreement with the of theoretical values. For the most general rotor-bearing system twelve coefficients are proposed, namely, four inertia, four damping, and four stiffness terms. A survey of the relevant literature further reveals that a full twelve coefficient model is appropriate in some cases and in other cases a simplified eight or six coefficient model may be used [20, 21].

1.1.2 Vibration Control

The literature relevant to the cause and the remedy of the vibration of rotor-bearing systems has been reviewed in this section. A rotor running on bearings has a threshold speed; above which it becomes unstable, this instability is characterized as sub-synchronized whirling. Cross-coupling stiffnesses (K_{xy}, K_{yx}) destabilize the system [19]. Newkirk and Taylor (1925) first reported that the oil whirl occurred only in lightly loaded oil-film bearings operated at a very small eccentricity ratio [22]. Reddi and Trumpler [23] investigated the phenomenon of oil whirl in full (360-deg.) and partial (180-deg.) journal bearings. Their study reveals that, to achieve successful design one must consider a system consisting of bearings and rotors. Many researchers worked on balancing techniques for rigid and flexible rotor-bearing systems [1, 24].

Modern machines are highly complex and therefore, in addition to unbalance in rotor, there are many reasons for vibrations. The rotors used in modern machines are highly flexible. These are generally mounted on more than two bearings and rotate at very high speeds. The instability in these machines is generally produced by aerodynamic forces on impeller wheels, friction in the stressed rotor and hydrodynamic forces in their bearings [2].

Studies that have been conducted to control the vibration of rotor-bearing systems can broadly be classified into two groups: passive vibration control; and active vibration control. Squeeze-film dampers (SFD) have been used in past and are in use today as successful devices for passive vibration control. These dampers were first applied in 1889 by C. A. Parson to its turbo rotor bearings. Brow Bovery of Switzerland incorporated SFD in its turbo chargers in 1939 [19]. Many investigators worked on the feasibility of controlling synchronous and nonsynchronous vibration of rotor-bearing systems using squeeze-film dampers [2, 3, 4]. The squeeze film damper improved the stability of a rotor-bearing system. However, an SFD has limited use if several modes of vibration are excited at the same time.

Realizing the limitation of a passive SFD, studies on an active SFD were carried out [5, 25]. An active SFD was found to be superior to a passive SFD. The performance of electromagnetic dampers as active vibration controllers has been investigated. It is found that such a damper offers improved control of the vibrational behavior of the system [6, 7]. In order to achieve improved control strategies an investigation has been conducted to determine the feasibility of applying control inputs through non-rotating components of machines [8]. Studies have been performed to investigate the relative suitability of different approaches of modern control theory for active vibration control [26-28].

1.1.3 Optimal Control.

The primary objective of most control systems is to obtain a desired output from the controlled process. The optimal control theory gives the best possible input within limits imposed by physical constraints. The optimal control of a system is possible only if the system is controllable and observable [9]. The concepts of controllability and observability were introduced by Kalman [29]. Many researchers developed the techniques for checking the controllability and observability of a system [30-37]. Elmadany [27] used the optimal control theory in developing the SVFB and ISVFB controllers as applied to the active suspension system of a vehicle. S. Zaman [38] used an SVFB controller to study the effect of actuator position on the performance of a ground vehicle suspension system. Surgener and Hesketh [28] used an LQS and a generic model controller(GMC) in their study of air and fuel control in a furnace. These techniques based on the modern control theory have not been used in the vibration control of rotor-bearing systems, to the best of our knowledge.

1.2 Scope of the Proposed Research

The purpose of this work is to study the performance of different controllers, (built on the basis of modern control theory) when they are employed in a rotor-bearing system. In order to investigate the effect of different controllers on the active vibration control of a rotor-bearing system, the following procedure is adopted.

1 . Mathematical model of a rotor-bearing system is developed.

2 . State-variable feed back(SVFB), Integral-plus-State-variable feed back (ISVFB) and Linear quadratic servo (LQS) methods are used to design different controllers.

3 . Each of the developed controllers is simulated using a digital computer.

4 . The results obtained from step-3 are compared in order to examine their relative suitability for controlling a rotor-bearing system.

Chapter 2

Mathematical Modeling of Rotor-Bearing System

The aim of this chapter is to present two different mathematical models of rotor-bearing systems. Three different controllers conceived by using modern control theory will be applied on these models. It is assumed that the rotor-bearing system can be modeled by considering the rotor and bearing as lumped masses and connected by massless flexible shaft. This kind of model is generally used to study the influence of bearings and supports on rotor vibrations [2, 8, 13].

The configurations of the models are shown in Fig 2.1 and Fig 2.2. Model-I (see Fig2.1) consists of two lumped masses and a massless flexible shaft which is symmetrically supported on two plain oil-film journal bearings. The whole system is mounted on rigid supports [5]. Model II consists of three lumped masses and a

massless flexible shaft which is supported by plain journal bearings mounted on flexible supports. The three mass model of the rotor-bearing system is commonly used to study the influence of flexible supports on rotor vibrations [8, 13].

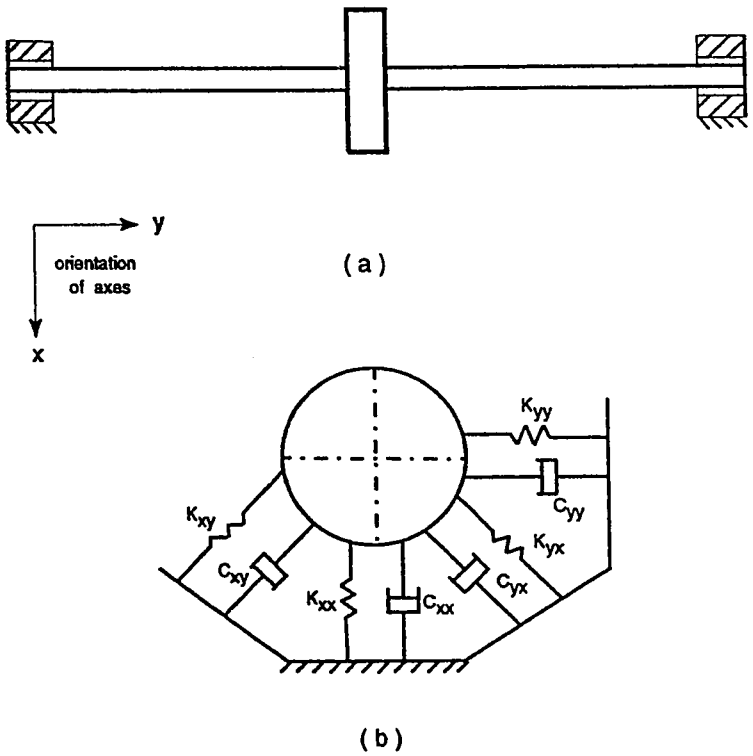

Figure 2.1: (a) Schematic diagram of a rotor-bearing system (Model-I). (b) Stiffness and damping coefficients of the fluid film in bearing.

In the dynamic analysis of the two models linearized stiffness and damping coefficients of hydrodynamic bearings are used. The analysis of a rotor-bearing system is greatly facilitated by the adoption of linearized models of the bearing stiffness and damping coefficients [8, 13]. Generally, for the sake of simplicity, the cross-coupling coefficients ($K_{xy}, K_{yx}, C_{xy}, C_{yx}$) of the oil film were assumed to be negligible [13, 23].

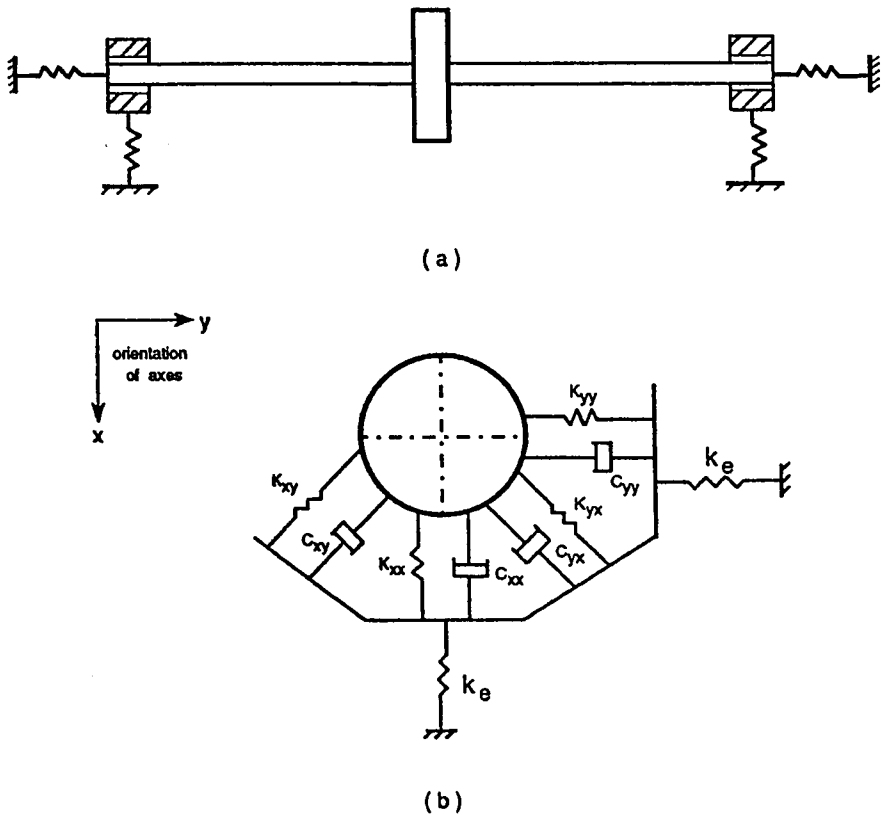

Figure 2.2: (a) Schematic diagram of a rotor-bearing system (Model-II). (b) Stiffness and damping coefficients of the fluid film in bearing and stiffness of flexible support.

This assumption obscures the fundamental notion of controllability of the lateral vibration modes from a single input [8]. Hence in deriving the mathematical models of the rotor-bearing system we have taken into consideration the cross-coupling effects of stiffness and damping coefficients of the oil-film. In both models the rotor is considered to be symmetrically supported on two plain oil-film bearings, each of which is characterized by eight linearized coefficients $(K_{xx}, K_{xy}, K_{yy}, K_{yx}, C_{xx}, C_{xy}, C_{yy}, C_{yx})$.

It is also assumed that the control forces can be exerted on all masses in both vertical and horizontal directions.

2.1 Equations of Motion of Model-I

A schematic diagram of a vibrating rotor-bearing system of model-I is shown in Fig 2.3. Each mass of the two-lumped-mass system has two degrees of freedom along the vertical and horizontal axes, i.e., in this case, the system has four degrees of freedom. The system has a journal mass (m_b) and mid-span mass(m_f) per bearing . The vertical displacements of the two masses m_b and m_f are x_b and x_f respectively; the horizontal displacements of m_b and m_f are y_b and y_f respectively. The stiffness of the rotor per bearing is k_f. The inputs applied vertically to the journal and mid-span masses are f_1 and f_2, respectively; f_3 and f_4 represent inputs in horizontal directions, applied to the journal and mid-span masses respectively. Applying Newton's second law of motion to the masses (m_b, m_f) of the system and simplifying one obtains the following equations :

$$\ddot{x_b} = \frac{f_1}{m_b} - \frac{K_{xx}}{m_b}(x_b) - \frac{K_{xy}}{m_b}(y_b) - \frac{C_{xx}}{m_b}(\dot{x_b}) - \frac{C_{xy}}{m_b}(\dot{y_b}) + \frac{K_f}{m_b}(x_f - x_b) \tag{2.1}$$

$$\ddot{x_f} = \frac{f_2}{m_f} - \frac{K_f}{m_f}(x_f - x_b) \tag{2.2}$$

$$\ddot{y_b} = \frac{f_3}{m_b} - \frac{K_{yy}}{m_b}(y_b) - \frac{K_{yx}}{m_b}(x_b) - \frac{C_{yy}}{m_b}(\dot{y_b}) - \frac{C_{yx}}{m_b}(\dot{x_b}) + \frac{K_f}{m_b}(y_f - y_b) \tag{2.3}$$

$$\ddot{y_f} = \frac{f_4}{m_f} - \frac{K_f}{m_f}(y_f - y_b) \tag{2.4}$$

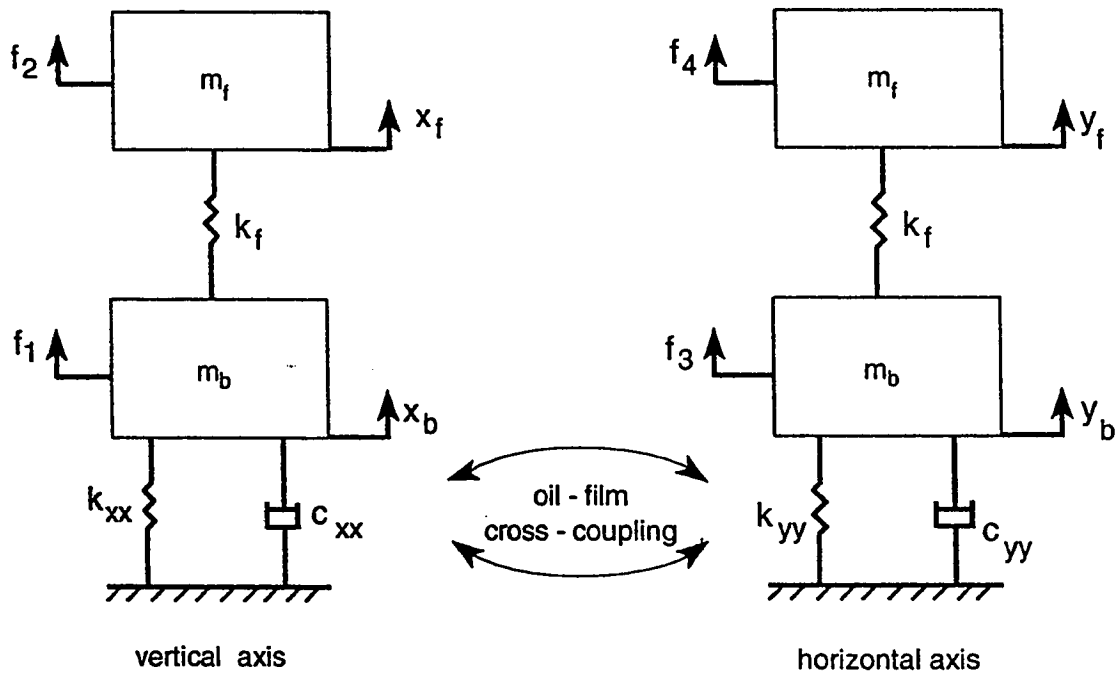

Figure 2.3: Schematic diagram of a vibrating rotor-bearing system for Model I.

2.1.1 State Variable Representation of Model I

A dynamic system consisting of a finite number of lumped elements may be described by ordinary differential equations in which time is the independent variable. By use of vector-matrix notation, an nth-order differential equation may be expressed by a first order vector-matrix differential equation [9]. The state-variable methods are particularly suited to digital-computer computations because of their time-domain approach. Furthermore , the multivariable nature of even the simplest configuration leads naturally to a state-space representation [8, 16, 27, 28].

A suitable set of state-variables for this model-I are as follows:

The state variables in the vertical direction are:

$x_1 = x_b$ = journal displacement; $x_2 = \dot{x_b}$= journal velocity;

$x_3 = x_f$ = mid-span displacement; and $x_4 = \dot{x_f}$= mid-span velocity.

The state variables in the horizontal direction are:

$x_5 = y_b$ =journal displacement; $x_6 = \dot{y_b}$= journal velocity;

$x_7 = y_f$ = mid-span displacement; and $x_8 = \dot{y_f}$= mid-span velocity.

Hence, the state-variable equations of the model are as given below:

$$\dot{x_1} = x_2 \tag{2.5}$$

$$\dot{x_2} = \frac{-(K_{xx} + K_f)}{m_b} x_1 - \frac{C_{xx}}{m_b} x_2 + \frac{K_f}{m_b} x_3 - \frac{K_{xy}}{m_b} x_5 - \frac{C_{xy}}{m_b} x_6 + \frac{f_1}{m_b} \tag{2.6}$$

$$\dot{x_3} = x_4 \tag{2.7}$$

$$\dot{x_4} = \frac{K_f}{m_f} x_1 - \frac{K_f}{m_f} x_3 + \frac{f_2}{m_f} \tag{2.8}$$

$$\dot{x_5} = x_6 \tag{2.9}$$

$$\dot{x_6} = \frac{-(K_{yy} + K_f)}{m_b} x_5 - \frac{C_{yy}}{m_b} x_6 - \frac{K_{yx}}{m_b} x_1 - \frac{C_{yx}}{m_b} x_2 + \frac{K_f}{m_b} x_7 + \frac{f_3}{m_b} \tag{2.10}$$

$$\dot{x_7} = x_8 \tag{2.11}$$

$$\dot{x_8} = \frac{K_f}{m_f} x_5 - \frac{K_f}{m_f} x_7 + \frac{f_4}{m_f} \tag{2.12}$$

It may be noted that equations 2.1 to 2.4 are rewritten in state variable form as 2.6,2.8,2.10 and 2.12 respectively . By using vector-matrix notation, this set of first-order differential equations can be written as follows:

$$\dot{\mathbf{X}} = \mathbf{AX} + \mathbf{Bu} \tag{2.13}$$

or

$$\begin{bmatrix} \dot{\mathbf{x}}_v \\ \dot{\mathbf{x}}_h \end{bmatrix} = \begin{bmatrix} \mathbf{A}_{11} & \mathbf{A}_{12} \\ \mathbf{A}_{21} & \mathbf{A}_{22} \end{bmatrix} \begin{bmatrix} \mathbf{x}_v \\ \mathbf{x}_h \end{bmatrix} + \begin{bmatrix} \mathbf{B}_{11} & \mathbf{B}_{12} \\ \mathbf{B}_{21} & \mathbf{B}_{22} \end{bmatrix} \begin{bmatrix} \mathbf{u}_v \\ \mathbf{u}_h \end{bmatrix} \tag{2.14}$$

Where the state-vectors of vertical motion $\mathbf{x}_v$ and horizontal motion $\mathbf{x}_h$, the vertical input $\mathbf{u}_v$ and horizontal input $\mathbf{u}_h$, the matrices $\mathbf{A}_{11}$, $\mathbf{A}_{12}$, $\mathbf{A}_{21}$, $\mathbf{A}_{22}$, $\mathbf{B}_{11}$, $\mathbf{B}_{12}$, $\mathbf{B}_{21}$ and $\mathbf{B}_{22}$ are defined as follows for Model I:

$$\mathbf{x}_v = \left\{ \begin{array}{cccc} x_1 & x_2 & x_3 & x_4 \end{array} \right\}^T ; \quad \mathbf{x}_h = \left\{ \begin{array}{cccc} x_5 & x_6 & x_7 & x_8 \end{array} \right\}^T$$

$$\mathbf{u}_v = \left\{ \begin{array}{cc} f_1 & f_2 \end{array} \right\}^T ; \quad \mathbf{u}_h = \left\{ \begin{array}{cc} f_3 & f_4 \end{array} \right\}^T$$

$$\mathbf{A}_{11} = \begin{bmatrix} 0 & 1 & 0 & 0 \\ \frac{-(K_{xx}+K_f)}{m_b} & \frac{-C_{xx}}{m_b} & \frac{K_f}{m_b} & 0 \\ 0 & 0 & 0 & 1 \\ \frac{K_f}{m_f} & 0 & \frac{-K_f}{m_f} & 0 \end{bmatrix}; \quad \mathbf{A}_{12} = \begin{bmatrix} 0 & 0 & 0 & 0 \\ \frac{-K_{xy}}{m_b} & \frac{-C_{xy}}{m_b} & 0 & 0 \\ 0 & 0 & 0 & 0 \\ 0 & 0 & 0 & 0 \end{bmatrix}$$

$$\mathbf{A}_{21} = \begin{bmatrix} 0 & 0 & 0 & 0 \\ \frac{-K_{yx}}{m_b} & \frac{-C_{yx}}{m_b} & 0 & 0 \\ 0 & 0 & 0 & 0 \\ 0 & 0 & 0 & 0 \end{bmatrix}; \quad \mathbf{A}_{22} = \begin{bmatrix} 0 & 1 & 0 & 0 \\ \frac{-(K_{yy}+K_f)}{m_b} & \frac{-C_{yy}}{m_b} & \frac{K_f}{m_b} & 0 \\ 0 & 0 & 0 & 1 \\ \frac{K_f}{m_f} & 0 & -\frac{K_f}{m_f} & 0 \end{bmatrix}$$

$$\mathbf{B}_{11} = \mathbf{B}_{22} = \begin{bmatrix} 0 & 0 \\ \frac{1}{m_b} & 0 \\ 0 & 0 \\ 0 & \frac{1}{m_f} \end{bmatrix}; \quad \mathbf{B}_{12} = \mathbf{B}_{21} = \begin{bmatrix} 0 & 0 \\ 0 & 0 \\ 0 & 0 \\ 0 & 0 \end{bmatrix}$$

2.2 Equations of Motion of Model-II

A schematic diagram of a vibrating rotor-bearing system for model-II is shown in Fig.2.4. The system has three masses, two masses (m_b and m_f) are same as those in model-I and the third mass is the bearing housing mass (m_e) and consequently

the system has six degrees of freedom. In this case f_1, f_2 and f_3 are the inputs applied to the bearing housing, journal and mid-span masses respectively in the vertical direction and f_4, f_5 and f_6 are the inputs applied to the bearing housing, journal and mid-span masses respectively in the horizontal direction. x_e, x_b, and x_f are the displacements of bearing housing (m_e), journal mass(m_b) and mid-span mass(m_f) in the vertical directions and y_e, y_b, and y_f are the displacements of bearing housing (m_e), journal mass(m_b) and mid-span mass(m_f) respectively in the horizontal directions. The following equations are derived by applying Newton's Second law of motion:

$$\ddot{x_e} = \frac{f_1}{m_e} + \frac{K_{xx}}{m_e}(x_b - x_e) + \frac{K_{xy}}{m_e}(y_b - y_e) + \frac{C_{xx}}{m_e}(\dot{x_b} - \dot{x_e}) + \frac{C_{xy}}{m_e}(\dot{y_b} - \dot{y_e}) - \frac{K_e}{m_e}(x_e) \quad (2.15)$$

$$\ddot{x_b} = \frac{f_2}{m_b} - \frac{K_{xx}}{m_b}(x_b - x_e) - \frac{K_{xy}}{m_b}(y_b - y_e) - \frac{C_{xx}}{m_b}(\dot{x_b} - \dot{x_e}) - \frac{C_{xy}}{m_b}(\dot{y_b} - \dot{y_e}) + \frac{K_f}{m_b}(x_f - x_b) \quad (2.16)$$

$$\ddot{x_f} = \frac{f_3}{m_f} - \frac{K_f}{m_f}(x_f - x_b) \quad (2.17)$$

$$\ddot{y_e} = \frac{f_4}{m_e} + \frac{K_{yy}}{m_e}(y_b - y_e) + \frac{K_{yx}}{m_e}(x_b - x_e) + \frac{C_{yy}}{m_e}(\dot{y_b} - \dot{y_e}) + \frac{C_{yx}}{m_e}(\dot{x_b} - \dot{x_e}) - \frac{K_e}{m_e}(y_e) \quad (2.18)$$

$$\ddot{y_b} = \frac{f_5}{m_b} - \frac{K_{yy}}{m_b}(y_b - y_e) - \frac{K_{yx}}{m_b}(x_b - x_e) - \frac{C_{yy}}{m_b}(\dot{y_b} - \dot{y_e}) - \frac{C_{yx}}{m_b}(\dot{x_b} - \dot{x_e}) + \frac{K_f}{m_b}(y_f - y_b) \quad (2.19)$$

$$\ddot{y_f} = \frac{f_6}{m_f} - \frac{K_f}{m_f}(y_f - y_b) \quad (2.20)$$

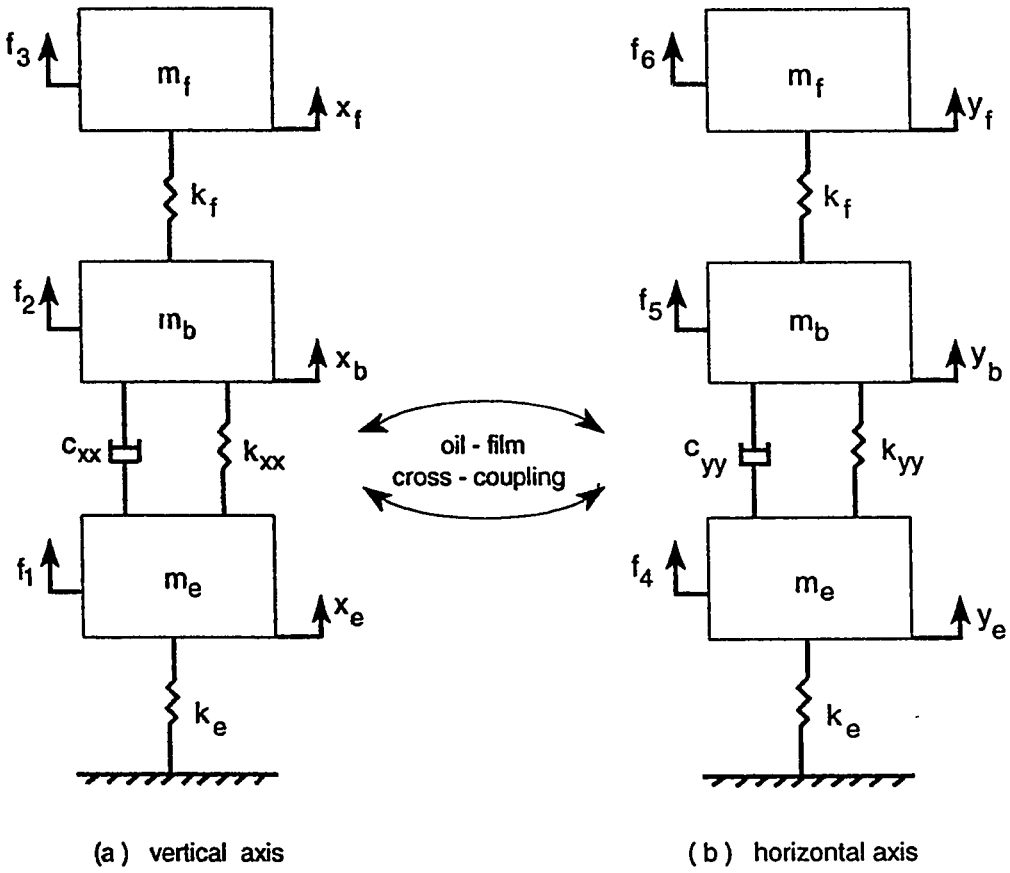

Figure 2.4: Schematic diagram of a vibrating rotor-bearing system for Model - II [8].

2.2.1 State Variable Representation of Model II

A suitable set of state-variables for Model II are as follows:

The state variables in the vertical direction are:

$x_1 = x_e$ = bearing housing displacement; $x_2 = \dot{x}_e$ =bearing housing velocity;

$x_3 = x_b$ =journal displacement; $x_4 = \dot{x}_b$ =journal velocity;

$x_5 = x_f$ =mid-span displacement; and $x_6 = \dot{x}_f$ =mid-span mass velocity.

The state variables in the horizontal direction are:

$x_7 = y_e$ =bearing housing displacement; $x_8 = \dot{y}_e$ =bearing housing velocity;

$x_9 = y_b$ =journal displacement; $x_{10} = \dot{y}_b$ =journal velocity;

$x_{11} = y_f$ =mid-span displacement; and $x_{12} = \dot{y}_f$ =mid-span velocity.

Hence, the state-variable equations of the model are as follows:

$$\dot{x}_1 = x_2 \tag{2.21}$$

$$\dot{x}_2 = \frac{-(K_{xx}+K_e)}{m_e}x_1 - \frac{C_{xx}}{m_e}x_2 + \frac{K_{xx}}{m_e}x_3 + \frac{C_{xx}}{m_e}x_4 - \frac{K_{xy}}{m_e}x_7 - \frac{C_{xy}}{m_e}x_8 + \frac{K_{xy}}{m_e}x_9 + \frac{C_{xy}}{m_e}x_{10} + \frac{f_1}{m_e} \tag{2.22}$$

$$\dot{x}_3 = x_4 \tag{2.23}$$

$$\dot{x}_4 = \frac{-(K_{xx}+K_f)}{m_b}x_3 - \frac{C_{xx}}{m_b}x_4 + \frac{K_{xx}}{m_b}x_1 + \frac{C_{xx}}{m_b}x_2 - \frac{K_{xy}}{m_b}x_9 - \frac{C_{xy}}{m_b}x_{10} + \frac{K_{xy}}{m_b}x_7 + \frac{C_{xy}}{m_b}x_8 + \frac{K_f}{m_b}x_5 + \frac{f_2}{m_b} \tag{2.24}$$

$$\dot{x}_5 = x_6 \tag{2.25}$$

$$\dot{x}_6 = \frac{K_f}{m_f}x_3 - \frac{K_f}{m_f}x_5 + \frac{f_3}{m_f} \tag{2.26}$$

$$\dot{x_7} = x_8 \tag{2.27}$$

$$\dot{x_8} = \frac{-(K_{yy}+K_e)}{m_e}x_7 - \frac{C_{yy}}{m_e}x_8 + \frac{K_{yy}}{m_e}x_9 + \frac{C_{yy}}{m_e}x_{10} - \frac{K_{yx}}{m_e}x_1 - \frac{C_{yx}}{m_e}x_2 + \frac{K_{yx}}{m_e}x_3 + \frac{C_{yx}}{m_e}x_4 + \frac{f_4}{m_e} \tag{2.28}$$

$$\dot{x_9} = x_{10} \tag{2.29}$$

$$\dot{x_{10}} = \frac{-(K_{yy}+K_f)}{m_b}x_9 - \frac{C_{yy}}{m_b}x_{10} + \frac{K_{yy}}{m_b}x_7 + \frac{C_{yy}}{m_b}x_8 - \frac{K_{yx}}{m_b}x_3 - \frac{C_{yx}}{m_b}x_4 + \frac{K_{yx}}{m_b}x_1 + \frac{C_{yx}}{m_b}x_2 + \frac{K_f}{m_b}x_{11} + \frac{f_5}{m_b} \tag{2.30}$$

$$\dot{x_{11}} = x_{12} \tag{2.31}$$

$$\dot{x_{12}} = \frac{K_f}{m_f}x_9 - \frac{K_f}{m_f}x_{11} + \frac{f_6}{m_f} \tag{2.32}$$

Equations 2.14 to 2.19 are rewritten in state variable form as 2.21, 2.23, 2.25, 2.27, 2.29 and 2.31 respectively . By using vector-matrix notation, this set of first-order differential equations can be rewritten as follows:

$$\dot{\mathbf{X}} = \mathbf{A}\mathbf{X} + \mathbf{B}\mathbf{u} \tag{2.33}$$

or

$$\begin{bmatrix} \dot{\mathbf{x}}_v \\ \dot{\mathbf{x}}_h \end{bmatrix} = \begin{bmatrix} \mathbf{A}_{11} & \mathbf{A}_{12} \\ \mathbf{A}_{21} & \mathbf{A}_{22} \end{bmatrix} \begin{bmatrix} \mathbf{x}_v \\ \mathbf{x}_h \end{bmatrix} + \begin{bmatrix} \mathbf{B}_{11} & \mathbf{B}_{12} \\ \mathbf{B}_{21} & \mathbf{B}_{22} \end{bmatrix} \begin{bmatrix} \mathbf{u}_v \\ \mathbf{u}_h \end{bmatrix} \tag{2.34}$$

Where the state-vectors of vertical motion $\mathbf{x}_v$ and horizontal motion $\mathbf{x}_h$, the vertical input $\mathbf{u}_v$ and horizontal input $\mathbf{u}_h$, the matrices $\mathbf{A}_{11}$, $\mathbf{A}_{12}$, $\mathbf{A}_{21}$, $\mathbf{A}_{22}$, $\mathbf{B}_{11}$, $\mathbf{B}_{12}$, $\mathbf{B}_{21}$

and $\mathbf{B}_{22}$ are defined as follows for Model II :

$$\mathbf{x}_v = \left\{ x_1 \quad x_2 \quad x_3 \quad x_4 \quad x_5 \quad x_6 \right\}^T ; \qquad \mathbf{x}_h = \left\{ x_7 \quad x_8 \quad x_9 \quad x_{10} \quad x_{11} \quad x_{12} \right\}^T$$

$$\mathbf{u}_v = \left\{ f_1 \quad f_2 \quad f_3 \right\}^T ; \qquad \mathbf{u}_h = \left\{ f_4 \quad f_5 \quad f_6 \right\}^T$$

$$\mathbf{A}_{11} = \begin{bmatrix} 0 & 1 & 0 & 0 & 0 & 0 \\ \frac{-(K_{xx}+K_e)}{m_e} & \frac{-C_{xx}}{m_e} & \frac{K_{xx}}{m_e} & \frac{C_{xx}}{m_e} & 0 & 0 \\ 0 & 0 & 0 & 1 & 0 & 0 \\ \frac{K_{xx}}{m_b} & \frac{C_{xx}}{m_b} & \frac{-(K_{xx}+K_f)}{m_b} & \frac{-C_{xx}}{m_b} & \frac{K_f}{m_b} & 0 \\ 0 & 0 & 0 & 0 & 0 & 1 \\ 0 & 0 & \frac{K_f}{m_f} & 0 & \frac{-K_f}{m_f} & 0 \end{bmatrix}$$

$$\mathbf{A}_{12} = \begin{bmatrix} 0 & 0 & 0 & 0 & 0 & 0 \\ \frac{-K_{xy}}{m_e} & \frac{-C_{xy}}{m_e} & \frac{K_{xy}}{m_e} & \frac{C_{xy}}{m_e} & 0 & 0 \\ 0 & 0 & 0 & 0 & 0 & 0 \\ \frac{K_{xy}}{m_b} & \frac{C_{xy}}{m_b} & \frac{-K_{xy}}{m_b} & \frac{-C_{xy}}{m_b} & 0 & 0 \\ 0 & 0 & 0 & 0 & 0 & 0 \\ 0 & 0 & 0 & 0 & 0 & 0 \end{bmatrix} ; \mathbf{A}_{21} = \begin{bmatrix} 0 & 0 & 0 & 0 & 0 & 0 \\ \frac{-K_{yx}}{m_e} & \frac{-C_{yx}}{m_e} & \frac{K_{yx}}{m_e} & \frac{C_{yx}}{m_e} & 0 & 0 \\ 0 & 0 & 0 & 0 & 0 & 0 \\ \frac{K_{yx}}{m_b} & \frac{C_{yx}}{m_b} & \frac{-K_{yx}}{m_b} & \frac{-C_{yx}}{m_b} & 0 & 0 \\ 0 & 0 & 0 & 0 & 0 & 0 \\ 0 & 0 & 0 & 0 & 0 & 0 \end{bmatrix}$$

$$\mathbf{A}_{22} = \begin{bmatrix} 0 & 1 & 0 & 0 & 0 & 0 \\ \frac{-(K_{yy}+K_e)}{m_e} & \frac{-C_{yy}}{m_e} & \frac{K_{yy}}{m_e} & \frac{C_{yy}}{m_e} & 0 & 0 \\ 0 & 0 & 0 & 1 & 0 & 0 \\ \frac{K_{yy}}{m_b} & \frac{C_{yy}}{m_b} & \frac{-(K_{yy}+K_f)}{m_b} & \frac{-C_{yy}}{m_b} & \frac{K_f}{m_b} & 0 \\ 0 & 0 & 0 & 0 & 0 & 1 \\ 0 & 0 & \frac{K_f}{m_f} & 0 & \frac{-K_f}{m_f} & 0 \end{bmatrix}$$

$$\mathbf{B}_{11} = \mathbf{B}_{22} = \begin{bmatrix} 0 & 0 & 0 \\ \frac{1}{m_e} & 0 & 0 \\ 0 & 0 & 0 \\ 0 & \frac{1}{m_b} & 0 \\ 0 & 0 & 0 \\ 0 & 0 & \frac{1}{m_f} \end{bmatrix}; \qquad \mathbf{B}_{12} = \mathbf{B}_{21} = \begin{bmatrix} 0 & 0 & 0 \\ 0 & 0 & 0 \\ 0 & 0 & 0 \\ 0 & 0 & 0 \\ 0 & 0 & 0 \\ 0 & 0 & 0 \end{bmatrix}$$

The modern control theory can be applied to these models for controlling the lateral vibrations of the rotor-bearing system. The controllability and observability of these models are investigated in Chapter 3.

Chapter 3

Controllability and Observability of a system

Concept of controllability and observability are of fundamental importance in modern control theory. They are considered necessary and sufficient conditions for the existence of a solution to a control problem. Whether or not a control solution exists for a system can be decided on the basis of the following conditions:

1. The possibility of transferring the system from any initial state to any other desired state in finite time by application of a suitable control input.

2. The possibility of determining the initial state if the output vector for a finite length of time is known.

Kalman [34] conceptualized these two basic conditions respectively as controllability and observability.

3.1 Controllability

The general form of the state equation of a system can be defined as:

$$\dot{\mathbf{X}} = \mathbf{AX} + \mathbf{Bu} \tag{3.1}$$

$$\mathbf{Y} = \mathbf{CX} \tag{3.2}$$

where, **A** is n×n matrix, **B** is n×p matrix and **C** is q×n matrix. A system is said to be completely controllable if every state variable of the process can be affected or controlled to reach a certain objective in finite time by some unconstrained control input u(t). If any one of the state variables is independent of u(t), then there would be no way of driving this particular state in finite time by means of a control effort, and this state is said to be uncontrollable . For a system or process if there exists any uncontrollable state, the system is said to be uncontrollable. Principally there are two types of controllability for a system or process, they are 'state variable controllability' and 'output controllability'.

A system is said to be completely state controllable if it is possible to transfer the system state from any initial state $x(t_0)$ to any other desired state $x(t_f)$ in specified finite time by a control vector u(t). The mathematical test of controllability can be performed either by the method developed by Kalman [34] or by the method

developed by Gilbert [39]. Output controllability is a property of the input-output description of a system [39]. A system is said to be completely output controllable if it is possible to construct an unconstrained control vector u(t) which will transfer any given initial output $y(t_o)$ to any final output $y(t_f)$ in a finite time interval [9]. It is to be noted that complete state controllability is neither necessary nor sufficient for complete output controllability [40]. However complete state controllability implies complete output controllability if and only if 'q' rows of matrix **C** are linearly independent [39, 40].

If the values of the elements of coefficient matrix **A** of state vector are not known with any certainty then rank testing, by Kalman's and Gilbert's method, becomes an unreliable operation. This practical problem can be overcome by examining the structural controllability of the system [8]. Structural controllability is a property that is as useful as controllability; it is introduced by Lin [30]. Lin [30] described the method to check the structural controllability of a pair (**A**,**B**) using graph theory. Shield and Pearson [31] extended the results of Lin [30] on structural controllability of single-input linear systems to multi-input linear systems. They developed an algorithm for determining the generic rank of a matrix called 'fixed-zero-rank-finder (FZRF). An algorithm derived by Burrows and Sahinkaya [32] enables the structural controllability of fairly complex system to be determined by inspection, without the aid of a computer. Pillou and Rech [33] developed an algorithm for determining the generic rank of structured systems. However, the algorithm developed by Burrows

and Sahinkaya [32] is much easier to apply than any other method suggested by other researchers, and it yields directly information concerning the number of inputs required, and their points of application, to ensure the controllability. For the controllability test of the systems considered in chapter-2 the algorithm developed by Burrows and Sahinkaya [32] is applied.

3.2 Observability

The concept of observability is dual to the concept of controllability. Simply speaking, controllability studies the possibilities of steering the state from the input and observability studies the possibilities of estimating the state from the output [39]. For a system to be observable, it must be possible to determine the state of the undisturbed system from the knowledge of the output of the system over some time interval. For the system described by the equations 3.1 and 3.2, a state x_o is observable at time t_o if and only if it can be uniquely determined from the observation of output y(t) over the interval(t_o,t). Finally if every state at time t_o can be determined from the measurements of output y(t) then the system is said to be completely observable [9, 39, 45].

The concept of observability is useful in solving the problem of reconstructing the immeasurable state variables from measurable ones in the minimum possible length of time [9, 44, 45]. Particularly for the rotor-bearing system as considered in our

study, the variables to be measured would be the velocity and displacement of each of three masses in both horizontal and vertical planes [8]. One way to achieve this is to use six accelerometers with the velocity and displacement signals being obtained by integrating the acceleration signals. However four of these accelerometers have to be attached to rotating components (for the Model II) and it would require additional equipment in order to extract the signals. If non-contacting transducers are used to monitor the mass displacements then differentiations of the signals will be required to obtain the velocity records, and the problems associated with this approach are well known. Hence an alternative approach is required which dispenses with the need of measuring all the system states or which is capable of predicting the immeasurable states. Kalman's principle of duality gives an analogy between controllability and observability. The principle of duality states that the pair **(A,B)** is controllable if $(\mathbf{A}^T, \mathbf{B}^T)$ is observable and the pair **(A,C)** is observable if the pair $(\mathbf{A}^T, \mathbf{C}^T)$ is controllable [9, 34]. Thus the controllability and observability are dual concepts.

The controllability and observability of the models of rotor-bearing systems considered in our study are tested by the methods described by Burrows and Suhinkaya [32]. The procedure of controllability and observability test is presented in Appendix-B. The proposed rotor-bearing system is found completely controllable and observable, therefore, the controllers derived from modern control theory can be applied on this system.

Chapter 4

Response Characteristics of Model I

In this Chapter an attempt is made to study the response of the rotor-bearing system assuming that its bearings are mounted on rigid supports. The responses have been studied by considering the system without a controller as well as with each of the following controllers, separately:

- State variable feedback (SVFB) controller [27, 45, 46].
- Integral plus state variable feedback (ISVFB) controller [27, 39, 47].
- Linear quadratic servo(LQS) controller [28, 39]

At first the response of the system without a controller owing to an external disturbance is presented; then the description of each controller and its performance

characteristics are presented. Finally, the relative suitability of these controllers is discussed.

4.1 System without a Controller

The dynamic equation of the system have been obtained in Chapter 2. The coefficient matrices **A** and **B** have been calculated by using the parameter values given in the following section. The resultant **A** and **B** matrices of the system are presented in Appendix C.

4.1.1 Parameter values and Simulation

Critical dimensions of Rotor and Journal Bearing

The critical dimensions of the rotor-bearing system are shown Fig. 4.1. The effective

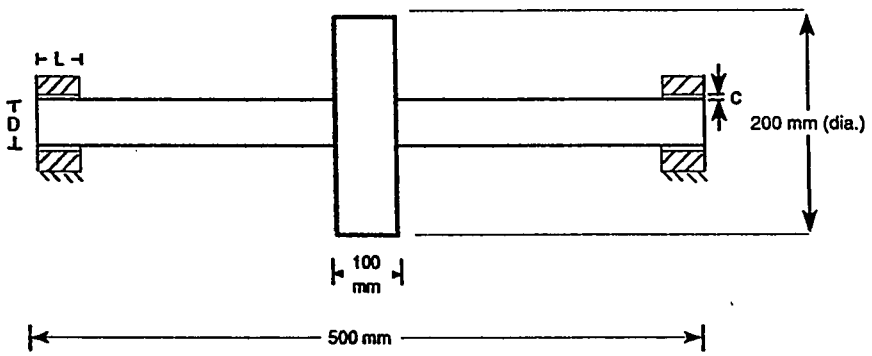

Figure 4.1: Schematic diagram of a rotor mounted on journal bearings.

masses per bearing and the necessary bearing dimensions are:

m_b = 0.2 kg, m_f = 12.33 kg;

load per bearing W = 189.87 N, radial clearance, c = 0.051 mm;

diameter of journal, D = 51 mm, land length of bearing, L = 12 mm.

Burrows and Stanway [20] considered the bearing as a multi-input, multi-output plant and applying state-space techniques, they developed a coherent strategy for identification of oil-film dynamics. But their work is restricted to rigid rotors. Kamal and Asfar [42] considered a more general model of rotor-bearing system and applied system identification techniques to estimate the oil-film coefficients. They developed a scheme to identify the modal parameters of the rotor-bearing system from which the damping and stiffness coefficients can be determined. However, our objective is to study the performance of the controllers so we have considered the oil-film parameters from the available data [43]. The following non-dimensional bearing parameters are used at eccentricity ratio, ϵ_o=0.8 [43]:

k_{xx} = 9.042, k_{xy} = 5.326, k_{yy} = 1.848, k_{yx} = -0.674;

c_{xx} = 8.177, c_{xy} = 1.915, c_{yy} = 1.128, c_{yx} = 1.915.

The computed values of oil-film stiffness coefficients($K_{xx} = k_{xx}\frac{W}{c}$ etc.) [19, 24, 42] are,

K_{xx} = 3.3663×10^7 N/m, K_{xy} = 1.9828×10^7 N/m;

K_{yy} = 6.88×10^6 N/m, K_{yx} = -2.5093×10^6 N/m.

Damping coefficients depend on the shaft speed($C_{xx} = c_{xx}\frac{W}{\omega c}$ etc., where ω is shaft

speed in rad/s); the computed values of damping coefficients for different shaft speeds are given in table 4.1.

Shaft speed(rpm)	Damping coefficients(Ns/m)			
N	C_{xx}	C_{xy}	C_{yy}	C_{yx}
500	5.8141×10^5	1.3616×10^5	8.0204×10^4	1.3616×10^5
1500	1.9380×10^5	4.5387×10^4	2.6735×10^4	4.5387×10^4
2500	1.1628×10^5	2.7232×10^4	1.6041×10^4	2.7232×10^4
3000	9.6901×10^4	2.2694×10^4	1.3367×10^4	2.2694×10^4
3500	8.3058×10^4	1.9452×10^4	1.1458×10^4	1.9452×10^4
4500	6.4601×10^4	1.5129×10^4	8.9116×10^3	1.5129×10^4
10000	2.9097×10^4	6.8081×10^3	4.0102×10^3	6.8081×10^3
15000	1.9380×10^4	4.5387×10^3	2.6735×10^3	4.5387×10^3

Table 4.1: Damping coefficients of Oil-film bearings at different shaft speeds.

Simulation

The dynamic response of the mathematical model of the system thus developed is simulated on an IBM compatible Personal Computer using the software package 'PC-MATLAB' [44]. Other computational work like determination of journal bearing parameters and damping ratios of the vibration of the system has been executed on a digital computer IBM3090-150E OS/VM/CMs. A FORTRAN compiler is used for this purpose. Graphical displays of the results are obtained with the help of PC-MATLAB and Interactive Chart Utility(ICU, installed in IBM3090-150E) software packages.

4.1.2 Response of the System Without a Controller

The eigenvalues of the coefficient matrix 'A' obtained at different shaft speeds are given in Table 4.2. The influence of the cross-coupling terms (K_{xy},K_{yx},C_{xy} and C_{yx}) on the stability of the system can be observed from this table. At lower shaft speeds all the eigenvalues are negative but at higher speeds (e.g. 10000rpm and above) two of the eigenvalues are positive complex numbers. On the other hand when the cross coupling terms are neglected the eigenvalues of the coefficient matrix ' A' are negative for all shaft speeds (the values are not shown here), indicating that the system is stable for any shaft speed. It implies that the cross coupling terms must be in included in the model to identify bearing characteristics and to control vibrations. The response of the vertical deflection of the mid-span of the shaft owing to a unit step external disturbance at the mid-span is shown in Fig. 4.2. The figure displays a plot of the deflection of the shaft against time. This response is obtained for a shaft speed of 500 rpm. The figure shows that the system is stable (at lower speed system is stable see Table 4.2). Oscillations about the equilibrium position occurred and each successive amplitude diminishes from the preceding amplitude which indicates that the response is underdamped. The horizontal deflection of the mid-span is also shown in this figure and the nature of oscillations displayed is similar. When a unit step disturbance is applied horizontally at the same location similar responses have been observed (graphs are not included). In this case, the

peak value of the horizontal deflection is larger than that of the vertical deflection. The study is repeated for shaft speeds of 1500, 2500, 3000, 3500, 4500, 10000 and 15000 rpm. The values of first two consecutive amplitudes(x_A, x_B), their times of occurrence(t_A, t_B) and the damping ratio(ζ) for different shaft speeds are given in Table 4.3 and Table 4.4. The values mentioned in the Tables 4.3 and 4.4 have been obtained from the response curves of mid-span deflection using the method of logarithmic decrement of the amplitude.

500 rpm	1500 rpm	4500 rpm
-3.0800(10^6)	-1.0264(10^6)	-3.4149(10^5)
-2.2760(10^5)	-7.4762(10^4)	-2.0930(10^4)
-77.945 + 65.022i	-33.581 + 1067.1i	-3.9972(10^3)
-77.945 - 65.022i	-33.581 - 1067.1i	-9.2428(10^2)
-11.488 + 1072.5i	-456.31 + 793.54i	-80.432 + 1028.1i
-11.488 - 1072.5i	-456.31 - 793.54i	-80.432 - 1028.1i
-155.42 + 1048.2i	-253.39 + 251.15i	-29.994 + 575.62i
-155.42 - 1048.2i	-253.39 - 251.15i	-29.994 - 575.62i

10000 rpm	15000 rpm
-1.5235(10^5)	-1.0015(10^5)
-5506.8 + 7712.5i	-3567.3 + 8852.8i
-5506.8 - 7712.5i	-3567.3 - 8852.8i
-1894.1	-2874.3
-88.303 + 957.82i	-73.379 + 9287.7i
-88.303 - 957.82i	-73.379 - 9287.7i
14.870 + 623.58i	18.629 + 639.94i
14.870 - 623.58i	18.629 - 639.94i

Table 4.2: Eigenvalues of coefficient matrix 'A' at different shaft speeds.

Shaft speed(N) rpm	Amplitude(x_A) m	Amplitude(x_B) m	Time(t_A) sec	Time(t_B) sec
500	4.889×10^{-8}	3.481×10^{-8}	15.4×10^{-3}	50.0×10^{-3}
1500	4.143×10^{-8}	1.286×10^{-8}	13.8×10^{-3}	50.0×10^{-3}
2500	3.103×10^{-8}	0.552×10^{-8}	14.9×10^{-3}	45.7×10^{-3}
3000	3.143×10^{-8}	0.428×10^{-8}	14.6×10^{-3}	43.8×10^{-3}
3500	3.143×10^{-8}	0.5×10^{-8}	15.4×10^{-3}	33.1×10^{-3}

Table 4.3: Consecutive peak values of the response of mid-span deflection and their time of occurrence at different shaft speeds.

Shaft speed(N) rpm	Damping ratio(ζ)	Frequency(f) Hz
500	54.0×10^{-3}	28.9
1500	183×10^{-3}	28.1
2500	265×10^{-3}	33.7
3000	302×10^{-3}	35.9
3500	281×10^{-3}	58.9

Table 4.4: Damping ratio and frequency of oscillation of mid-span mass (m_f). These values are obtained from the response curves of the vertical-deflection of the mid-span of the rotor at different shaft speeds.

4.1.3 Remarks on the Performance of the System without a Controller

Observation of the response curves reveals that the system exhibits stable and underdamped response owing to an external disturbance up to a shaft speed of 4500 rpm; the system is unstable when the rotor speed is 10000 rpm and above (see Table 4.2.). The damping coefficients of the oil-film decreases with the increase of the rotor speed and this influences the stability of the system. When the effect of cross-coupling terms are considered to be negligible (i.e. $K_{xy} = K_{yx} = C_{xy} = C_{yx} = 0$) the responses obtained show that the system is stable for any rotor speed.

It is observed that up to 3000 rpm, the values of x_B, t_B go on decreasing as the speed of shaft increases and the damping ratio (ζ) increases with the increase of speed (Table 4.3). At 3500 rpm the value of x_B is higher and the value of t_B and ζ are lower compared to the values at 3000 rpm. The frequency of vibration of the system first decreases when the speed is increased from 500 to 1500 rpm; then frequency increases with the increase of shaft the speed. The response curves of the mid-span deflection at a shaft speed 4500 rpm in Fig. 4.2 are not of similar nature to those at other speeds. One observes that the decrement of the amplitudes is not logarithmic in nature. This deviation is due to the effect of the cross-coupling terms and when the speed of the rotor is increased to 10000 rpm and above the system exhibits instability. All the results show that vibrations in the horizontal

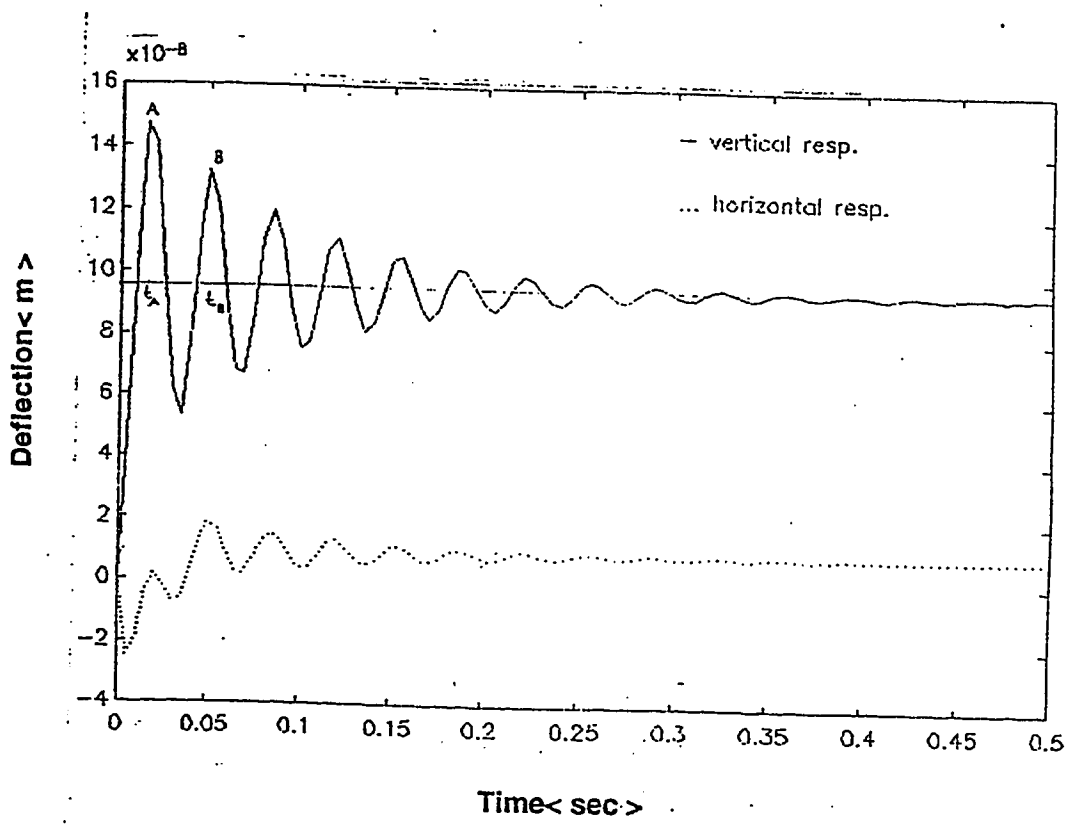

Figure 4.2: Response of the mid-span deflection at a shaft speed of 500 rpm when an external unit-step disturbance is applied at mid-span in the vertical direction(no controller is employed in the system).

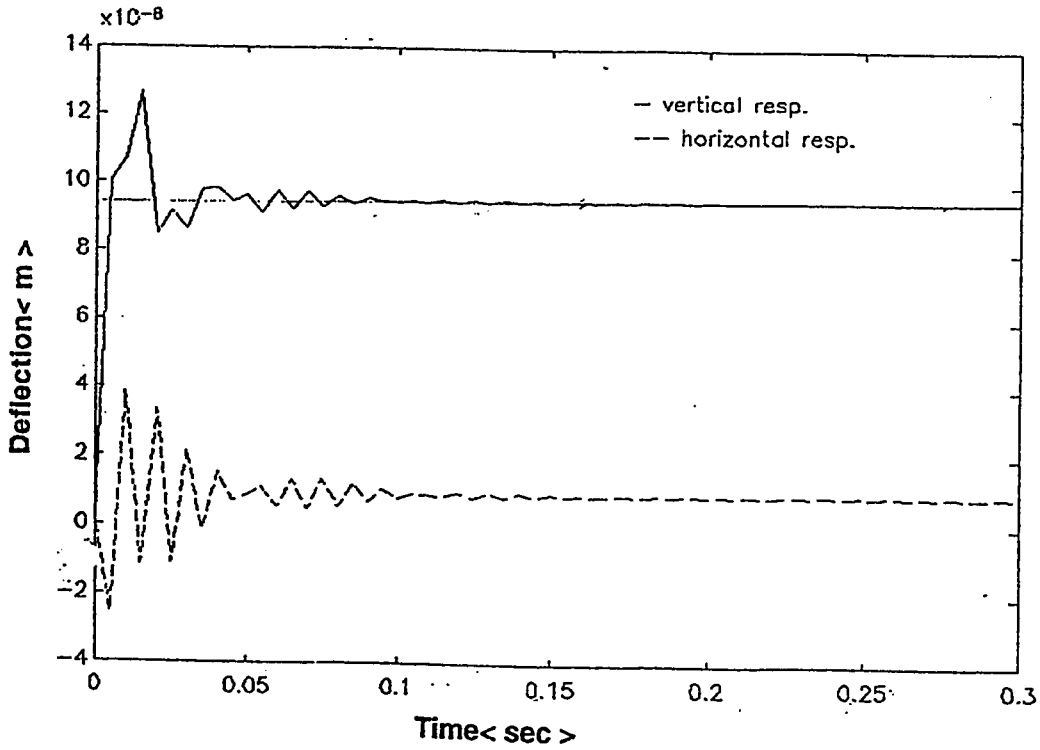

Figure 4.3: Response of the mid-span deflection at a shaft speed of 4500 rpm when an external unit-step disturbance is applied at mid-span in the vertical direction(no controller is employed in the system).

and vertical directions are in general not in phase.

4.2 State Variable Feedback Controller

State variable feedback is a widely used control technique of single input-single output (SISO) as well as multi-input multi-output(MIMO) systems [26, 27, 38]. In this method the states such as the displacements and velocities of each of the lumped masses of the rotor bearing system are fed back and added to the system input after being modified by a certain amount of gain. This makes the system a closed-loop system with overall characteristic equation being modified by a feedback gain.

4.2.1 The Closed-Loop Configuration of the System.

The dynamic equation of Model-I is given by,

$$\dot{\mathbf{X}} = \mathbf{A}\mathbf{X} + \mathbf{B}\mathbf{u} \tag{4.1}$$

where, the matrices **A**, **B** and **u** are described in Chapter 2. Owing to a disturbance there may be a change in the state of the system, and in practice a controller is responsible for driving the system ultimately to its original state. It is required to calculate [45, 47] the optimal feedback gain matrix **K** such that the feedback law,

$$\mathbf{u} = -\mathbf{K}\mathbf{X} \tag{4.2}$$

minimizes the cost function,

$$J = \int (\mathbf{X}^T \mathbf{Q} \mathbf{X} + \mathbf{u}^T \mathbf{R} \mathbf{u}) dt \tag{4.3}$$

The gain can be calculated from the related steady state algebraic Ricatti equation [45, 47]:

$$\mathbf{P}\mathbf{A} + \mathbf{A}^T\mathbf{P} - \mathbf{P}\mathbf{B}\mathbf{R}^{-1}\mathbf{B}^T\mathbf{P} + \mathbf{Q} = 0 \tag{4.4}$$

$$\mathbf{K} = \mathbf{R}^{-1}\mathbf{B}^T\mathbf{P} \tag{4.5}$$

The derivational details of equations (4.2) to (4.5) are given in Appendix B. The designer selects the weighting matrices $\mathbf{Q}$ and $\mathbf{R}$ to achieve the desired gain matrix $\mathbf{K}$. To keep the tuning exercise as straight-forward as possible , the off-diagonal elements of $\mathbf{Q}$ have been set to zero [28, 39]; since $\mathbf{u}$ is a vector matrix the off-diagonal elements of $\mathbf{R}$ are also zero. The following $\mathbf{Q}$ and $\mathbf{R}$ matrices may be used:

$$\mathbf{Q} = \begin{bmatrix} q_1 & 0 & 0 & 0 & 0 & 0 & 0 & 0 \\ 0 & q_2 & 0 & 0 & 0 & 0 & 0 & 0 \\ \vdots & \vdots & \vdots & \vdots & \vdots & \vdots & \vdots & \vdots \\ \vdots & \vdots & \vdots & \vdots & \vdots & \vdots & \vdots & \vdots \\ 0 & 0 & 0 & 0 & 0 & 0 & q_7 & 0 \\ 0 & 0 & 0 & 0 & 0 & 0 & 0 & q_8 \end{bmatrix} \tag{4.6}$$

where,q_1,q_2, ·····, q_8 represent the weight factors, the designer places on the constraints of the state variables x_1, x_2, ·····, x_8. The larger the value of q_i relative to other value of q, the more control effort is spent to regulate x_i(t).

$$\mathbf{R} = \begin{bmatrix} r_1 & 0 & 0 & 0 \\ 0 & r_2 & 0 & 0 \\ 0 & 0 & r_3 & 0 \\ 0 & 0 & 0 & r_4 \end{bmatrix} \tag{4.7}$$

Where, r_1, r_2, r_3 and r_4 represent the weight factors to be applied to the control inputs u_1, u_2, u_3 and u_4. If a disturbance du is applied on the system, the dynamic equation of state variable feedback is given by,

$$\dot{\mathbf{X}} = (\mathbf{A} - \mathbf{BK})\mathbf{X} + \mathbf{B}.d\mathbf{u} = \mathbf{A}_c\mathbf{X} + \mathbf{B}.d\mathbf{u} \tag{4.8}$$

The closed-loop system equation when the disturbance du = 0 is given by,

$$\dot{\mathbf{X}} = (\mathbf{A} - \mathbf{BK})\mathbf{X} \tag{4.9}$$

Since the system under consideration is controllable and observable as shown in Chapter 3, the regulator $\mathbf{A}_c$ will provide a stable closed-loop system [27]. The adopted coefficient matrices and resultant gain and regulator matrices are shown in Appendix C. Fig. 4.4 is a typical representation of the state variable feedback system.

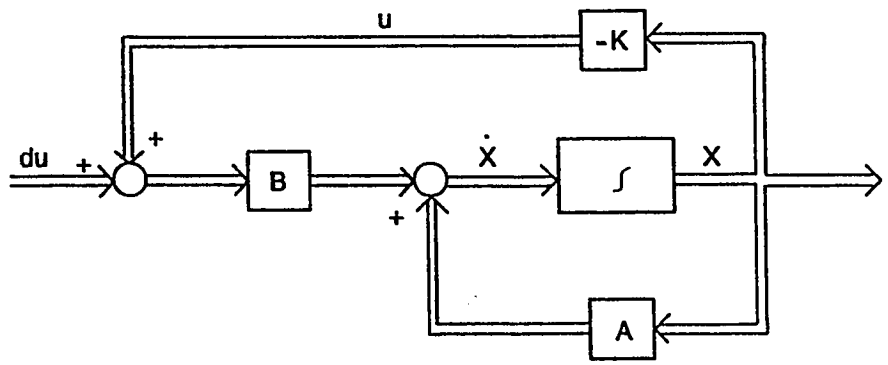

Figure 4.4: Block diagram representation of the system with a State Variable Feedback Controller.

4.2.2 Selection of Weighting Factors

A series of simulation have been conducted for selecting the appropriate weighting matrices **Q** and **R**. The following procedures have been employed for the selection of the weighting matrices:

1. Initially the value of the elements of the matrices **Q** and **R** have been taken as 1, to observe the response of the system.

2. Relative weights of elements in **Q** and **R** are revised to give the desired response.

3. The relative weights of the elements r_1, r_2, r_3, r_4 of the matrix **R** have been revised until the desired response is achieved.

The mid-span deflection has to be minimized, therefore, the state variables x_3 and x_7 corresponding to the vertical and horizontal mid-span displacement have to be

controlled effectively. Consequently, weightages given to q_3 and q_7 are higher relative to the other values of q. The inputs u_2 and u_4 which affect directly the states x_3 and x_7 would be given more weightage than the other inputs and hence the weighting factors r_2 and r_4 would be set to a higher value than other weighting factors. Based on the simulation with different trial values, the following sets of weighting factors are selected:

- the first set of values of weighting factors are: q_1=q_2= $\cdots\cdots$= q_8=1; and r_1=r_3 = 10^{-10}, r_2=r_4= 10^{-8}; and
- the second set of values of weighting factors are: q_3=q_7=10^6,q_1=q_2= q_4 = q_5= q_6= q_8=1; and r_1=r_3 = 10^{-10}, r_2=r_4= 10^{-8}.

4.2.3 Response of the System With an SVFB Controller

When an SVFB controller with the first set of weighting factors is employed the response of the mid-span deflection of the rotor-bearing system owing to an external unit-step disturbance is as shown in Fig. 4.5. Fig. 4.5 is obtained by plotting the vertical displacement of the mid-span against time when the speed of the shaft is 500 rpm. The effect of the shaft speed on the performance of the controller has been studied by considering the shaft speeds of 1500, 2500, 3000, 3500,4500, 10000, 15000 rpm. The response curves corresponding to these speeds are similar to the one in Fig. 4.5, so they are not presented here.

The result shown by the graph in Fig. 4.6. is the response of the mid-span deflection when the second set of weighting factors is used. The effect of the shaft speed on the performance of the controller has been studied by considering shaft speeds of 1500, 2500, 3000, 3500,4500, 10000, 15000 rpm. The response curves corresponding to these speeds are similar to the one in Fig. 4.6, therefore, they are not presented here.

When the same disturbance is applied horizontally at the mid-span, the results of vertical and horizontal deflection are similar to those in Fig. 4.5 and Fig. 4.6.

The performance characteristics such as the rise time(t_r), settling time(t_s), delay time(t_d) and steady-state value [45] obtained from the response curves corresponding to shaft speeds of 500, 1500, 2500, 3000, 3500, 4500, 10000 and 15000 rpm, have been given in Table 4.5.

Shaft speed(N)	rise time(t_r)	delay time(t_d)	settling time(t_s)	steady-state
rpm	10^{-3}sec.	10^{-3}sec.	sec.	10^{-8}m
500	4.348	2.717	.0326	7.129
1500	4.348	2.717	.0136	7.581
2500	4.348	2.717	.0103	7.613
3000	4.348	2.717	.0125	7.613
3500	4.348	2.717	.00978	7.581
4500	4.348	2.717	.0125	7.548
10000	3.846	2.564	.0128	7.437
15000	3.846	2.564	.0103	7.437

Table 4.5: Performance characteristics, t_r, t_d, t_s and steady-state value of mid-span response of the system with an SVFB controller having the second set of weighting factors and disturbance is applied vertically at mid-span.

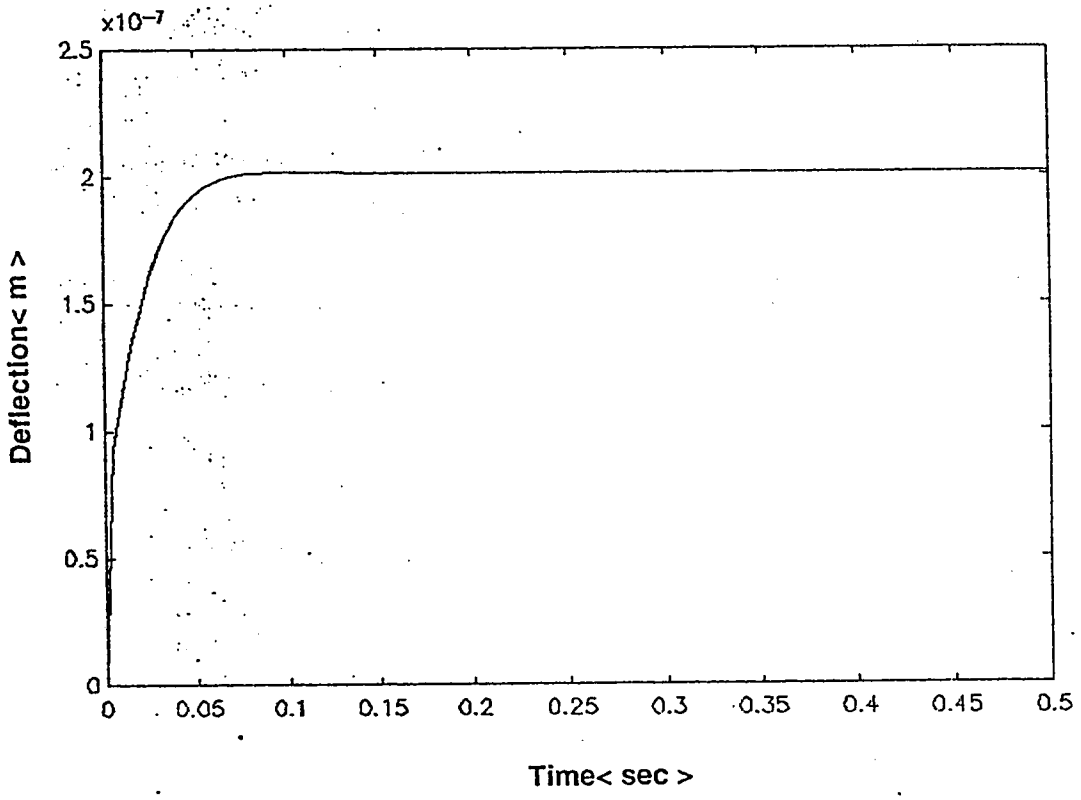

Figure 4.5: Response of mid-span vertical deflection of rotor with an SVFB controller having the first set of weighting factors and subjected to a unit step external disturbance (the response is at shaft speed of 500 rpm).

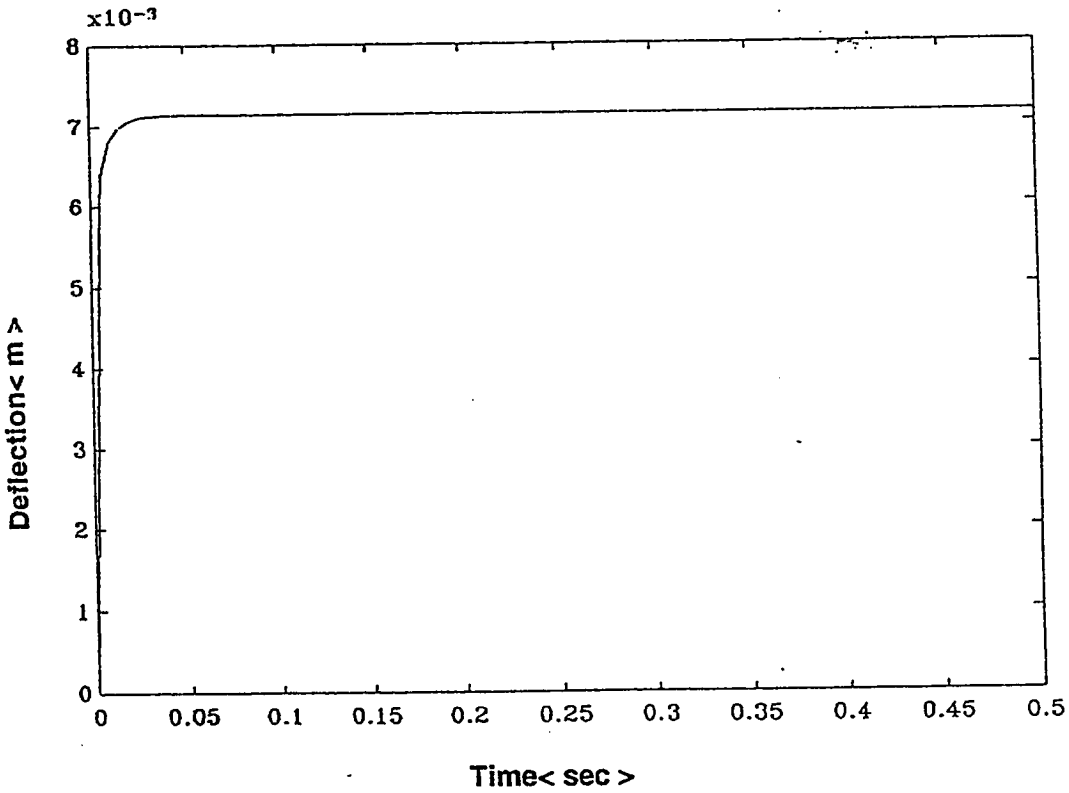

Figure 4.6: Response of mid-span vertical deflection of rotor with an SVFB controller having the second set of weighting factors and when a unit step external disturbance is applied vertically at mid-span (the response is at shaft speed of 500 rpm).

4.2.4 Remarks on the Performance of the System With an SVFB Controller

One observes that in the present case an SVFB controller exhibits well damped response. The system is found to be stable. Observation of Fig. 4.2 and Fig. 4.5 reveals that a steady state non-zero displacement occurs due to a step disturbance. The steady-state deflection for the system with an SVFB controller is $2(10^{-7})$m compared to $0.95(10^{-7})$m for the system without a controller. But the system reaches the steady-state after 0.185s, while without a controller the system reaches the steady-state in 0.5s. This indicates that when a controller with the first set of weighting factors is employed the settling time is less than the system without a controller. When a controller with the second set of weighting factors is used response is better (see Fig. 4.5 and Fig. 4.6) in that the steady-state deflection is only $7.161(10^{-8})$m which is 25% lower than that achieved without a controller. The settling time in this case is to $3.26(10^{-2})$s which indicates that the system approaches the steady-state faster than any of the previous systems. Hence by proper tuning of the weighting matrices a desired level of steady-state value of the mid-span deflection can be achieved by an SVFB controller.

Table 4.5 shows that the rise time (t_r) and the delay time (t_d) are 4.348s and 2.717s respectively, upto a shaft speed of 4500 rpm. For shaft 10000 rpm and above rise time decreases to $3.846(10^{-3})$s and delay time increases to $2.564(10^{-3})$s. This im-

value of (t_r) and (t_d) changes when the speed of rotor crosses the critical speed (the critical speed of rotor is 8200 rpm). The settling time is highly influenced by the shaft speed (Table 4.5). The value of the steady-state deflection increases with the increase of shaft speed up to the speed of 2500 rpm and then the steady-state value decreases with the speed of shaft when the speed is above 3000 rpm (the steady-state value at 3000 and 2500 rpm is same. Table 4.5).

4.3 Integral Plus State Variable Feedback Controller

To improve the steady state response of the mid-span displacements of the rotor bearing system, the system state equations (2.13)[Chapter-2] are appended with two state variables x_9(t) and x_{10}(t) such that: $\dot{x}_9 = x_3$, and $\dot{x}_{10} = x_7$, where, x_3 and x_7 are the vertical and horizontal displacements of mid-span lumped mass, m_f.

$$\begin{bmatrix} \dot{x}_9 \\ \dot{x}_{10} \end{bmatrix} = \begin{bmatrix} 0 & 0 & 1 & 0 & 0 & 0 & 0 & 0 \\ 0 & 0 & 0 & 0 & 0 & 0 & 1 & 0 \end{bmatrix} \begin{bmatrix} x_1 \\ x_2 \\ x_3 \\ \vdots \\ x_8 \end{bmatrix} = \mathbf{CX} \tag{4.10}$$

or,

$$[\dot{z}] = \mathbf{CX} \tag{4.11}$$

We add to the system variables, 'the integral state', z(t) defined by,

$$z_1 = \int x_3 dt \ \ or \ \ x_9 = \int x_3 dt \tag{4.12}$$

$$z_2 = \int x_7 dt \ \ or \ \ x_{10} = \int x_7 dt \tag{4.13}$$

Now equation (4.9) can be rewritten by augmenting the original system(2.13) as follows:

$$\begin{bmatrix} \dot{X} \\ \dots \\ \dot{z} \end{bmatrix} = \begin{bmatrix} A & \vdots & 0 \\ \dots & \dots & \dots \\ C & \vdots & 0 \end{bmatrix} \begin{bmatrix} X \\ \dots \\ z \end{bmatrix} + \begin{bmatrix} B \\ \dots \\ 0 \end{bmatrix} u \tag{4.14}$$

$$\dot{\hat{\mathbf{X}}} = \mathbf{A}_a \hat{\mathbf{X}} + \mathbf{B}_a \mathbf{u} \tag{4.15}$$

Hence the new state vector is $\hat{\mathbf{X}} = \begin{bmatrix} X \\ \dots \\ z \end{bmatrix}$ and has a dimension of 10×1.

The doubt which arises is whether the new system (4.11) is controllable by the input **u**. However, if the original system defined by equation(2.13) is controllable this augmented system is also controllable [39].

The control law gives,

$$\mathbf{u} = -\mathbf{K}\hat{\mathbf{X}} \tag{4.16}$$

which minimizes the performance index

$$J = \frac{1}{2}\int_0^\infty (\hat{\mathbf{X}}^T \mathbf{Q}_a \hat{\mathbf{X}} + \mathbf{u}^T \mathbf{R} \mathbf{u}) dt \tag{4.17}$$

where, $\mathbf{Q}_a$ is a 10×10 matrix and it is given by,

$$\mathbf{Q}_a = \begin{bmatrix} Q & 0 & 0 \\ 0 & q_9 & 0 \\ 0 & 0 & q_{10} \end{bmatrix} \tag{4.18}$$

The control vector (4.11) may be written as follows:

$$\mathbf{u} = -\mathbf{K}_1\mathbf{X} - \mathbf{K}_2\mathbf{z} \tag{4.19}$$

This implies a proportional plus integral control action. If disturbance du is applied on the system the dynamic equation of an ISVFB is given by,

$$\dot{\hat{\mathbf{X}}} = (\mathbf{A}_a - \mathbf{B}_a K)\hat{\mathbf{X}} + \mathbf{B}_a.d\mathbf{u} = \mathbf{A}_c\hat{\mathbf{X}} + \mathbf{B}_a.d\mathbf{u} \tag{4.20}$$

The block diagram in Fig. 4.7 illustrates the elements of the overall feedback control system.

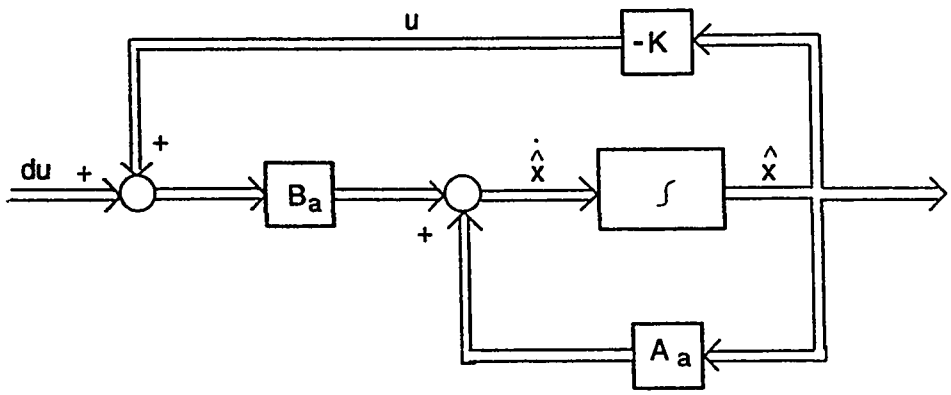

Figure 4.7: Block diagram representation of the system with an Integral plus state variable feedback controller.

4.3.1 Selection of Weighting factors

The weighting matrix for the state variables is,

$$\mathbf{Q}_a = \begin{bmatrix} Q & \vdots & 0 & 0 \\ \cdots & \cdots & \cdots & \cdots \\ 0 & \vdots & q_9 & 0 \\ 0 & \vdots & 0 & q_{10} \end{bmatrix} \tag{4.21}$$

where **Q** and **R** are the same as in the case of the SVFB controller, the weighting factors q_9 and q_{10} are augmented for improving the steady state performance of the mid-span deflection. The simulation has been performed by considering the following weighting factors:

- the first set of values of weighting factors are: $q_3 = q_7 = 10^6$, $q_1 = q_2 = q_4 = q_5 = q_6 = q_8 = q_9 = q_{10} = 1$; and $r_1 = r_3 = 10^{-10}$, $r_2 = r_4 = 10^{-8}$; and
- the second set of values of weighting factors are: $q_3 = q_7 = q_9 = q_{10} = 10^6$, $q_1 = q_2 = q_4 = q_5 = q_6 = q_8 = 1$; and $r_1 = r_3 = 10^{-10}$, $r_2 = r_4 = 10^{-8}$

The adopted augmented matrices ($\mathbf{A}_a$, $\mathbf{B}_a$, $\mathbf{Q}_a$) for an ISVFB controller and the final gain and regulator matrices (**K** and $\mathbf{A}_c$) are given in Appendix C.

4.3.2 Response of the System With an ISVFB Controller

At first the response of the mid-span deflection has been obtained by using the first set of weighting factors and applying a unit step disturbance at the mid-span in the vertical direction. Fig. 4.8 shows the graph obtained by plotting the value of the mid-span deflection for a shaft speed of 500 rpm. The steady-state deflection in this case is found to be $7.129(10^{-8})$m and settling time is 0.0322s. This result is obtained for a shaft speed of 500 rpm. In order to observe the effect of the shaft speed on the performance of the controller the simulation has been repeated for shaft speeds of 1500, 2500, 3000, 3500,4500, 10000 and 15000 rpm. The response curves are similar to those shown in Fig. 4.8; these are not included. However, the settling time(t_s), rise time(t_r), delay time(t_d) and steady-state deflection values have been obtained from these response curves and they are presented in Table 4.6.

For the second set of weighting factors the response curve of the mid-span vertical deflection is as shown in Fig. 4.9. The graph of Fig. 4.9 has been obtained at a shaft speed of 500 rpm. The response curves for shaft shaft speeds of 1500, 2500, 3000, 3500,4500, 10000 and 15000 rpm are similar to those in Fig. 4.9. The settling time (t_s), peak value (M_p) obtained from the response curves for these speeds have been presented in Table 4.7.

Shaft speed(N)	rise time(t_r)	delay time(t_d)	settling time(t_s)	steady-state
rpm	10^{-3}sec.	10^{-3}sec.	sec.	10^{-8}m
500	4.301	2.688	.0322	7.129
1500	4.301	2.688	.0103	7.581
2500	4.301	2.688	.0100	7.613
3000	4.301	2.688	.0124	7.613
3500	4.301	2.688	.00977	7.581
4500	4.301	2.688	.0120	7.548
10000	3.846	2.564	.0128	7.437
15000	3.846	2.564	.0103	7.437

Table 4.6: Performance characteristics, t_r, t_d, t_s and steady-state value of mid-span response of the rotor of the system with an ISVFB controller having the first set of weighting factors and disturbance is applied vertically at mid-span.

Shaft speed(N)	peak value(M_p)	time of peak value(t_p)	settling time(t_s)	steady-state
rpm	10^{-8}m	sec.	sec.	m
500	4.44	0.487	6.76	0
1500	4.74	0.487	6.76	0
2500	4.81	0.487	6.76	0
3000	4.72	0.487	6.76	0
3500	4.72	0.487	6.76	0
4500	4.7	0.487	6.76	0
10000	4.654	0.487	6.74	0
15000	4.654	0.487	6.74	0

Table 4.7: Performance characteristic values, M_p, t_p and t_s of mid-span response of the system with an ISVFB controller having the second set of weighting factors and disturbance is applied vertically at mid-span.

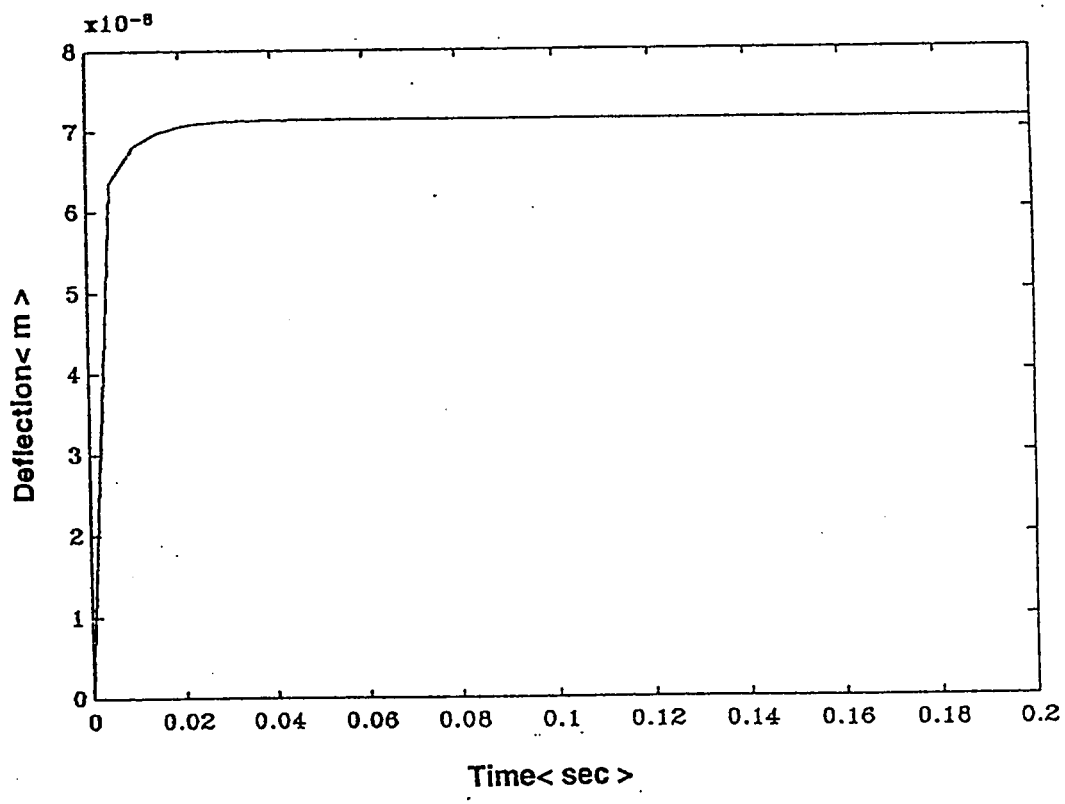

Figure 4.8: Response of the mid-span vertical deflection of the rotor of the system with an ISVFB controller with the first set of weighting factors when a unit step external disturbance is apllied vertically at mid-span (the response is at shaft speed of 500 rpm).

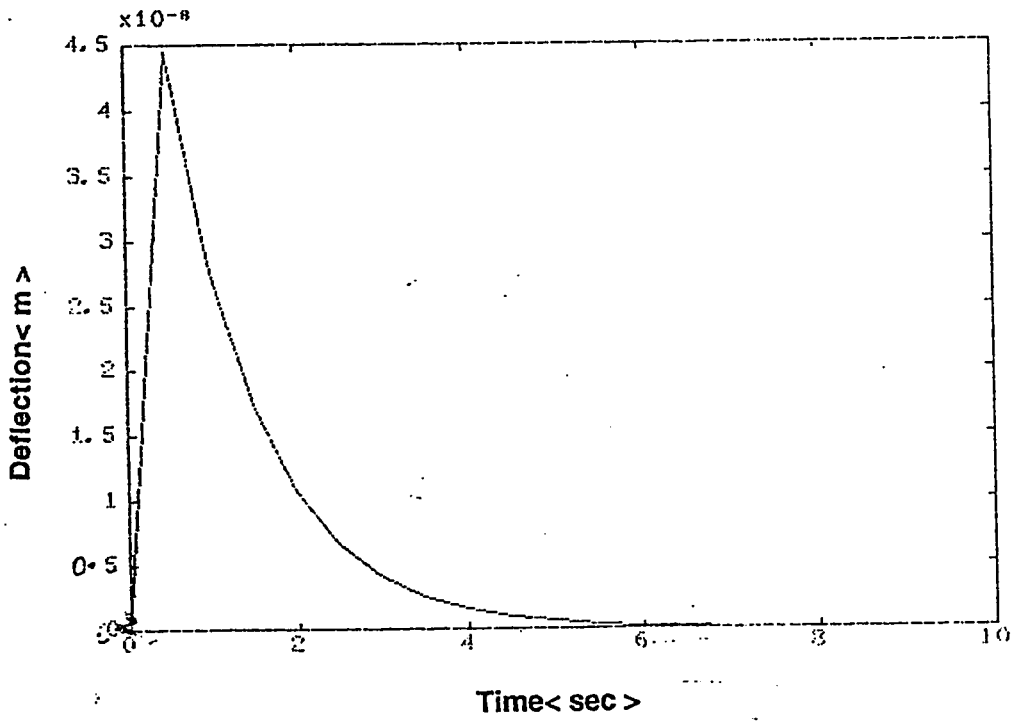

Figure 4.9: Response of the mid-span vertical deflection of rotor with an ISVFB controller with the second set of weighting factors whenma unit step external disturbance is applied vertically at mid-span (the response is at a shaft speed of 500 rpm).

4.3.3 Remarks on the Performance of the System With an ISVFB Controller

The response of an ISVFB controller with the first set of weighting factors is not very different from the response of an SVFB controller with the second set of weighting factors (see Tables 4.5 and 4.6). The variations of t_s, t_r, t_d and steady state-deflection with the shaft speed for the case of an ISVFB controller with the first set of weighting factors are similar in trend to that of an SVFB controller with the second set of weighting factors.

When an ISVFB controller with the second set of weighting factors is used the steady-state value of the mid-span deflection is zero (Fig. 4.9). From the response of the mid-span vertical deflection when an ISVFB controller with the second set of weighting factors is employed, it is observed that the system reaches the zero steady-state deflection just after 6s, and the peak value is $4.44(10^{-8})$m when the rotor speed is 500 rpm (Fig. 4.9). Table 4.7 shows that the settling time is 6.76s for a rotor speed of upto 4500 rpm, and the settling time reduces to 6.74s when the speed is 10000 rpm and above. The time required to reach the peak value is 0.487s for any speed. The peak value increases as the shaft speed increases from 500 to 2500 rpm, as the speed further increases the peak value decreases till the shaft speed is 3000 rpm, between 3000 and 4500 rpm peak value is almost constant. When the speed of the rotor is above the critical speed (critical speed of rotor is 8200 rpm)

the peak value decreases to $4.654(10^{-8})$m (Table 4.7). It can be concluded that an ISVFB controller can be used to achieve any steady-state deflection by adjusting the weighting factors q_9 and q_{10}.

4.4 Linear Quadratic Servo(LQS) Controller

An LQS controller introduces integral action by differentiation and augmentation of the original system matrices [28]. Consider the equation (4.11),

$$[\dot{z}] = \mathbf{CX}$$

or

$$\mathbf{y} = \mathbf{CX} \tag{4.22}$$

Derivative forms of equation (4.22) and the original system (see equation 2.13) can be written as,

$$\dot{\mathbf{y}} = \mathbf{C}\dot{\mathbf{X}} \tag{4.23}$$

$$\ddot{\mathbf{X}} = \mathbf{A}\dot{\mathbf{X}} + \mathbf{B}\dot{\mathbf{u}} \tag{4.24}$$

Augmentation of equation (4.23) and equation (4.24) gives the following form of the system:

$$\begin{bmatrix} \dot{\mathbf{y}} \\ \cdots \\ \ddot{\mathbf{X}} \end{bmatrix} = \begin{bmatrix} \mathbf{0} & \vdots & \mathbf{C} \\ \cdots & \cdots & \cdots \\ \mathbf{0} & \vdots & \mathbf{A} \end{bmatrix} \begin{bmatrix} \mathbf{y} \\ \cdots \\ \dot{\mathbf{X}} \end{bmatrix} + \begin{bmatrix} 0 \\ \cdots \\ \mathbf{B} \end{bmatrix} \dot{\mathbf{u}} \tag{4.25}$$

$$\dot{\hat{\mathbf{z}}} = \mathbf{A}_a\hat{\mathbf{z}} + \mathbf{B}_a\mathbf{v} \tag{4.26}$$

Where, $\hat{\mathbf{z}} = \begin{bmatrix} \mathbf{y} \\ \dots \\ \dot{\mathbf{X}} \end{bmatrix}$ and $\mathbf{v} = d\mathbf{u}/dt$, $\mathbf{A}_a$ and $\mathbf{B}_a$ are augmented system matrices.

The cost function for the LQS design now can be written as,

$$J = \frac{1}{2}\int_0^\infty (\hat{\mathbf{z}}^T\mathbf{Q}_a\hat{\mathbf{z}} + \mathbf{v}^T\mathbf{R}\mathbf{v})dt \tag{4.27}$$

where, the weighting of the output $\mathbf{y}$ is accounted for by it's presence in the $\mathbf{z}$ vector.

The associated algebraic riccati equation is,

$$\mathbf{P}\mathbf{A}_a + \mathbf{A}_a{}^T\mathbf{P} - \mathbf{P}(\mathbf{B}_a\mathbf{R}^{-1}\mathbf{B}_a{}^T)\mathbf{P} + \mathbf{Q}_a = 0 \tag{4.28}$$

Weighting matrix $\mathbf{Q}_a$ is a 10×10 matrix as follows:

$$\mathbf{Q}_a = \begin{bmatrix} q_9 & 0 & 0 & 0 & 0 & 0 & 0 & 0 \\ 0 & q_{10} & 0 & 0 & 0 & 0 & 0 & 0 \\ 0 & 0 & 0 & 0 & 0 & 0 & 0 & 0 \\ \vdots & \vdots & \vdots & \vdots & \vdots & \vdots & \vdots & \vdots \\ 0 & 0 & 0 & 0 & 0 & 0 & 0 & 0 \\ 0 & 0 & 0 & 0 & 0 & 0 & 0 & 0 \end{bmatrix} \tag{4.29}$$

The optimal gain matrix becomes:

$$\mathbf{K} = \mathbf{R}^{-1}\mathbf{B}_a{}^T\mathbf{P} \tag{4.30}$$

The control law can now be written as:

$$\mathbf{v} = \dot{\mathbf{u}} = -\mathbf{K}_1\mathbf{y} - \mathbf{K}_2(\mathbf{A}\mathbf{X} + \mathbf{B}\mathbf{u}) \tag{4.31}$$

where, $\mathbf{K}_1$ and $\mathbf{K}_2$ are appropriate matrices obtained by partitioning feedback gain matrix $\mathbf{K}$ i.e.,

$$\mathbf{K} = \left[\mathbf{K}_1 \ \vdots \ \mathbf{K}_2 \right] \tag{4.32}$$

If disturbance du is applied on the system then the dynamic equation of an LQS system is given by,

$$\dot{\hat{\mathbf{z}}} = (\mathbf{A}_a - \mathbf{B}_a\mathbf{K})\hat{\mathbf{z}} + \mathbf{B}_a.d\mathbf{u} = \mathbf{A}_c\hat{\mathbf{z}} + \mathbf{B}_a.d\mathbf{u} \tag{4.33}$$

The block diagram shown in Fig 4.10 illustrates the elements of the overall feedback control system.

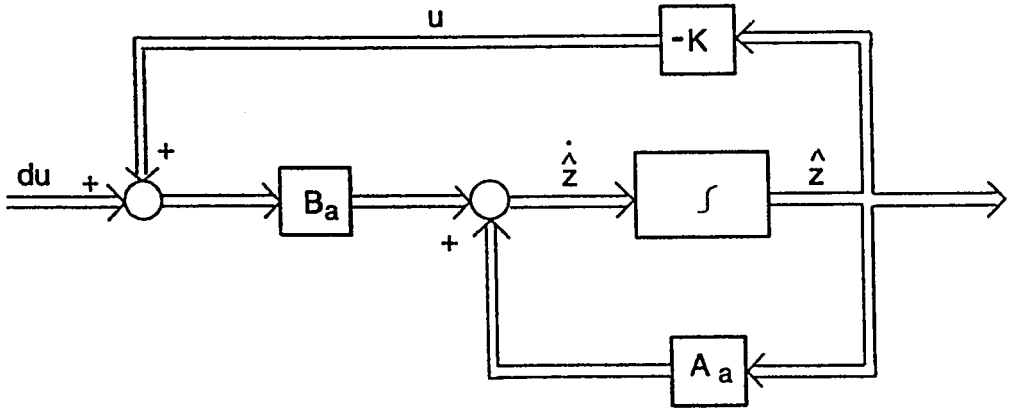

Figure 4.10: Block diagram representation of the system with an LQS controller [28].

4.4.1 Selection of Weighting Factors

In this approach one weights the errors directly therefore, weighting matrix $\mathbf{Q}_a$ is as follows:

$$\mathbf{Q}_a = \begin{bmatrix} q_9 & 0 & 0 & 0 & 0 & 0 & 0 & 0 \\ 0 & q_{10} & 0 & 0 & 0 & 0 & 0 & 0 \\ 0 & 0 & 0 & 0 & 0 & 0 & 0 & 0 \\ \vdots & \vdots & \vdots & \vdots & \vdots & \vdots & \vdots & \vdots \\ 0 & 0 & 0 & 0 & 0 & 0 & 0 & 0 \\ 0 & 0 & 0 & 0 & 0 & 0 & 0 & 0 \end{bmatrix}_{10\times 10}$$

The simulation has been performed by considering the following sets of weighting factors:

- the first set of values of weighting factors are : $q_9 = q_{10} = 1$; and $r_1 = r_3 = 10^{-10}$, $r_2 = r_4 = 10^{-8}$; and
- the second set of values of weighting factors are: $q_9 = q_{10} = 10^6$, and $r_1 = r_3 = 10^{-10}$, $r2 = r_4 = 10^{-8}$.

The augmented matrices $\mathbf{A}_a$, $\mathbf{B}_a$ and $\mathbf{Q}_a$ of the system, and the resultant gain matrix $\mathbf{K}$ and controller matrix $\mathbf{A}_c$ are given in Appendix C.

4.4.2 Response of the System With an LQS Controller

The performance of an LQS controller has been studied using the same disturbance as in the previous sections(4.1.2 and 4.2.1). The results obtained by employing an LQS controller are presented in Fig. 4.11 and 4.12. The response of the mid-span vertical deflection when an LQS controller with the first set of weighting factors is employed is shown in Fig. 4.11, which is for a rotor speed of 500 rpm. The responses obtained for rotor speeds of 1500, 2500, 3000, 3500,4500, 10000 and 15000 rpm are similar to the one shown in Fig. 4.11; they are not included. The values of (M_p), (t_p), (t_s) and steady deflection obtained from the response curves of the corresponding different rotor speeds are presented in Table 4.8.

Fig. 4.12 displays a graph between the vertical mid-span deflection and time when an LQS controller with the second set of weighting factors has been employed in the system. This result has been obtained at a shaft speed of 500 rpm. With the second set of weighting factors the simulation has been repeated for shaft speeds of 1500, 2500, 3000, 3500, 4500, 10000 and 15000 rpm. The values of (M_p), (t_p), (t_s) and steady-state deflection are obtained from these response curves; they have been presented in Table 4.9.

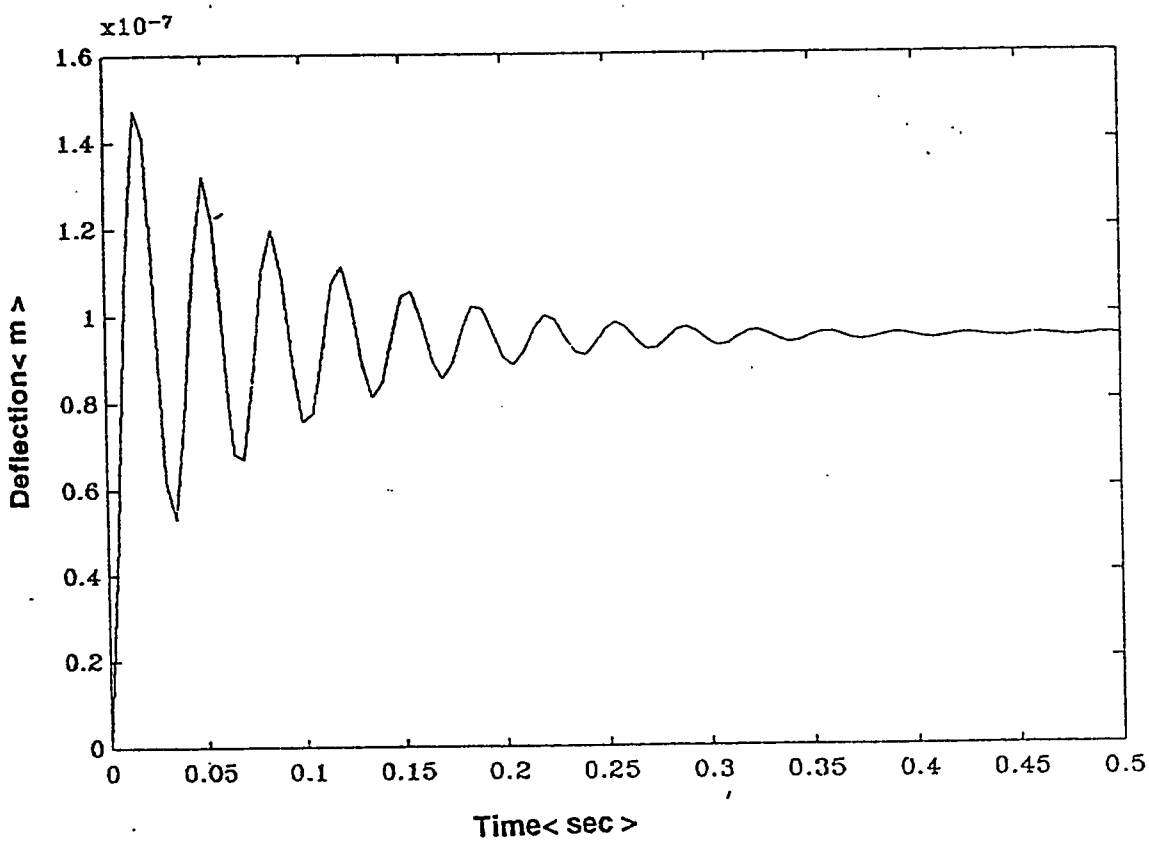

Figure 4.11: Response of mid-span deflection of the rotor with an LQS controller having the first set of weighting factors, when subjected to a unit step external disturbance is applied vertically at mid-span (the response is at a shaft speed of 500 rpm).

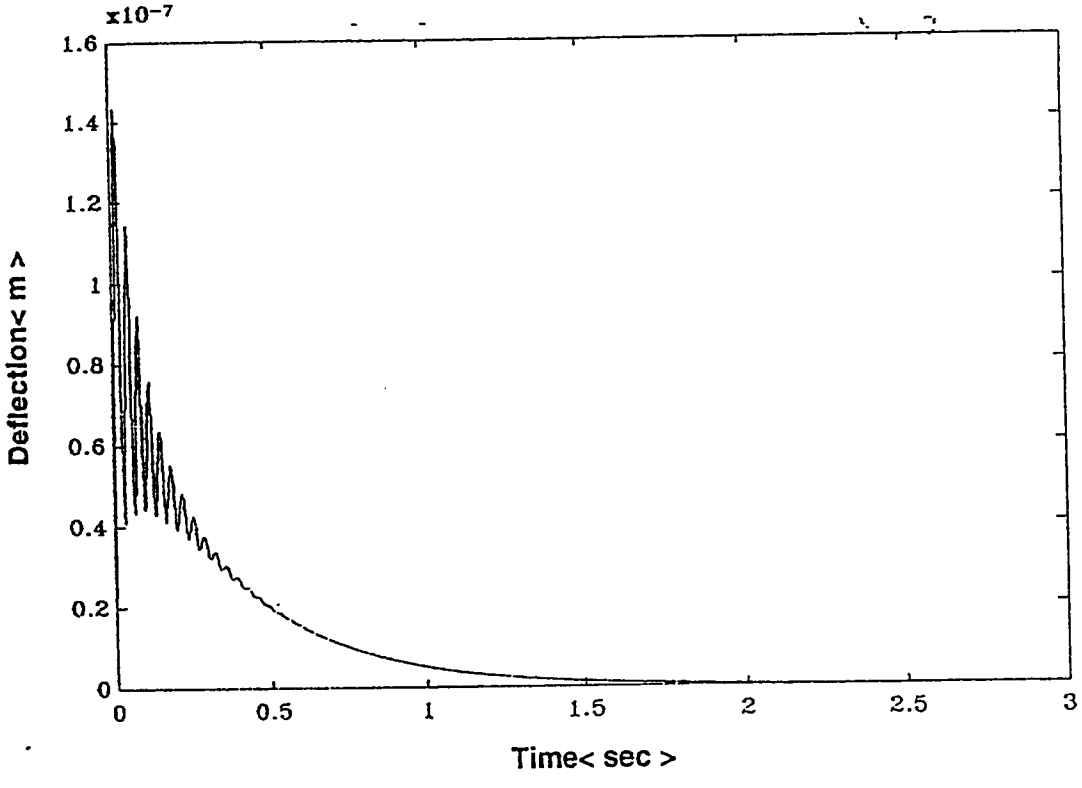

Figure 4.12: Response of mid-span deflection of the rotor with an LQS controller having the second set of weighting factors, when subjected to a unit step external disturbance is applied vertically at mid-span (the response is at a shaft speed of 500 rpm).

Speed(N)	peak value(M_p)	time of peak value(t_p)	settling time(t_s)	steady-state
rpm	10^{-7}m	sec.	sec.	10^{-8}m
500	1.4867	.0162	.483	8.84
1500	1.348	.0149	.1878	9.49
2500	1.268	.0149	.1189	9.49
3000	1.257	.0149	.1122	9.49
3500	1.257	.0149	.1081	9.49
4500	1.284	.0149	.1486	9.49
10000	1.242	.00921	.3868	9.58
15000	1.392	.0103	.2718	9.714

Table 4.8: Performance characteristic values, M_p, t_p, t_s and steady-state value of mid-span response of the system with an LQS controller having the the first set of weighting factors and disturbance is applied vertically at mid-span.

Speed(N)	peak val.(M_p)	time of peak value(t_p)	settling time(t_s)	steady-state
rpm	10^{-7}m	10^{-3}sec.	sec.	m
500	1.437	15	2.0	0
1500	1.289	15	2.032	0
2500	1.206	15	2.032	0
3000	1.193	15	2.081	0
3500	1.195	15	2.081	0
4500	1.202	15	2.032	0
10000	1.193	8.947	2.0635	0
15000	1.335	10.256	2.338	0

Table 4.9: Performance characteristic values, M_p, t_p, t_s and steady-state value of mid-span response of the system with an LQS controller having the second set of weighting factors and disturbance is applied vertically at mid-span.

4.4.3 Remarks on the Performance of the System With an LQS Controller

Comparison of Figures 4.2 and 4.11 reveals that the system incorporating an LQS controller with the first set of weighting factors responds in the same way as the system without a controller for the rotor speed upto 4500 rpm. Thus the controller does not serve the purpose very well when the first set of weighting factors are employed as long as the system is stable. But above the critical speed when the systems becomes unstable the LQS controller with the first set of weighting factors makes the system stable and damps out the vibration due to the disturbance (Table 4.8). When the second set of weighting factors are used an improvement in the performance of the controller has been achieved (Fig. 4.12). The graph of Fig. 4.12 shows initial oscillations of the system before reaching a steady-state deflection of zero. From Figures 4.9 and 4.12 one observes that the system with an LQS controller reaches the steady state value in 2s and with an ISVFB controller it reaches the steady state in 6s. It means that an LQS controller responds faster than an ISVFB controller in controlling the vibration of the system. The results obtained by employing the second set of weighting factors show that there is always some initial oscillation of the mid-span vertical deflection before it reaches the steady-state value of zero. However, duration of oscillations decreases as the shaft speed increases. The results also reveal that the peak value decreases as the shaft speed increases from

500 to 3000 rpm; when the speed is above 3000 rpm the peak value increases with the increase of speed (Table 4.9). At 10000 rpm the peak value again decreases to $1.193(10^{-7})$m and at 15000 rpm it increases to $1.335(10^{-7})$m. On the other hand settling time increases from 2.0s to 2.032s when speed of the rotor is increased from 500 to 1500 rpm it is 2.032s at a speed of 2500 rpm. When the speed is increased above the critical speed of the rotor the value of t_s again increases with the increase of the speed. The value of t_p remains constant ($15(10^{-3})$s) when the speed of the rotor is below the critical speed (critical speed of the rotor is 8200 rpm), and above the critical speed the value of t_p increases with the increase of the speed (Table 4.9).

4.5 Relative Suitability of different Controllers

Digital simulations have been carried out to study the performance of SVFB, ISVFB and LQS controllers. It is revealed from the results that the behavior of system can be controlled by properly selecting the elements of the weighting matrices Q and R. The disturbance rejection qualities offered by an ISVFB controller with the first set of weighting factors is not very different from those offered by an SVFB controller with the second set of weighting factors (see Fig. 4.6 and Fig. 4.8). However, when the second set of weighting factors are used an improvement in the performance of an ISVFB controller is observed in that the integral action of the controller assures a final value of the mid-span vertical deflection of zero. When an LQS controller is

used with the first set of weighting factors the system behaves in the same way as the original system without a controller when the rotor runs below the critical speed. Both the LQS and the ISVFB controllers with their second set of weighting factors ensure a steady-state deflection of zero for the horizontal and vertical directions. The favorable feature of an LQS controller is that it responds faster than an ISVFB controller. On the other hand the advantage of an ISVFB controller over an LQS controller is that it brings the system to a steady state deflection of zero without any oscillation in the system. For any shaft speed a higher peak value is observed in the case of an LQS controller than that in the case of an ISVFB controller.

It can be concluded that for a system that requires a quick control action in controlling the vibration due to any disturbance, the LQS controller is preferable, while for a system that requires a non-oscillatory response of the system to a disturbance an SVFB or an ISVFB controller is preferred. For a system that can tolerate a low level steady state deflection an SVFB controller is suitable. For a system that requires a zero steady state deflection and oscillation free control action against a disturbance, an ISVFB controller, is preferable.

4.6 Implementation of the Controllers

In order to obtain the data for the different states, the simplest way is to use accelerometers, with the velocity and displacement signals being obtained by integrating the acceleration signals. For the rotating components, as in this case, accelerometers with additional equipment (e.g., a telemetry system) can be used to extract the signals. The non-contacting transducers can also be used, these devices would give the displacements of the mass, then differentiating the signals velocity of the mass can be obtained.

In order to apply the required input force to the rotor, to suppress the vibration, a contactless force generator can be used. The electromagnetic dampers (EDM) [6], electroviscous dampers (EVD) [48], active magnetic bearings (AMB) [49] and piezoelectric actuator [50] are the devices that can be used to control the vibration of the rotor.

If the practical measurement of any of the states is not possible due to the inaccessibility of that point, then the unmeasurable state can be predicted , if the system is observable. It is shown in Appendix A that the system considered in this study is observable. Similarly if an input force can not be applied to an inaccessible point of the rotor, the vibration of that point can be controlled by applying control force on some other accessible point, if the system is completely controllable having the input applied on the accessible point.

Chapter 5

Response Characteristics of Model II

The rotor-bearing system is asumed to comprise of three lumped masses, namely, the mid-span mass (m_f), the journal mass(m_b) and the bearing housing mass (m_e). The rotor system is symmetrically supported on two plain-oil film journal bearings and the bearing housing is mounted on flexible supports. The model is shown in Fig. 2.2 (Chapter 2) and its mathematical description is given in Chapter 2. The attention, in this chapter, is focused on studying the effects of three different control (SVFB, ISVFB and LQS) systems on the overall performance of the model. The description of these control systems has been given in the Chapter 4. The behavior of the system in the presence of an external disturbance when no control system is employed is given in Section 5.1. The performance of a state variable feedback (SVFB) control

system when an external disturbance is applied is discussed in Section 5.2, the performance parameters of ISVFB and LQS control systems are included in Sections 5.3 and Section 5.4 respectively. The effects of stiffness of the flexible supports on the performance of the system with and without a controller have been presented in Section 5.5.

5.1 System Without a Controller

The dynamic equations of the system represented by model II have been obtained in Chapter 4. The coefficient matrices A and B have been calculated by using the parameter values given in the following section. The resultant A and B matrices used in the simulation of the system are presented in Appendix C.

5.1.1 Parameter values for simulation

The dynamic equations of the rotor-bearing system (model-II) in state-variable form have been presented by using matrix-notation(see equation 2.32). In the computation of coefficient matrices the following parameters for the rotor-bearing system have been used :

$m_b = 0.2$ kg, $m_f = 12.33$kg, $m_e = 0.85$ kg;

radial clearance of the bearing = C = 0.051 mm;

diameter of the journal = D = 51 mm, the land length = L = 12 mm;

stiffness of the shaft $K_f = 142 \times 10^7$ N/m, stiffness of each support $k_e = 0.01k_f$ [19]; and

the values of bearing stiffness and damping coefficients are presented in Chapter 4 (Section 4.1.2)

5.1.2 Response of the System Without a controller

In order to study the performance of model II of the rotor bearing system (see Fig. 2.2 and Fig. 2.4) a unit step-disturbance is applied on the model. The response of the mid-span vertical and horizontal deflections (i.e., the variation of the displacement of the mid-span lumped mass, m_f with time) is shown in Figures 5.1 and 5.2 when an external disturbance is applied vertically at the bearing housing and mid-span respectively. These responses have been obtained for a shaft speed of 500 rpm. The peak values of horizontal and vertical deflections are 10^{-6} m and $11(10^{-6})$m when the disturbance is applied at the mid-span (Figs. 5.1 and 5.2) for both the cases. Steady-state values and settling times are almost the same for both the cases. The graphs further reveal that the system is stable at a shaft speed of 500 rpm. Simulations have been performed for shaft speeds of 1500, 2500, 3000, 3500, 4500, 10,000 and 15,000 rpm; the results show that the system is unstable. The eigenvalues of the coefficient matrix 'A' at different shaft is presented in in the Table 5.1.

500 rpm	1500 rpm	4500 rpm
-3.8047(10^6)	-1.2680(10^6)	-4.2209(10^5)
-2.8136(10^5)	-9.2979(10^4)	-2.8368(10^4)
-100.82 + 3844.6i	-304.66 + 3823.9i	-983.72 + 3592.4i
-100.82 - 3844.6i	-304.66 - 3823.9i	-983.72 - 3592.4i
-7.4553 + 3847i	-22.326 + 3846.1i	-65.910 + 3838.0i
-7.4553 - 3847i	-22.326 - 3846.1i	-65.910 - 3838.0i
-78.188 + 64.094i	-237.41 + 192.52i	-746.92 + 648.14i
-78.188 - 64.094i	-237.41 - 192.52i	-746.92 - 648.14i
-0.51715 + 101.68i	0.058095 + 101.71i	0.053008 + 101.85i
-0.51715 - 101.68i	0.058095 - 101.71i	0.053008 - 101.85i
-0.075392 + 102.54i	-0.088421 + 102.46i	-0.047090 + 102.40i
-0.075392 - 102.54i	-0.088421 - 102.46i	-0.047090 - 102.40i

10000 rpm	15000 rpm
-1.8875(10^5)	-1.2457(10^5)
-5674.2 + 5605i	-3833.1 + 8242.7i
-5674.2 - 5605i	-3833.1 - 8242.7i
-136.66 + 3805.0i	-3.219(10^3)
-136.66 - 3805.0i	-185.02 + 3761.1i
-2.8865(10^3)	-185.02 - 3761.1i
-531.83 + 2116.7i	-197.12 + 2248.3i
-531.83 - 2116.7i	-197.12 - 2248.3i
0.026388 + 101.87i	0.017859 + 101.87i
0.026388 - 101.87i	0.017859 - 101.87i
-0.026388 + 102.39i	-0.015503 + 102.39i
-0.026388 - 102.39i	-0.015503 - 102.39i

Table 5.1: Eigenvalues of coefficient matrix 'A' at different shaft speeds.

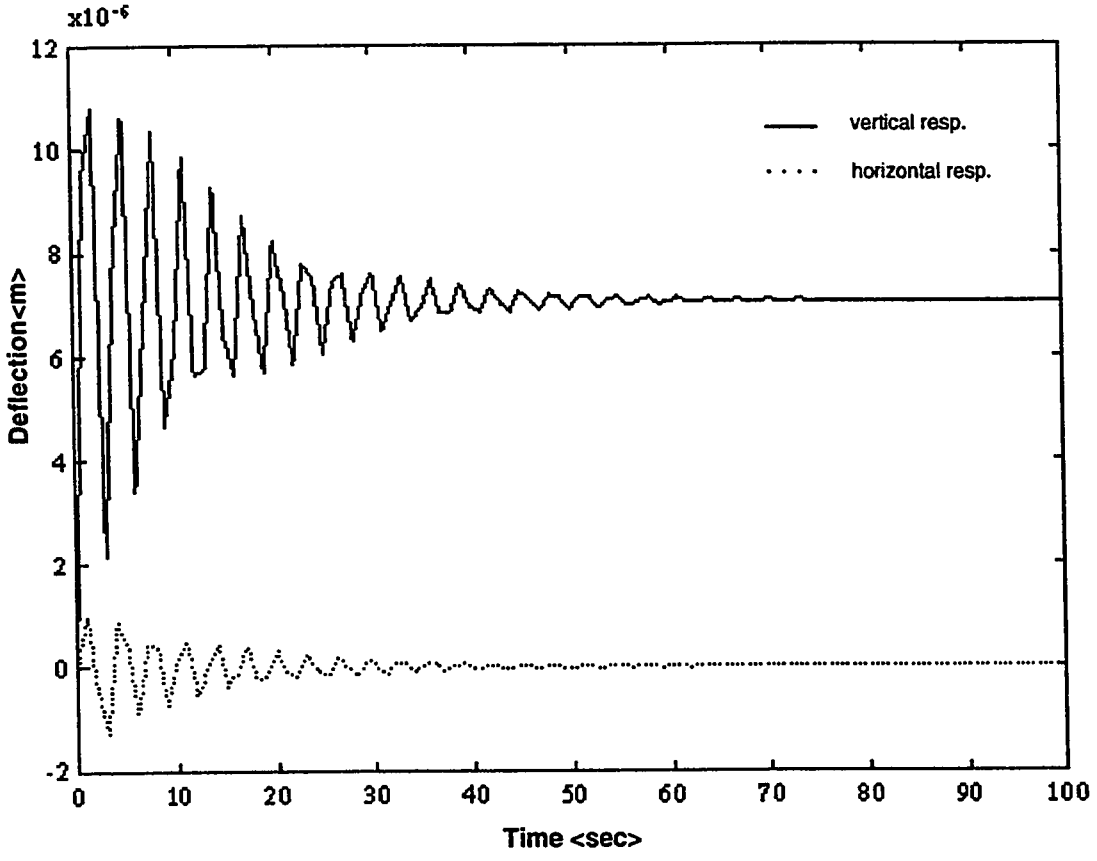

Figure 5.1: Response of the mid-span deflection at a shaft speed of 500 rpm when an external unit-step disturbance is applied at the bearing housing in the vertical direction(no controller is employed in the system).

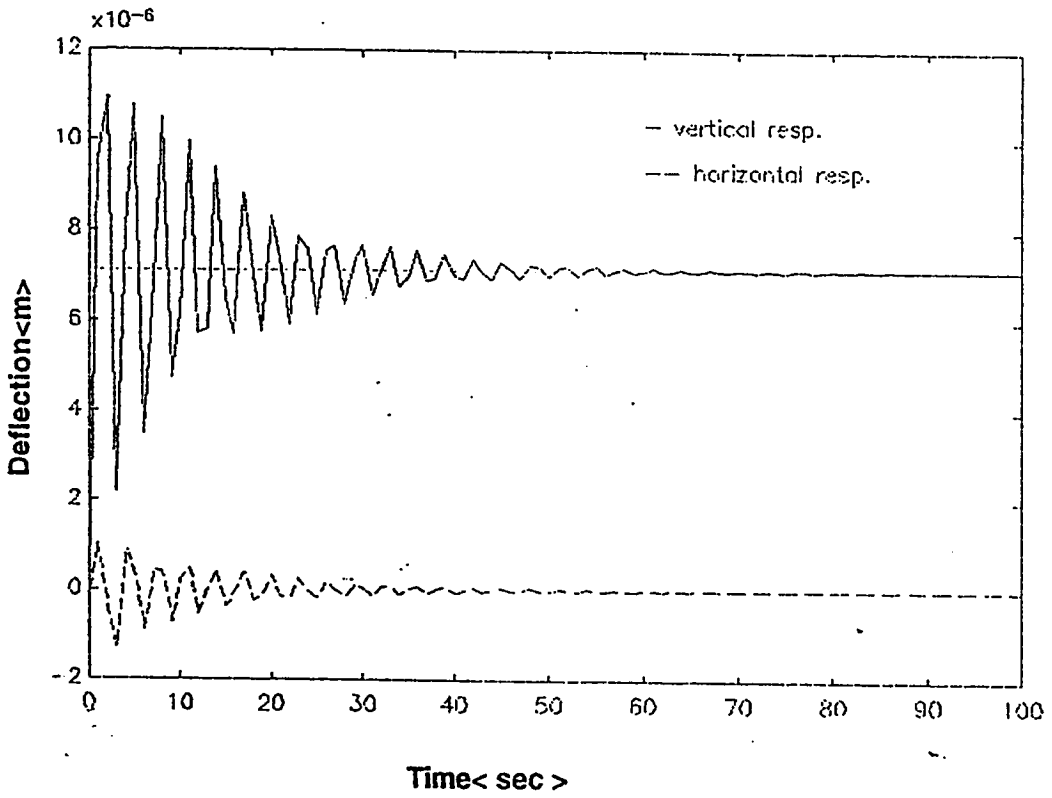

Figure 5.2: Response of the mid-span deflection at a shaft speed of 500 rpm when an external unit-step disturbance is applied at the mid-span in the vertical direction(no controller is employed in the system).

5.1.3 Remarks on the Performance of the System Without a Controller

The system is observed stable at a shaft speed of 500 rpm. At a shaft speed higher than or equal to 1500 rpm the system is unstable. Table 5.1 shows that all the eigenvalues are negative at a shaft speed of 500 rpm, it indicates that the system is stable. For the shaft speeds 1500, 2500, 3000, 3500, 4500, 10,000 and 15,000 rpm, two eigenvalues are positive for each speed, so at these shaft speeds the system is unstable. The eigenvalues shown in the Table 5.1 are obtained when the cross-coupling stiffness and damping coefficients (K_{xy}, K_{yx}, C_{xy}, C_{yx}) of oil-film are taken into consideration. When the eigenvalues of the matrix 'A' are simulated considering the cross-coupling terms as negligible (i.e., $K_{xy} = K_{yx} = C_{xy} = C_{yx} = 0$), then the eigenvalues obtained are all positive for any shaft speed. The simulation results also show that the system is stable for any shaft speed when the cross-coupling terms are considred negligible, these results are not shown here. The influence of the cross-coupling term in the stability of the system is awared, therefore, it is not suitable to neglect the cross-coupling terms in the study of the vibration of rotor-bearing system.

5.2 System With an SVFB Controller

The equation of the system, with the state variable feedback (SVFB) controller, in closed-loop form is given by

$$\dot{\mathbf{X}} = (\mathbf{A} - \mathbf{BK})\mathbf{X} \tag{5.1}$$

To determine a suitable gain matrix $\mathbf{K}$ we have to select suitable weighting matrices $\mathbf{Q}$ and $\mathbf{R}$ and then get the gain matrix by using the following equations:

$$\mathbf{PA} + \mathbf{A}^T\mathbf{P} - \mathbf{PBR}^{-1}\mathbf{B}^T\mathbf{P} + \mathbf{Q} = 0 \tag{5.2}$$

$$\mathbf{K} = \mathbf{R}^{-1}\mathbf{B}^T\mathbf{P} \tag{5.3}$$

The derivational details of equation 5.1 to 5.3 are presented in Appendix B. The block diagram of the controller is as shown in Fig. 4.4 (Chapter 4).

5.2.1 Selection of Weighting Factors

The simplest form of the weighting matrix $\mathbf{Q}$ one can use is a diagonal matrix :

$$\mathbf{Q} = \begin{bmatrix} q_1 & 0 & 0 & \cdots & \cdots & 0 & 0 \\ 0 & q_2 & 0 & \cdots & \cdots & 0 & 0 \\ \vdots & \vdots & \vdots & \vdots & \vdots & \vdots & \vdots \\ \vdots & \vdots & \vdots & \vdots & \vdots & \vdots & \vdots \\ 0 & 0 & 0 & \cdots & \cdots & q_{11} & 0 \\ 0 & 0 & 0 & \cdots & \cdots & 0 & q_{12} \end{bmatrix} \tag{5.4}$$

Where q_1, q_2,$\cdots$, q_{12} represent the weight factors, the designer places on the state variables x_1,x_2,$\cdots$,x_{12}. In the study of the performance of different controllers, the responses of vertical and horizontal deflection of mid-span are considered. The state variables x_5 and x_{11} represent the vertical and horizontal deflection of the mid-span respectively(see Section 2.2.1); therefore, considerable weightage would be given to q_5 and q_{11} relative to other values of q. Similarly the simplest form of the weighing matrix **R** that can be used is a diagonal matrix.

$$\mathbf{R} = \begin{bmatrix} r_1 & 0 & 0 & 0 & 0 & 0 \\ 0 & r_2 & 0 & 0 & 0 & 0 \\ \vdots & \vdots & \vdots & \vdots & \vdots & \vdots \\ 0 & 0 & 0 & 0 & 0 & r_6 \end{bmatrix} \tag{5.5}$$

Where, r_1,r_2,r_3,$\cdots$,r_6 represent the amount of weight to be given to control inputs. The response of the mid-span deflection are considered for comparative study, the inputs u_3 and u_6 corresponding to the mid-span would be given more weightage than the other inputs. Finally the weighting factors r_3 and r_6 corresponding to u_3 and u_6 would be given higher values than the other values of 'r'. After conducting several trial simulations, the following sets of weighting factors are selected:

- the first set of weighting factors are: $q_1=q_2=q_3=\cdots\cdots=q_{12}=1$ and $r_3=r_6=10^{-8}$, $r_1=r_2=\cdots\cdots=10^{-10}$; and

- the second set of weighting factors are $q_5=q_{11}=10^6$, $q_1=q_2=q_3=\cdots\cdots=q_{12}=1$ and $r_3=r_6=10^{-8}$, $r_1=r_2=\cdots\cdots=10^{-10}$.

The final gain matrix K and control matrix $\mathbf{A_c}$ are presented in Appendix C.

5.2.2 Response of the System With an SVFB Controller

The results of the simulation presented in Fig.5.3 and Fig. 5.4 have been obtained for the first set of weighting factors. Fig 5.3 shows the response of the vertical deflection of the the mid-span for a shaft speed of 500 rpm. Generally the graphs are obtained for a time step of 0.05 sec., the time steps are changed to smaller or greater value (0.005sec, or 0.5sec) where it is required to get clear and informative curves. Fig 5.3(a) represents the response of the mid-span deflection when the disturbance is applied vertically at the bearing housing and Fig 5.3(b) represents the response of same deflection of the mid-span when the disturbance is applied at the mid-span in the vertical direction. The simulation has been repeated for shaft speeds of 1500, 2500, 3000, 3500,4500, 10000 and 15000 rpm. Fig 5.4(a) and Fig 5.4(b) represent the response of the mid-span deflection for a shaft speed of 4500 rpm considering disturbances at the bearing housing and at the mid-span respectively. The response characteristics for other shaft speeds are similar to those in Fig. 5.4. The value of

rise time (t_r) and delay time (t_d), settling time (t_s) and steady-state value obtained from the response urves for the above mentioned shaft speeds are presented in Tables 5.2 and 5.3.

Figs 5.5 and 5.6 show the response of the mid-span deflection with the second set of weighting factors. The time step is 0.05s. Fig 5.5(a) and 5.5(b) show the graphs of the vertical deflection of the mid-span at a shaft speed of 500 rpm when the disturbances are applied at the bearing-housing and the mid-span respectively. Fig 5.6(a) and 5.6 (b) represents the response of the mid-span at a shaft speed of 4500 rpm.

When the simulation is performed at shaft speeds of 1500, 2500, 3000,3500, 10000 and 15000 rpm results are similar in nature to those in Figures 5.5 and 5.6 are obtained. The values of t_r, t_d, t_s and steady-state values obtained from the response curves are presented in Tables 5.4 and 5.5.

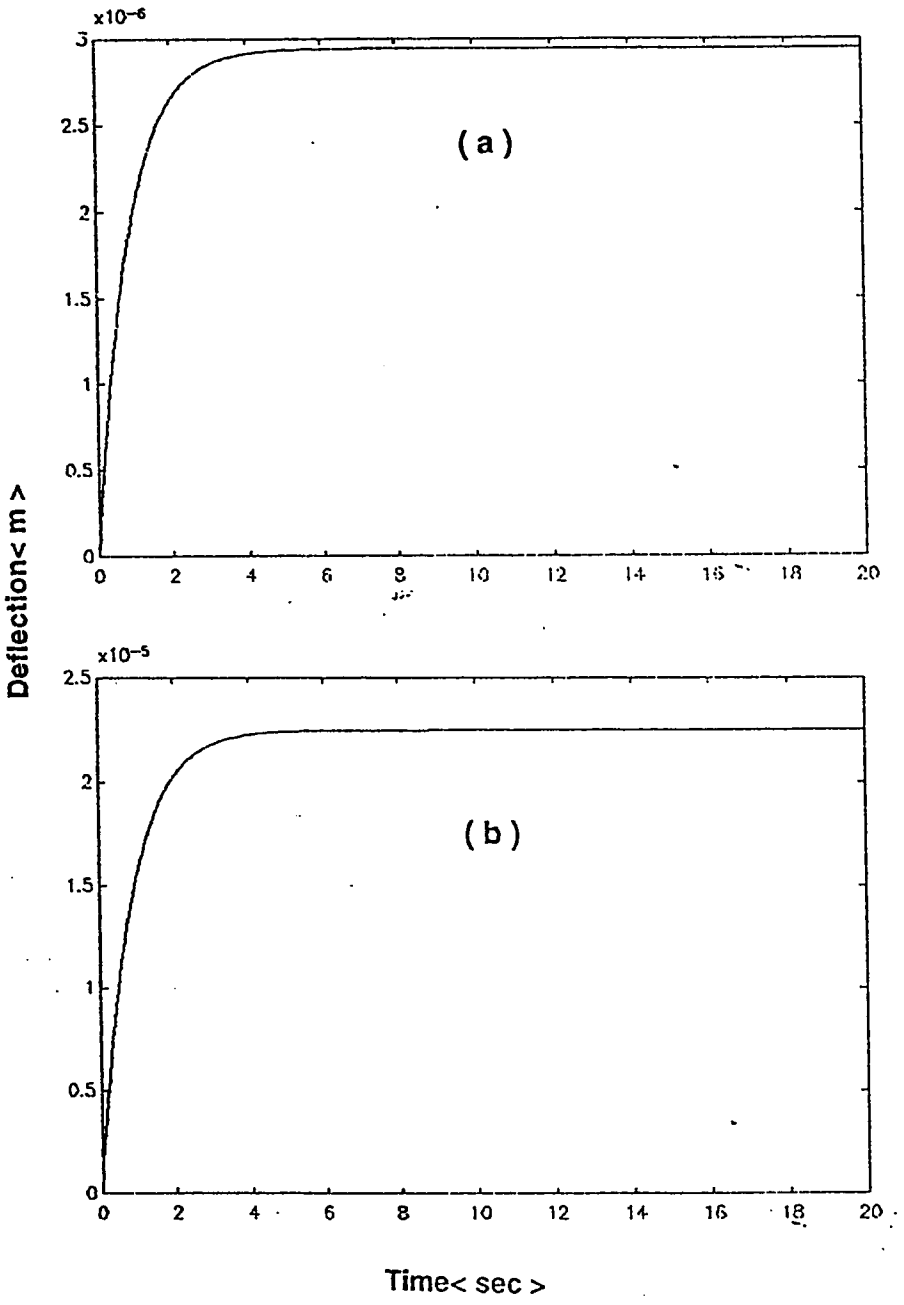

Figure 5.3: Response of the mid-span deflection at a shaft speed of 500 rpm when an external unit-step disturbance is applied in vertical direction at (a) bearing housing, (b) mid-span (when an SVFB controller with the first set of weighting factors is employed in the system).

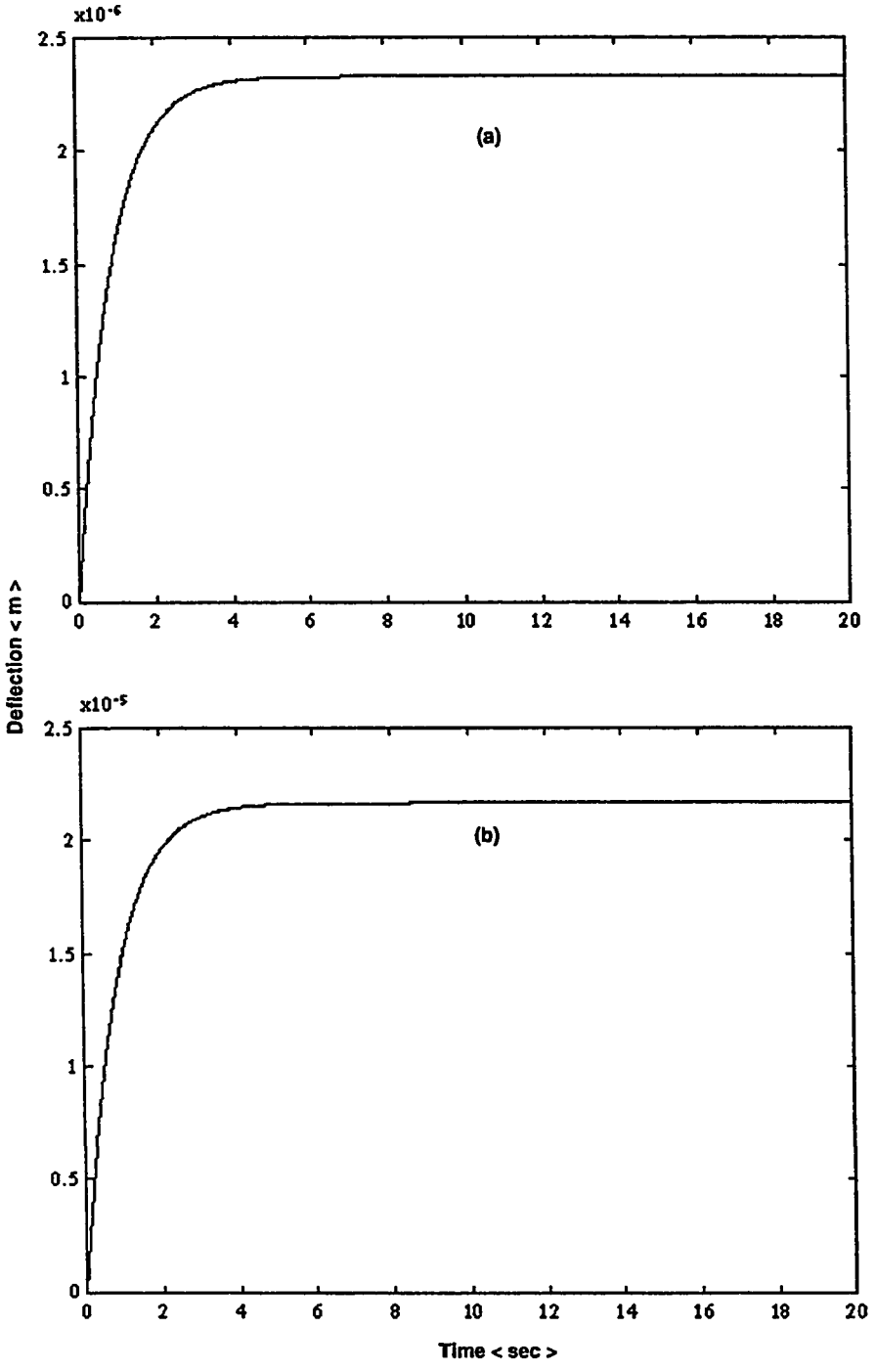

Figure 5.4: Response of the mid-span deflection at a shaft speed of 4500 rpm when an external unit-step disturbance is applied in the vertical direction at: (a) bearing housing, (b) mid-span (when an SVFB controller with the first set of weighting factors is employed in the system).

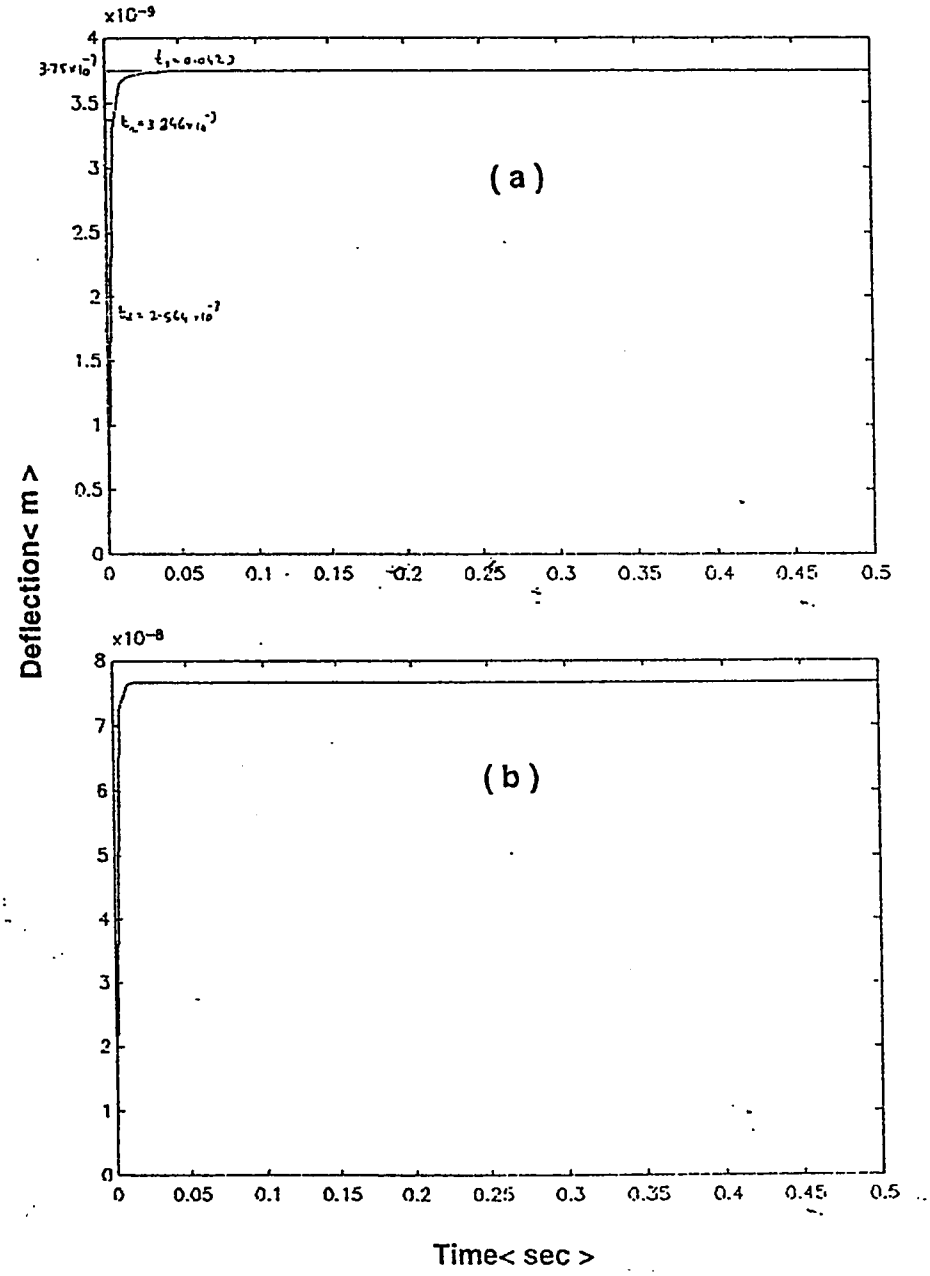

Figure 5.5: Response of the mid-span deflection at a shaft speed of 500 rpm when an external unit-step disturbance is applied in the vertical direction at: (a) bearing housing, (b) mid-span (when an SVFB controller with the second set of weighting factors is employed is the system).

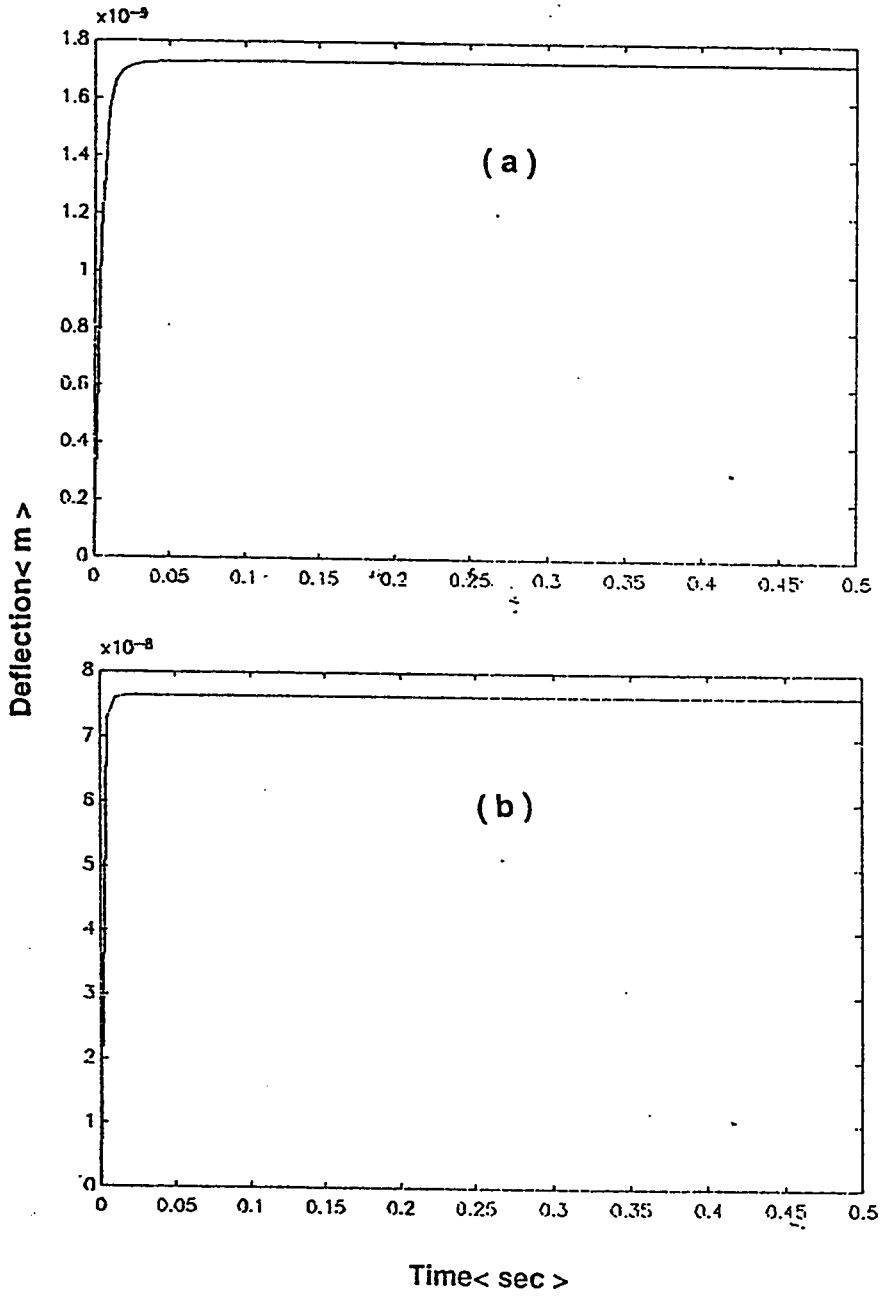

Figure 5.6: Response of the mid-span deflection at a shaft speed of 4500 rpm when an external unit-step disturbance is applied in the vertical direction at: (a) bearing housing, (b) mid-span (when an SVFB controller with the second set of weighting factors is employed in the system).

Shaft speed(N)	rise time(t_r)	delay time(t_d)	settling time(t_s)	steady-state
rpm	sec.	sec.	sec.	10^{-6}m
500	1.8974	0.6154	7.1795	2.942
1500	1.8974	0.6154	6.2564	2.698
2500	1.8974	0.6154	5.487	2.524
3000	1.8974	0.6154	5.9487	2.442
3500	1.8974	0.6154	6.256	2.394
4500	1.8974	0.6154	6.564	2.317
10000	1.8947	0.579	5.158	2.306
15000	1.8947	0.579	6.474	2.34

Table 5.2: Performance characteristics, t_r, t_d, t_s and steady-stale value of mid-span response of the system with an SVFB controller having the first set of weighting factors and disturbance is applied vertically at bearing housing.

Shaft speed(N)	rise time(t_r)	delay time(t_d)	settling time(t_s)	steady-state
rpm	sec.	sec.	sec.	10^{-5}m
500	1.8974	0.6154	8.8178	2.25
1500	1.8974	0.6154	5.9487	2.231
2500	1.8974	0.6154	5.9487	2.202
3000	1.8974	0.6154	5.7436	2.192
3500	1.8974	0.6154	5.7436	2.183
4500	1.8974	0.6154	6.154	2.183
10000	1.8947	0.579	6.579	2.142
15000	1.8947	0.579	5.8947	2.142

Table 5.3: Performance characteristics, t_r, t_d, t_s and steady-state value of mid-span response of the system with an SVFB controller having the first set of weighting factors and disturbance is applied vertically at mid-span.

Shaft speed(N)	rise time(t_r)	delay time(t_d)	settling time(t_s)	steady-state
rpm	10^{-3}sec.	10^{-3}sec.	sec.	10^{-9}m
500	3.864	2.564	.0423	3.75
1500	7.692	2.564	.0385	2.895
2500	7.692	2.564	.05	2.327
3000	7.692	2.564	.05	2.125
3500	7.692	3.846	.0385	1.962
4500	8.974	3.846	.0718	1.7285
10000	9.211	3.947	0.0474	1.4
15000	9.211	3.947	0.0579	1.433

Table 5.4: Performance characteristics, t_r, t_d, t_s and steady-state value of mid-span response of the system with an SVFB controller having the second set of weighting factors and disturbance is applied vertically at bearing housing.

Shaft speed(N)	rise time(t_r)	delay time(t_d)	settling time(t_s)	steady-state
rpm	10^{-3}sec.	10^{-3}sec.	sec.	10^{-8}m
500	3.846	2.564	.0128	7.625
1500	3.846	2.564	.0128	7.625
2500	3.846	2.564	.0128	7.625
3000	3.846	2.564	.0128	7.625
3500	3.846	2.564	.0128	7.625
4500	3.846	2.564	.0167	7.625
10000	3.947	2.632	0.0361	7.581
15000	3.947	2.632	0.0184	7.588

Table 5.5: Performance characteristics, t_r, t_d, t_s and steady-state value of mid-span response of the system with an SVFB controller having the second set of weighting factors and disturbance is applied vertically at mid-span.

5.2.3 Remarks on the Performance of the System With an SVFB Controller

The mid-span deflection of the system with a state variable feedback controller shows a better damped response than that of the system without a controller (Fig. 5.3 to 5.6). For an SVFB controller with the first set of weighting factors the steady-state values are $2.942(10^{-6})$m and $2.25(10^{-5})$; when the second set of weighting factors are used the steady state values reduce to $3.75(10^{-9})$m and $7.625(10^{-8})$m; all these values are for a shaft speed of 500 rpm (see Figures 5.3(a-b) and 5.5(a-b)).

Tables 5.2 and 5.3 show that the rise time is 1.8947s when the SVFB controller with the first set of weighting factors is employed. The simulation results give the same rise time for all shaft speed whether the disturbance is applied at bearing housing or mid-span. The steady-state value of the mid-span deflection decreases as the speed of the shaft speed is increased from 500 to 4500 rpm. The steady-state deflection value does not change when the speed is increased from 10000 to 15000 rpm. The delay time is 0.6154s for a shaft speed of up to 4500 rpm and 0.579s at or above the shaft speed 10000 rpm (Tables 5.2 and 5.3).

Tables 5.4 and 5.5 show that the SVFB controller with the second set of weighting factors, responds quite faster than the controller with the first set of weighting factors, in controlling the vibration of the system. The steady-state deflection value decreases with the increase of shaft speed (up to the speed of 10000 rpm, the value

increases from $1.4(10^{-9})$m to $1.4333(10^{-9})$m when the speed increases from 10000 to 150000 rpm) when the disturbance is applied at bearing housing (see Table 5.4). The steady-state value remains $7.625(10^{-8})$ up to the shaft speed of 4500 rpm, when the disturbance is applied at mid-span, the steady-state value is $7.581(10^{-8})$m and $7.588(10^{-8})$m when the shaft speed is 10000 and 15000 rpm respectively (see Table 5.5).

5.3 System With an ISVFB Controller

An integral plus state variable feedback (ISVFB) controller uses an integral feedback for improving steady state performance of the system when a disturbance is applied. Since the comparative study is focussed on the response of the mid-span deflection of the rotor bearing system, it is of interest to use an integral feedback of the mid-span displacements x_5 and x_{11} in vertical and horizontal directions (see Section 2.2.1). To obtain a steady state value of zero for the mid-span deflections, the following equations, namely (5.6) and (5.7) are appended to the system state equations(2.32)

$$\dot{x}_{13} = x_5 \tag{5.6}$$

$$\dot{x}_{14} = x_{11} \tag{5.7}$$

or in matrix form,

$$\begin{bmatrix} \dot{x}_{13} \\ \dot{x}_{14} \end{bmatrix} = \begin{bmatrix} 0 & 0 & 0 & 0 & 1 & 0 & 0 & 0 & 0 & 0 & 0 & 0 \\ 0 & 0 & 0 & 0 & 0 & 0 & 0 & 0 & 0 & 0 & 1 & 0 \end{bmatrix} \begin{bmatrix} x_1 \\ x_2 \\ \vdots \\ x_{12} \end{bmatrix} \tag{5.8}$$

$$\dot{\mathbf{Z}} = \mathbf{CX} \tag{5.9}$$

Hence the augmented system equation is given by,

$$\begin{bmatrix} \dot{X} \\ \dots \\ \dot{Z} \end{bmatrix} = \begin{bmatrix} A_{11} & A_{12} & \vdots & 0 \\ A_{21} & A_{22} & \vdots & \\ \dots & \dots & \dots & \dots \\ \mathbf{C} & & \vdots & 0 \end{bmatrix} \begin{bmatrix} \mathbf{X} \\ \dots \\ \mathbf{Z} \end{bmatrix} + \begin{bmatrix} \mathbf{B} \\ \dots \\ 0 \end{bmatrix} \mathbf{u} \tag{5.10}$$

or

$$\dot{\hat{\mathbf{X}}} = \mathbf{A}_a\hat{\mathbf{X}} + \mathbf{B}_a\mathbf{u} \tag{5.11}$$

5.3.1 Selection of Weighting Factors

The weighting matrix for the state variables is,

$$\mathbf{Q}_a = \begin{bmatrix} Q & \vdots & 0 & 0 \\ \cdots & \cdots & \cdots & \\ 0 & \vdots & q_{13} & 0 \\ 0 & \vdots & 0 & q_{14} \end{bmatrix} \tag{5.12}$$

The response of mid-span deflection is simulated by considering the following sets of weighting factors:

- the first set of weighting factors are: $q_5=q_{11}=10^6$, $q_1=q_2=q_3=\cdots\cdots=q_{12}=q_{13}=q_{14}=1$ and $r_3=r_6=10^{-8}$, $r_1=r_2=\cdots\cdots=10^{-10}$; and
- the second set of weighting factors are $q_5=q_{11}=q_{13}=q_{14}=10^6$, $q_1=q_2=q_3=\cdots\cdots=q_{12}=1$ and $r_3=r_6=10^{-8}$, $r_1=r_2=\cdots\cdots=10^{-10}$.

The augmented matrices $\mathbf{A}_a$, $\mathbf{B}_a$ and $\mathbf{Q}_a$ and the final gain matrix $\mathbf{K}$, control matrix $\mathbf{A}_c$ for this system are presented in Appendix C.

5.3.2 Response of the System With an ISVFB controller

The results of the simulation of the mid-span deflection are presented in graphical form in the figures Fig. 5.7 to 5.12, and the values of t_r, t_s, t_d and steady state value for different shaft speeds are presented in Tables 5.6 to 5.9.

The results obtained using the first set of weighting factors are shown in Figs. 5.7 and 5.8. Fig 5.7 (a) and Fig 5.7 (b) represent the response of the mid-span vertical deflection at a shaft speed 500 rpm when a disturbance is applied vertically at the bearing housing and the mid-span respectively. Fig 5.8 (a) and Fig 5.8 (b) represent the response of the mid-span vertical deflection at a shaft speed 4500 rpm when a disturbance is applied vertically at the bearing housing and the mid-span respectively. In the same way responses are simulated repeatedly for shaft speeds of 1500, 2500,3000, 3500, 10000 and 15000 rpm. The performance curves obtained at theses speeds are of similar nature as shown in the Figs. 4.7 and 4.8. The performance characteristics t_r ,t_d, t_s and steady-state values obtained from the performance curves are presented in Tables 5.6 and 5.7.

The results obtained by using the second set of weighting factors are displayed through Fig 5.9 to Fig 5.12. Figs. 5.9 and 5.10 show the response of the mid-span vertical deflection for a disturbance applied in the vertical direction at the bearing housing when shaft speeds are 500 and 4500 rpm respectively. Fig 5.9 (a) and Fig 5.10 (a) show the results obtained for a time span of 0.5s with the time step of 0.005s.

Fig 5.9 (b) and 5.10 (b) show the results obtained for a time span of 20s with the time step of 0.05s. The peak value (M_p), time to reach the peak value (t_p) and settling time (t_s) are obtained from the response curves for shaft speeds of 500, 1500, 2500, 3000, 3500, 4500, 10000 and 15000 rpm. These values are presented in Table 5.8. Fig. 5.11 and Fig. 5.12 represent the response curves of the mid-span deflection for shaft speeds of 500 rpm and 4500 rpm respectively. When a disturbance is applied at the mid-span of the rotor bearing system. The peak value (M_p), time to reach the peak value (t_p) and the settling time (t_s) obtained from the response curves of different shaft speeds of 500, 1500, 2500, 3000, 3500, 4500, 10000 and 15000 rpm are presented in Table 5.9.

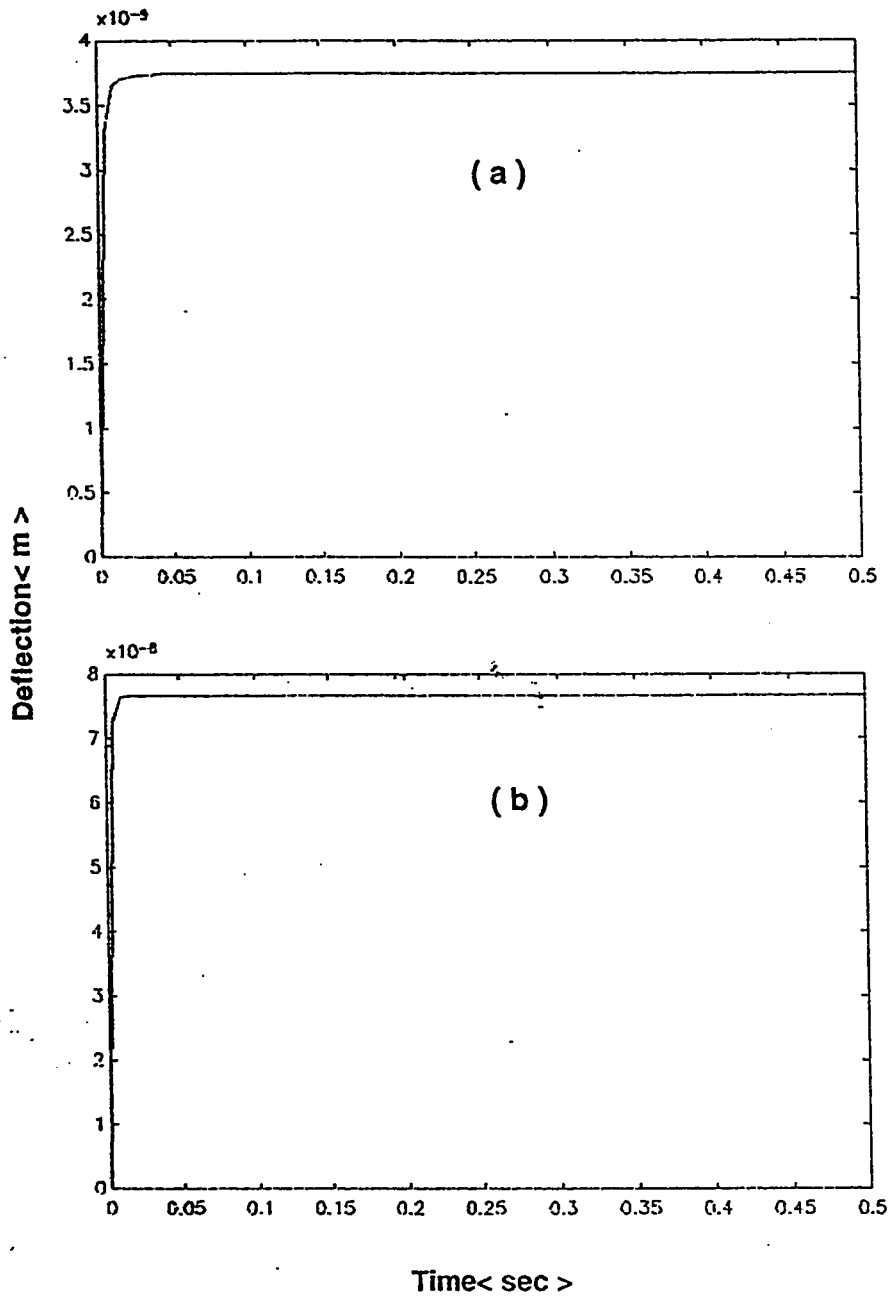

Figure 5.7: Response of the mid-span deflection at a shaft speed of 500 rpm when an external unit-step disturbance is applied in the vertical direction at: (a) bearing housing, (b) mid-span (when an ISVFB controller with the first set of weighting factors is employed in the system).

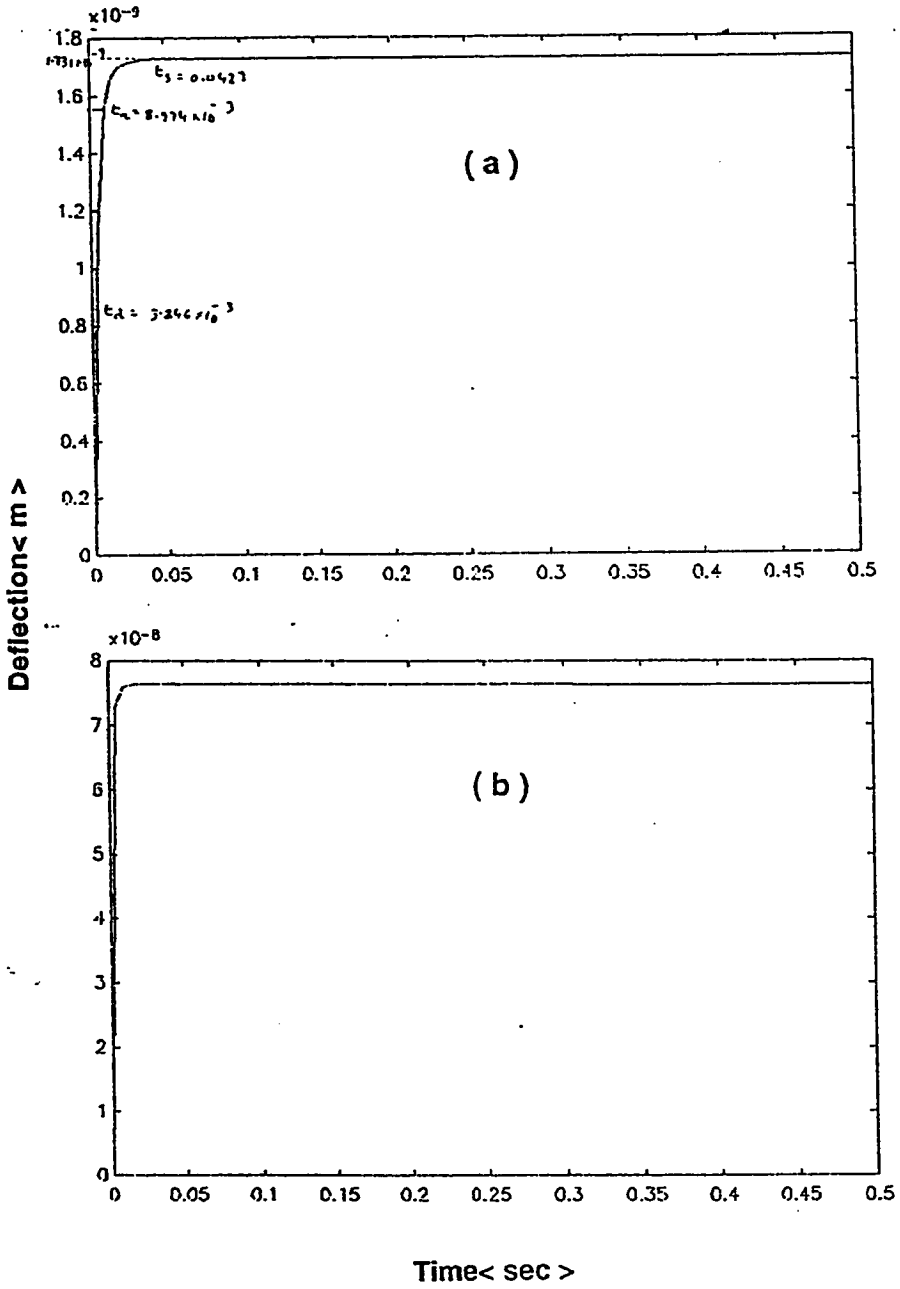

Figure 5.8: Response of the mid-span deflection at a shaft speed of 4500 rpm when an external unit-step disturbance is applied in the vertical direction at: (a) bearing housing, (b) mid-span (when an ISVFB controller with the first set of weighting factors is employed in the system).

Shaft speed(N)	rise time(t_r)	delay time(t_d)	settling time(t_s)	steady-state
rpm	10^{-3}sec.	10^{-3}sec.	sec.	10^{-9}m
500	3.864	2.564	.041	3.75
1500	7.692	2.564	.0.0385	2.884
2500	7.692	2.564	.05	2.327
3000	7.692	2.564	.05	2.125
3500	7.692	3.846	.0423	1.954
4500	8.974	3.846	.0423	1.731
10000	9.211	5.263	.0474	1.4
15000	9.211	5.263	.0579	1.433

Table 5.6: Performance characteristic values, t_r, t_d, t_s and steady-state value of mid-span response of the system with an ISVFB controller having the first set of weighting factors and disturbance is applied vertically at bearing housing.

Shaft speed(N)	rise time(t_r)	delay time(t_d)	settling time(t_s)	steady-state
rpm	10^{-3}sec.	10^{-3}sec.	sec.	10^{-8}m
500	3.846	2.564	.014	8.312
1500	3.846	2.564	.0128	7.625
2500	3.846	2.564	.0128	7.625
3000	3.846	2.564	.0128	7.625
3500	3.846	2.564	.0128	7.625
4500	3.846	2.564	.0179	7.625
10000	3.947	2.632	0.0151	7.558
15000	3.947	2.632	0.0151	7.524

Table 5.7: Performance characteristic values, t_r, t_d, t_s and steady-state value of mid-span response of the system with an ISVFB controller having the first set of weighting factors and disturbance is applied vertically at mid-span.

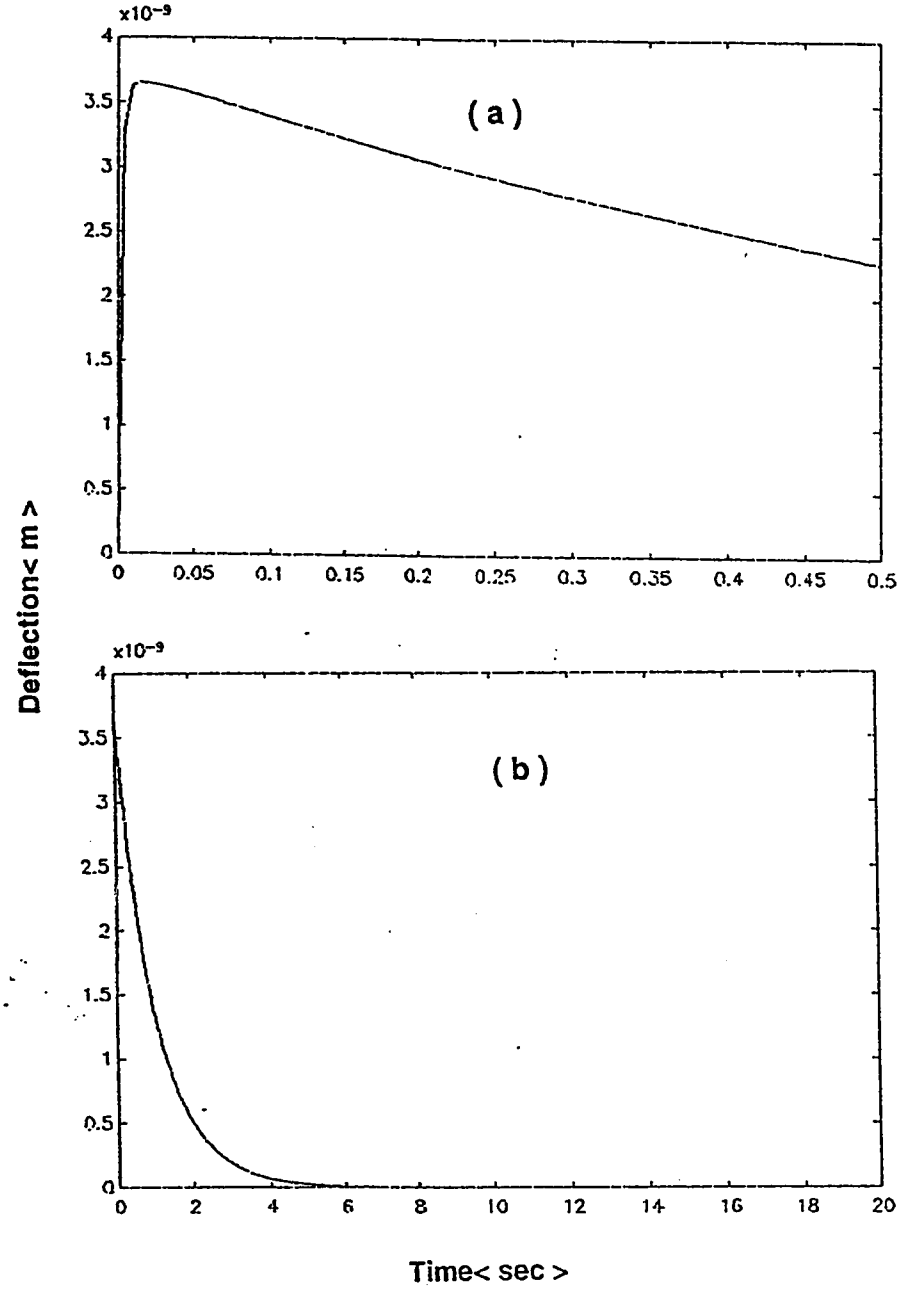

Figure 5.9: Response of the mid-span deflection at a shaft speed of 500 rpm when an external unit-step disturbance is applied at bearing housing in the vertical direction(when an ISVFB controller with the second set of weighting factors is employed on the system) for: (a) time step of 0.005 sec., (b) time step of 0.05 sec.

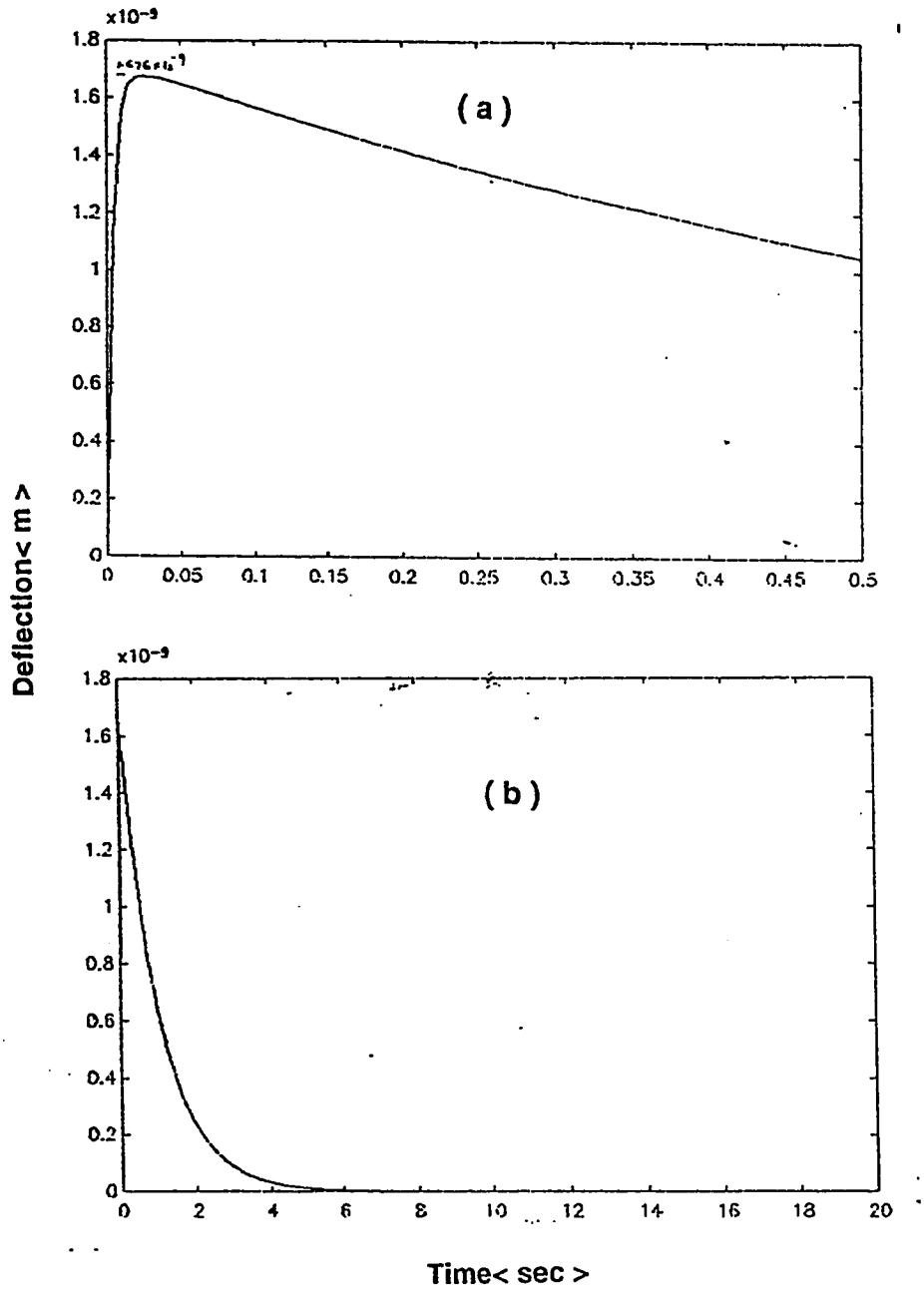

Figure 5.10: Response of the mid-span deflection at a shaft speed of 4500 rpm when external unit-step disturbance is applied at bearing housing in the vertical direction(when an ISVFB controller with the second set of weighting factors is employed in the system) for: (a) time step of 0.005 sec., (b) time step of 0.05sec.

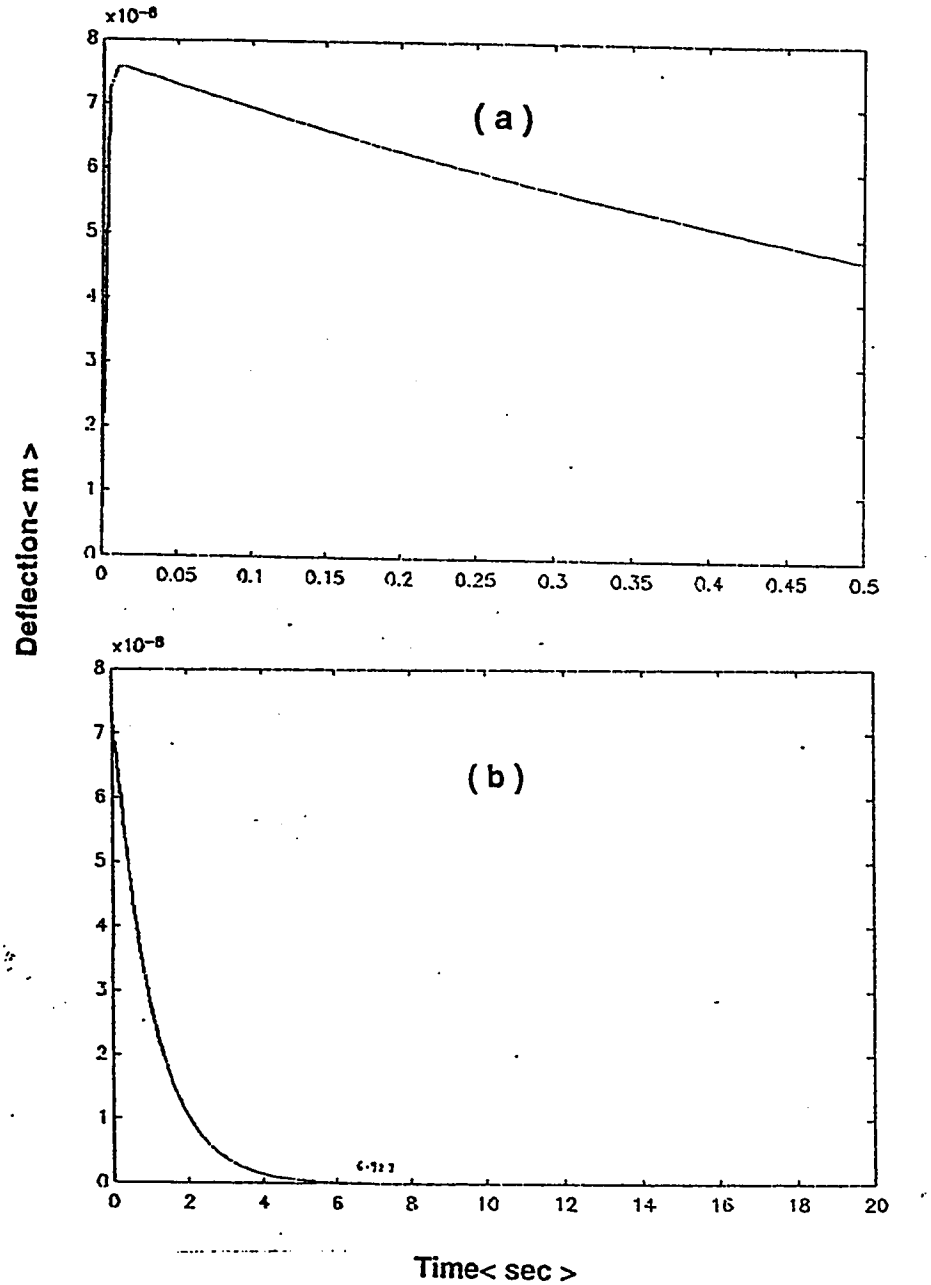

Figure 5.11: Response of the mid-span deflection at a shaft speed of 500 rpm when an external unit-step disturbance is applied at the mid-span in the vertical direction(when an ISVFB controller with the second set of weighting factors is employed in the system) for: (a) time step of 0.005 sec., (b) time step of 0.05 sec.

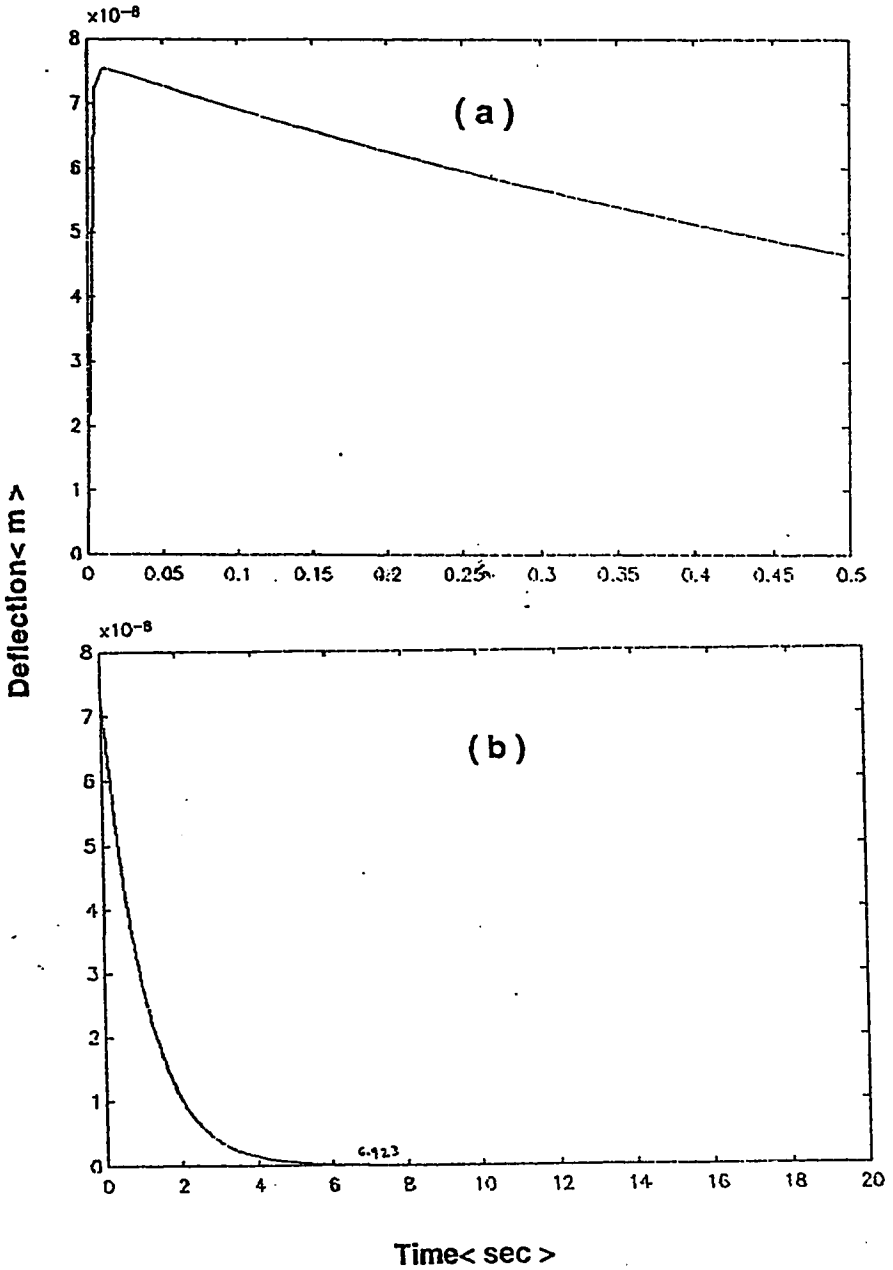

Figure 5.12: Response of the mid-span deflection at a shaft speed of 4500 rpm when an external unit-step disturbance is applied at mid-span in the vertical direction(when an ISVFB controller with the second set of weighting factors is employed in the system) for: (a) time step of 0.005 sec., (b) time step of 0.05 sec.

Shaft speed(N)	peak value(M_p)	time of peak value(t_p)	settling time(t_s)
rpm	10^{-9}m	sec.	sec.
500	3.656	.0141	6.923
1500	2.802	.0231	6.923
2500	2.212	.0551	6.923
3000	2.058	.0231	6.923
3500	1.90	.0231	6.923
4500	1.676	.0231	6.923
10000	1.354	.0237	6.105
15000	1.375	.0276	6.105

Table 5.8: Performance characteristic values, M_p, t_p and t_s of mid-span response of the system with an ISVFB controller having the second set of weighting factors and disturbance is applied vertically at bearing housing.

Shaft speed(N)	peak value(M_p)	time of peak value(t_p)	settling time(t_s)
rpm	10^{-8}m	sec.	sec.
500	7.5625	.0103	6.923
1500	7.5625	.0103	6.923
2500	7.5625	.0551	6.923
3000	7.5625	.0103	6.923
3500	7.5625	.0103	6.923
4500	7.5625	.0103	6.923
10000	7.476	.0105	6.105
15000	7.476	.0105	6.105

Table 5.9: Performance characteristic values, M_p, t_p and t_s of mid-span response of the system with an ISVFB controller with the second set of weighting factors and disturbance is applied vertically at mid-span.

5.3.3 Remarks on the Performance of the System With an ISVFB Controller

The performance curves of the integral plus state variable feedback (ISVFB) controller with the first set of weighting factors are of similar trend to those obtained in the case of SVFB controller with the second set of weighting factor (see Figs. 5.5, 5.6,5.7 and 5.8). The performance characteristic values t_r ,t_d, t_s and steady-state values are almost equal to that of the values obtained in the SVFB controller (see Tables 5.4, 5.5, 5.6 and 5.7).

The ISVFB controller with the second set of weighting factors responds to a disturbance well in that it achieves a steady state value of zero (Figs. 5.9 to 5.12). The settling time (t_s) is 6.923s for a shaft speed up to 4500 rpm and 6.105s for shaft speed 10000 rpm and above (Table 5.8 and 5.9). For a disturbance applied at the bearing housing the peak value (M_p) decreases as the shaft speed increases, for shaft speeds of up to 10000 rpm, when the speed is increased from 10000 to 15000 rpm the value of M_p increases from $1.354(10^{-9})$m to $1.375(10^{-9})$m (Table 5.8). When the disturbance is applied at the mid-span the value of M_p is $7.5625(10^{-8})$m for shaft speeds of up to 4500 rpm and the value of M_p decreases to $7.476(10^{-8})$m for a shaft speed of 10000 rpm and above (Table 5.9). The time (t_p) required to reach the peak value is 0.0141s and 0.0551s for shaft speeds 500 and 2500 rpm respectively, for other shaft speeds below the critical shaft speed (8200 rpm) the value of t_p is

0.0231s. When the speed is above the critical speed then the value of t_p increases with the speed of the shaft (Table 5.8). For a disturbance at the the mid-span the value of t_p at a shaft speed of 2500 rpm is 0.0551s, for other shaft speeds below the critical shaft speed the value is 0.0103s, above the critical shaft speed the value of t_p increases to 0.0105s (Table 5.9).

5.4 System With an LQS Controller

In order to obtain steady state values of zero for the mid-span deflections, the system state equation (2.32) are appended with two state variables x_{13} and x_{14} and these two state variables represent the deflections of mid-span (x_5, x_{11}):

$$\mathbf{Y} = \begin{bmatrix} x_{13} \\ x_{14} \end{bmatrix} = \begin{bmatrix} 0 & 0 & 0 & 0 & 1 & 0 & 0 & 0 & 0 & 0 & 0 & 0 \\ 0 & 0 & 0 & 0 & 0 & 0 & 0 & 0 & 0 & 0 & 1 & 0 \end{bmatrix} \begin{bmatrix} x_1 \\ x_2 \\ \vdots \\ \vdots \\ x_{12} \end{bmatrix} \tag{5.13}$$

$$\mathbf{Y} = \mathbf{C}\mathbf{X} \tag{5.14}$$

$$\dot{\mathbf{Y}} = \mathbf{C}\dot{\mathbf{X}} \tag{5.15}$$

The derivative form of the original system equations (2.32) can be written as:

$$\ddot{\mathbf{X}} = \begin{bmatrix} A_{11} & A_{12} \\ A_{21} & A_{22} \end{bmatrix} \begin{bmatrix} \dot{X}_v \\ \dot{X}_h \end{bmatrix} + \begin{bmatrix} B_{11} & B_{12} \\ B_{21} & B_{22} \end{bmatrix} \begin{bmatrix} \dot{U}_v \\ \dot{U}_h \end{bmatrix} \tag{5.16}$$

$$\ddot{\mathbf{X}} = \mathbf{A}\dot{\mathbf{X}} + \mathbf{B}\dot{\mathbf{u}} \tag{5.17}$$

Augmentation of equations (5.15) and (5.17) gives the following form of the system equation,

$$\begin{bmatrix} \dot{Y} \\ \cdots \\ \ddot{X} \end{bmatrix} = \begin{bmatrix} 0 & \vdots & C \\ \cdots & \cdots & \cdots \\ 0 & \vdots & A \end{bmatrix} \begin{bmatrix} \mathbf{Y} \\ \cdots \\ \dot{\mathbf{X}} \end{bmatrix} + \begin{bmatrix} 0 \\ \cdots \\ B \end{bmatrix} \dot{\mathbf{u}} \tag{5.18}$$

$$\dot{\hat{\mathbf{Z}}} = \mathbf{A}_a \hat{Z} + \mathbf{B}_a \mathbf{v} \tag{5.19}$$

where, $\hat{Z} = \begin{bmatrix} Y \\ \cdots \\ \dot{X} \end{bmatrix}$, $\mathbf{v} = \dot{\mathbf{u}}$ and $\mathbf{A}_a$, $\mathbf{B}_a$ are augmented system matrices. These matrices are presented in Appendix C. The structure of the controller as implemented is given in Fig. 4.10 (Chapter 4).

5.4.1 Selection of Weighting Factors

The weighting matrix for the state variables is $\mathbf{Q}_a$ given as,

$$\mathbf{Q}_a = \begin{bmatrix} q_{13} & 0 & 0 & \cdots & \cdots & 0 \\ 0 & q_{14} & 0 & \cdots & \cdots & 0 \\ 0 & 0 & 0 & \cdots & \cdots & 0 \\ \cdots & \cdots & \cdots & \cdots & \cdots & \cdots \\ \cdots & \cdots & \cdots & \cdots & \cdots & \cdots \\ 0 & 0 & 0 & \cdots & \cdots & 0 \end{bmatrix}_{14\times 14} \tag{5.20}$$

The response of mid-span deflection is simulated by considering the following sets of weighting factors:

- the first set of weighting factors are: q_{13}=q_{14}=1 and r_3=r_6=10^{-8}, r_1=r_2= ..... = 10^{-10}; and
- the second set of weighting factors are: q_{13} = q_{14}= 10^6, and r_3=r_6=10^{-8}, r_1=r_2= ..... = 10^{-10}.

The resultant gain and control matrices are presented in Appendix C.

5.4.2 Response of the System With an LQS controller

Fig 5.13 and Fig. 5.14 show the response of the mid-span deflection in the vertical direction for shaft speeds of 500 and 4500 rpm respectively. The LQS controller with the first set of weighting factors is applied in this case. Fig. 5.13(a) and Fig 5.14(a) show the response of the mid-span deflection when a disturbance is applied at the bearing-housing. Fig 5.13(b) and 5.14(b) show the response of the mid-span deflection when a disturbance is applied at the mid-span. Similar trend of responses has been observed for shaft speeds of 1500, 2500, 3000, 3500, 10000 and 15000 rpm. Tables 5.10 and 5.11 present the peak value (M_p), time to reach the peak value (t_p), settling time (t_s) and steady-state value of the mid-span deflection of the rotor. The values are obtained from the response curves of the system for different shaft speeds. Figures 5.15 and 5.16 show the response of the mid-span deflection of the system

with an LQS controller with the second set of weighting factors for shaft speeds of 500 and 4500 rpm respectively. Fig. 5.15(a) and Fig. 5.16(a) are the responses obtained when a disturbance is applied at the bearing housing. Fig 5.15(b) and 5.16(b) show the response curves when a disturbance is applied at the mid-span. Responses are also obtained for shaft speeds of 1500, 2500,3000,3500, 10000 and 15000 rpm; in these cases, responses are similar to those shown in Figures 5.15 and 5.16; and therefore, they are not presented here. However, the performance characteristics M_p, t_p, t_s and steady-state value obtained from the responses for these speeds are presented in Tables 5.12 and 5.13.

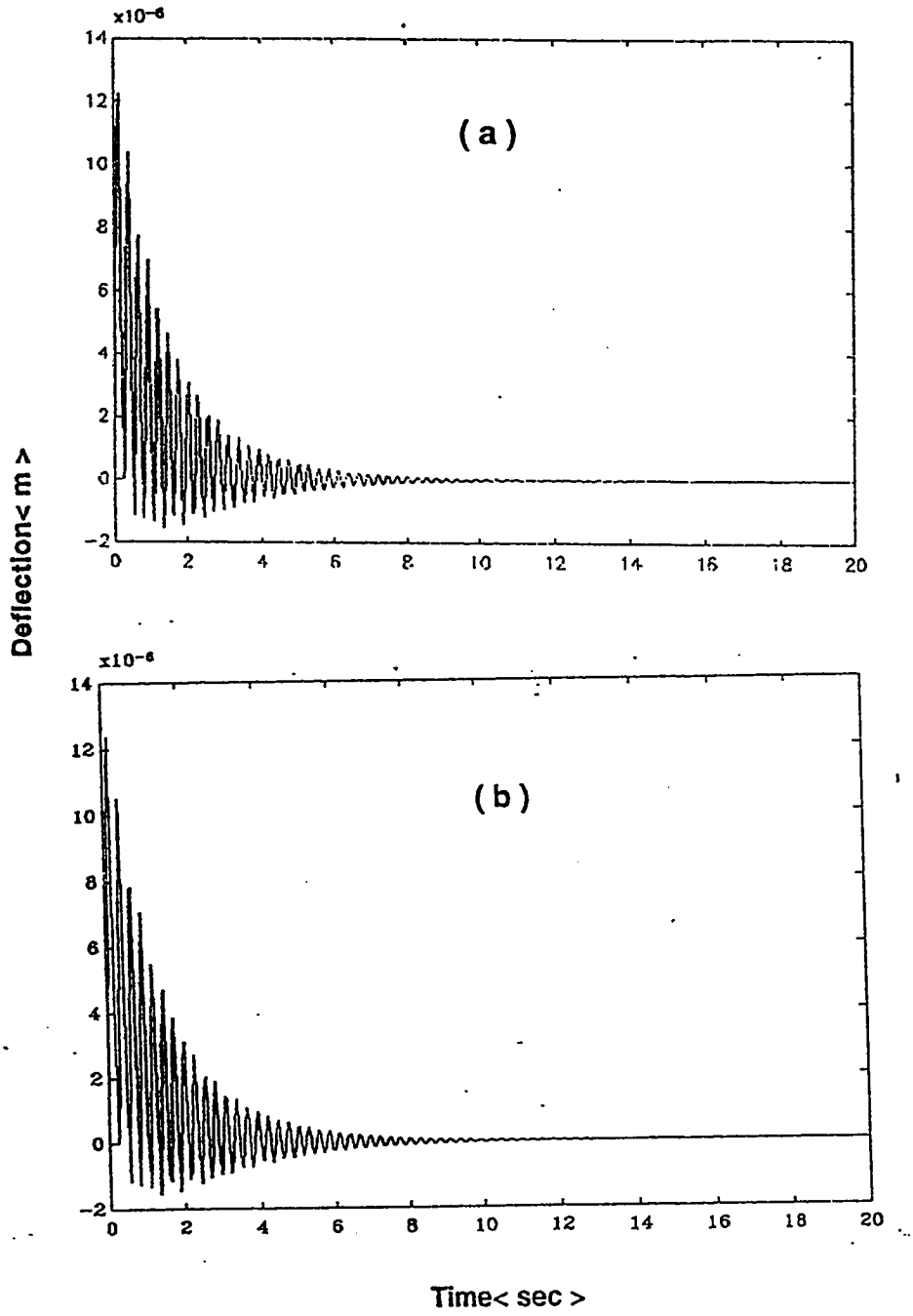

Figure 5.13: Response of the mid-span deflection at a shaft of speed of 500 rpm when an external unit-step disturbance is applied in the vertical direction at: (a) bearing housing, (b) mid-span (when an LQS controller with the first set of weighting factors is employed in the system).

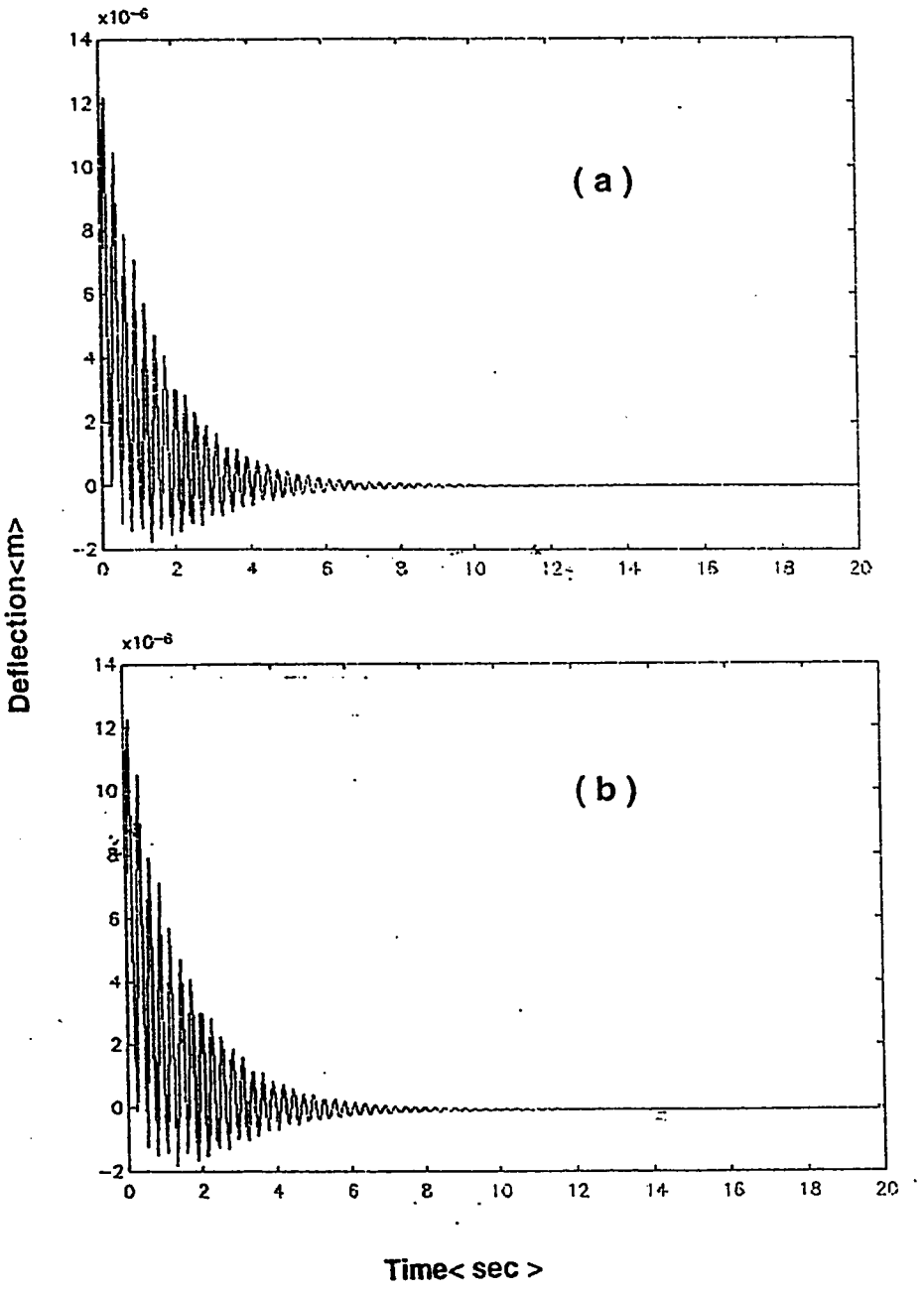

Figure 5.14: Response of the mid-span deflection at a shaft speed of 4500 rpm when an external unit-step disturbance is applied in the vertical direction at: (a) bearing housing, (b) mid-span (when an LQS controller with the first set of weighting factors is employed in the system).

Speed(N)	peak value(M_p)	time of peak value(t_p)	settling time(t_s)	s.s. value
rpm	10^{-6}m	sec.	sec.	m
500	12.25	0.154	13.85	0
1500	12.25	0.154	13.64	0
2500	12.25	0.154	13.85	0
3000	12.25	0.154	13.64	0
3500	12.25	0.154	13.64	0
4500	12.25	0.154	13.64	0
10000	12.285	0.158	11.947	0
15000	12.285	0.158	11.947	0

Table 5.10: Performance characteristic values, t_r, t_d, t_s and steady-state value of mid-span response of the system with an LQS controller having the first set of weighting factors and disturbance is applied vertically at bearing housing.

Speed(N)	peak value(M_p)	time of peak value(t_p)	settling time(t_s)	s.s. value
rpm	10^{-6}m	sec.	sec.	10^{-7}m
500	12.375	0.154	14.25	0
1500	12.375	0.154	14.154	0
2500	12.375	0.154	13.85	0
3000	12.25	0.154	11.743	-1.25
3500	12.25	0.154	11.743	-1.25
4500	12.25	0.154	11.743	-1.25
10000	12.429	0.158	11.947	0
15000	12.429	0.158	11.947	0

Table 5.11: Performance characteristic values, t_r, t_d, t_s and steady-state value of mid-span response of the system with an LQS controller having the first set of weighting factors and disturbance is applied vertically at mid-span.

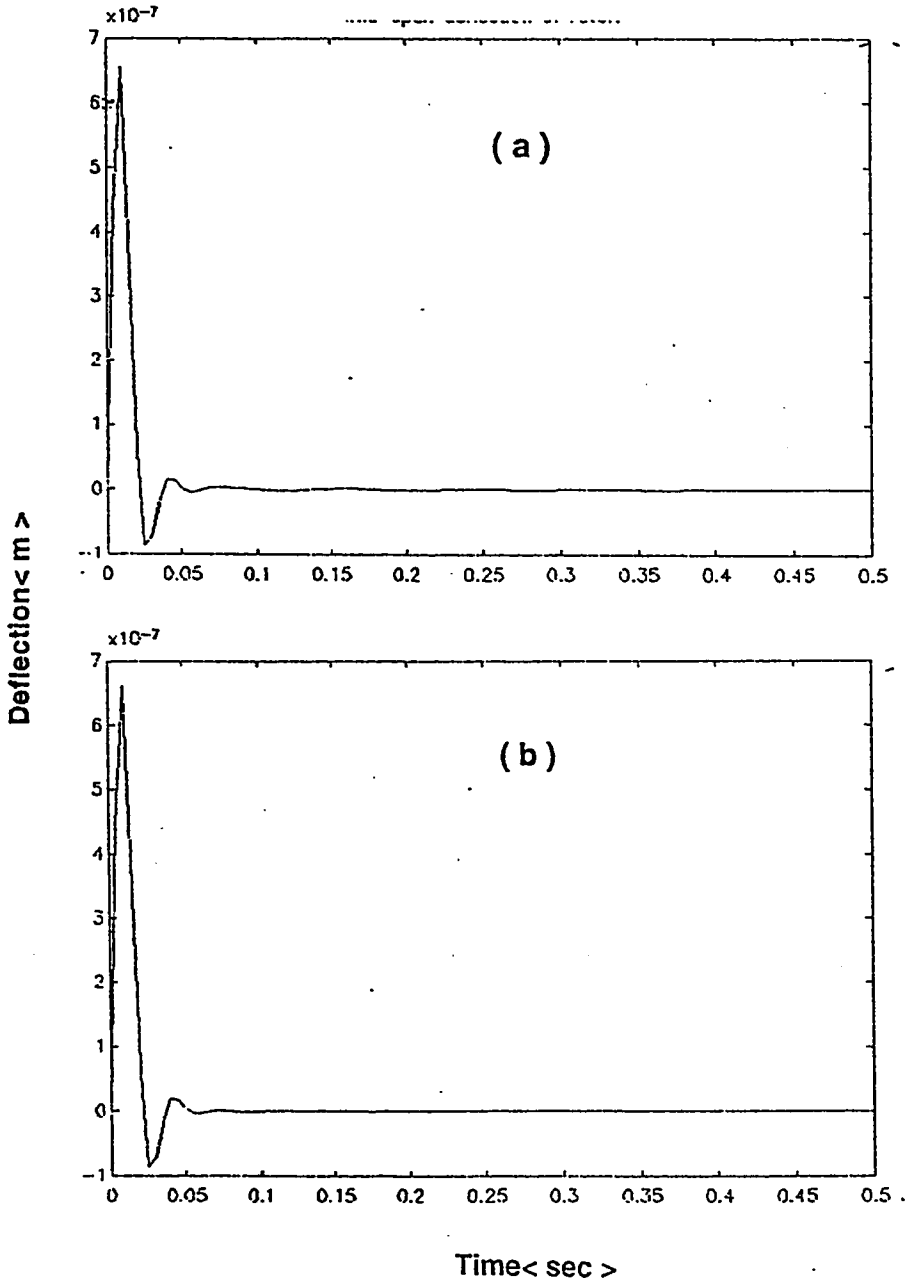

Figure 5.15: Response of the mid-span deflection at a shaft speed of 500 rpm when an external unit-step disturbance is applied in the vertical direction at: (a) bearing housing, (b) mid-span (when an LQS controller with the second set of weighting factors is employed in the system).

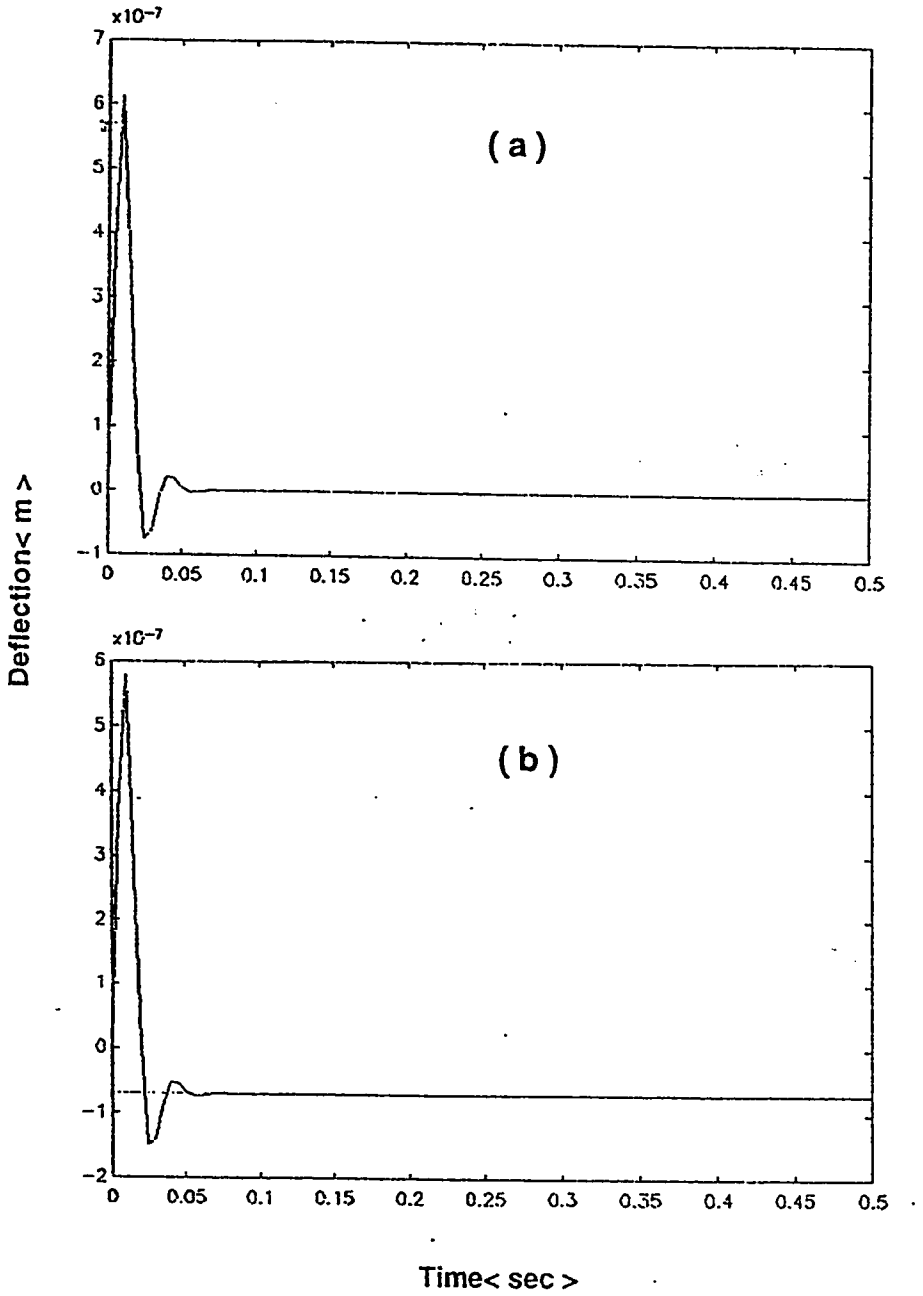

Figure 5.16: Response of the mid-span deflection at a shaft speed of 4500 rpm when an external unit-step disturbance is applied in the vertical direction at: (a) bearing housing, (b) mid-span (when an LQS controller with the second set of weighting factors is employed in the system).

Speed(N)	Max. peak value(M_p)	time of max.peak(t_p)	settling time(t_s)	s.s. value
rpm	10^{-7}m	sec.	sec.	m
500	6.5625	.0103	0.378	0
1500	6.5625	0.0103	0.132	0
2500	6.5625	0.0103	0.0692	0
3000	6.5625	0.0103	0.0974	0
3500	6.5625	0.0103	0.0795	0
4500	6.5625	0.0103	0.0679	0
10000	6.5238	0.00921	0.06579	0
15000	6.5238	0.00921	0.06579	0

Table 5.12: Performance characteristic values, M_p, t_p, t_s and steady-state value of mid-span response of the system with an LQS controller having the the second set of weighting factors and disturbance is applied vertically at bearing housing.

Speed(N)	peak val.(M_p)	time of peak value(t_p)	settle time(t_s)	S.S.value
rpm	10^{-7}m	sec.	sec.	10^{-8}m
500	6.625	.0103	.1808	0
1500	6.625	0.0103	0.0923	0
2500	6.625	0.0103	0.0923	0
3000	5.8125	0.0103	0.0846	-6.875
3500	5.8125	0.0103	0.0782	-6.875
4500	5.8125	0.0103	0.0782	-6.875
10000	6.619	0.00921	0.06579	0
15000	6.619	0.00921	0.06579	0

Table 5.13: Performance characteristic values, M_p, t_p, t_s and steady-state value of mid-span response of the system with an LQS controller having the second set of weighting factors and disturbance is applied vertically at mid-span.

5.4.3 Remarks on the Performance of the System With an LQS Controller

Figs 5.13 and 5.14 show the deflections of the mid-span when an LQS controller with the first set of weighting factors is used in the system. These figures show that the system exhibits an oscillatory behavior before reaching the steady state value. The peak value (M_p) of these oscillations is 12.25 (10^{-6})m for any shaft speed, below the critical shaft speed, when the disturbance is applied at the bearing housing. When the shaft speed is above the critical speed then the value of M_p increases to 12.285(10^{-6})m (see Table 5.10). On the other hand when the disturbance is applied at the mid-span the value of M_P is found as 12.375(10^{-6})m for shaft speeds of 500 to 2500 rpm, and the value of M_P changes to 12.25×10^{-6}m for shaft a speed at 3000 rpm and above, for the shaft speed above the critical value M_P increases to 12.429×10^{-6}m (see Table 5.11). The steady-state value of the responses for all shaft speeds is zero when the disturbance is at the bearing housing; on the other hand when the disturbance is applied at the mid-span the steady state value of the response is -1.25×10^{-7}m for a shaft speed of 3000 rpm and above and zero for a shaft speed of less than 3000 rpm. From Tables 5.10 and 5.11 it is noted that the time required to reach the peak value(t_p) is 0.154s and t_P is independent of the shaft speed when the speed is below the critical value. For the shaft speed above the critical value t_p increases to 0.158s.

When the LQS controller with the second set of weighting factors is used system's disturbance rejection quality is improved (see Figures 5.15 and 5.16). The peak value is lower compared to that in the previous case. The value of t_p is 0.0103s for the shaft speed below the critical value and it decreases to 0.00921s for the shaft speed above the critical value (Tables 5.12 and 5.13). The steady state value for a shaft speed at and above 3000 rpm is $-6.875(10^{-8})$m when disturbance is at the mid-span; for other shaft speeds for all speeds when disturbance is at the bearing housing the steady state value is zero (Tables 5.12 and 5.13). The system with an LQS controller has a larger value of (M_p) as compared to those of the system with an ISVFB (Tables 5.8 to 5.13).

5.5 Effects of support stiffness on the response of the system

The results displayed in Section 5.1.1 to Section 5.1.4 have been obtained by assuming the stiffness of the support (K_e) to be 0.01 times the stiffness of the rotor (K_f) of the system (i.e., $K_e = 0.01K_f$) [19]. In this section the results presented are obtained by simulating the response of the mid-span when the stiffness of the support has the following values: $0.1K_f$, $1.0K_f$, $10K_f$ and $100K_f$. A shaft speed of 4500 and 15000 rpm is used in all the cases.

5.5.1 Response of the System for different values of the Support stiffness (K_e)

The response of the mid-span deflection of the rotor has been simulated by considering the system with and without a controller. Two sets of response curves obtained by applying a unit step disturbance vertically at bearing housing and at mid-span respectively. The characteristic values obtained from these performance curves are presented in the Tables 5.14 to 5.20. The simulation results obtained at a shaft speed of 4500 rpm (below the critical speed of the rotor) are presented in Tables 5.14 to 5.17. Tables 5.18 to 5.20 show the result when the the response is simulated at 15000 rpm (above the critical speed of the rotor). The results of the Table 5.14 show the values M_p, t_p, t_d, t_r, t_s of the response curves for different support stiffness, for the system without a controller, when the shaft speed is 4500 rpm. But for a shaft speed of 15000 rpm the system behavior without a controller is unstable for any value support stiffness. The controllers (SVFB, ISVFB and LQS) with the second set of weighting factors are used in simulation.

Parameters	Pos. of distrb.	k_e=0.01 k_f	k_e=0.1 k_f	k_e= k_f	k_e=10 k_f	k_e=100 k_f
M_p	a	unstable	unstable	1292	129.1	9.35
10^{-10}m	b	"	"	3027	174.3	1.267
t_p	a	"	"	5.128	3.077	15.4
10^{-3}sec.	b	"	"	"	"	"
s.-state	a	"	"	702.7	70.3	7.038
10^{-10}m	b	"	"	1662	1021.4	962.1
t_d	a	"	"	2.564	2.307	3.846
10^{-3}sec.	b	"	"	"	"	2.564
t_r	a	"	"	3.846	2.307	7.692
10^{-3}sec.	b	"	"	"	3.077	10.3
t_s	a	"	"	0.333	0.174	0.146
sec.	b	"	"	0.5	0.285	0.194

Table 5.14: Performance characteristic values, M_p, t_p, t_r, t_d, t_s and steady-state value of mid-span response of the system without a controller for different values of support-stiffness(k_e) and shaft running speed is 4500 rpm.

Parameters	Pos. of distrb.	k_e=0.01 k_f	k_e=0.1 k_f	k_e= k_f	k_e=10 k_f	k_e=100 k_f
M_p	a	-	-	-	-	-
	b	-	-	-	-	-
t_p	a	-	-	-	-	-
	b	-	-	-	-	-
s.-state	a	17.31	17.31	16.83	9.75	6.081
10^{-10}m	b	762.5	762.5	762.5	758	756.25
t_d	a	3.846	3.846	3.846	3.077	2.564
10^{-3}sec.	b	2.564	2.564	2.564	3.077	2.564
t_r	a	8.974	8.974	7.692	4.615	3.846
10^{-3}sec.	b	3.846	3.846	3.846	4.615	3.846
t_s	a	0.0718	0.0282	0.0138	0.0128	0.146
sec.	b	0.0167	0.0115	0.0128	0.0108	0.0167

Table 5.15: Performance characteristic values, M_p, t_p, t_r, t_d, t_s and steady-state value of mid-span response of the system with an SVFB controller having the the second set of weighting factors for different values of support-stiffness(k_e) and shaft running speed is 4500 rpm.

a→disturbance at bearing housing;

b→ disturbance at mid-span.

Parameters	Pos. of distrb.	k_e=0.01 k_f	k_e=0.1 k_f	k_e= k_f	k_e=10 k_f	k_e=100 k_f
M_p	a	16.48	16.55	16.0	9.31	-
10^{-10}m	b	728.1	728.1	728.1	725	-
t_p	a	23.1	23.1	20.5	10.3	-
10^{-3}sec.	b	10.3	10.3	10.3	10.3	-
s.-state	a	0	0	0	0	6.081
10^{-10}m	b	-	-	-	-	756.25
t_d	a	-	-	-	-	2.564
10^{-3}sec.	b	-	-	-	-	"
t_r	a	-	-	-	-	3.846
10^{-3}sec.	b	-	-	-	-	"
t_s	a	6.923	6.974	7.05	7.25	.0128
sec.	b	"	"	6.9	7.15	.0167

Table 5.16: Performance characteristic values, M_p, t_p, t_r, t_d, t_s and steady-state value of mid-span response of the system with an ISVFB controller having the the second set of weighting factors for different values of support-stiffness(k_e) and shaft running speed is 4500 rpm.

Parameters	Pos. of distrb.	k_e=0.01 k_f	k_e=0.1 k_f	k_e= k_f	k_e=10 k_f	k_e=100 k_f
M_p	a	6125	6569	1243	93.8	8.827
10^{-10}m	b	5813	7423	2930	1205	1205
t_p	a	10.3	10.3	5.128	10.3	15.4
10^{-3}sec.	b	"	"	"	"	"
s.-state	a	0	0	0	70.3	0
10^{-10}m	b	-687.5	0	0	0	0
t_d	a	-	-	-	-	-
	b	-	-	-	-	-
t_r	a	-	-	-	-	-
	b	-	-	-	-	-
t_s	a	0.0679	0.2256	0.5	1.864	2.323
sec.	b	0.0782	0.132	0.5	1.894	2.338

Table 5.17: Performance characteristic values, M_p, t_p, t_r, t_d, t_s and steady-state value of mid-span response of the system with an LQS controller having the the second set of weighting factors for different values of support-stiffness(k_e) and shaft running speed is 4500 rpm.

Parameters	Pos. of distrb.	k_e=0.01 k_f	k_e=0.1 k_f	k_e= k_f	k_e=10 k_f	k_e=100 k_f
M_p	a	-	-	-	-	-
	b	-	-	-	-	-
t_p	a	-	-	-	-	-
	b	-	-	-	-	-
s.-state	a	14.33	14.32	13.43	6.08	3.58
10^{-10}m	b	758.8	754.84	754.84	751.6	745.2
t_d	a	3.947	4.44	4.05	3.33	3.33
10^{-3}sec.	b	2.638	2.778	3.33	2.22	2.22
t_r	a	9.21	8.89	8.11	3.89	3.89
10^{-3}sec.	b	3.947	3.89	3.89	3.89	3.89
t_s	a	0.0579	0.0467	0.023	0.0122	0.01
sec.	b	0.0184	0.0122	0.0122	0.0089	0.0089

Table 5.18: Performance characteristic values, M_p, t_p, t_r, t_d, t_s and steady-state value of mid-span response of the system with an SVFB controller having the the second set of weighting factors for different values of support-stiffness(k_e) and shaft running speed is 15000 rpm.

Parameters	Pos. of distrb.	k_e=0.01 k_f	k_e=0.1 k_f	k_e= k_f	k_e=10 k_f	k_e=100 k_f
M_p	a	13.75	13.826	13.163	5.999	3.548
10^{-10}m	b	747.6	746.22	747.12	742.87	737.37
t_p	a	27.6	25	20	15	10
10^{-3}sec.	b	10.5	10	15	15	15
s.-state	a	0	0	0	0	0
10^{-10}m	b	0	0	0	0	0
t_d	a	-	-	-	-	-
10^{-3}sec.	b	-	-	-	-	-
t_r	a	-	-	-	-	-
10^{-3}sec.	b	-	-	-	-	-
t_s	a	6.105	6.161	6.161	6.429	6.46
sec.	b	"	6.071	"	6.25	6.339

Table 5.19: Performance characteristic values, M_p, t_p, t_r, t_d, t_s and steady-state value of mid-span response of the system with an ISVFB controller having the the second set of weighting factors for different values of support-stiffness(k_e) and shaft running speed is 15000 rpm.

Parameters	Pos. of distrb.	k_e=0.01 k_f	k_e=0.1 k_f	k_e= k_f	k_e=10 k_f	k_e=100 k_f
M_p	a	6523.8.2	6579.7	1306.6	98.113	10.042
10^{-10}m	b	6619	7430	3082.4	1375.6	1342.7
t_p	a	9.21	10.0	5.0	10.0	10
10^{-3}sec.	b	"	"	"	"	"
s.-state	a	0	0	0	0	0
10^{-10}m	b	0	0	0	0	0
t_d	a	-	-	-	-	-
	b	-	-	-	-	-
t_r	a	-	-	-	-	-
	b	-	-	-	-	-
t_s	a	0.06579	0.1133	0.4533	1.6081	1.9054
sec.	b	"	0.12	"	1.6486	1.9868

Table 5.20: Performance characteristic values, M_p, t_p, t_r, t_d, t_s and steady-state value of mid-span response of the system with an LQS controller having the the second set of weighting factors for different values of support-stiffness(k_e) and shaft running speed is 15000 rpm.

5.5.2 Remarks on the Effect of support stiffness

The effect of support stiffness (K_e) on the response of the system have been studied by considering the stiffness (K_e) as 0.01, 0.1, 1, 10 and 100 times of the rotor stiffness (K_f). The results show that the system without a controller exhibits an unstable response at 4500 rpm when $K_e = 0.01K_f$ and $0.1K_f$ (see Table 5.14). For $K_e = K_f$, $10K_f$ and $100K_f$ the system is found to be stable at a shaft speed of 4500 rpm. The magnitude of the peak value (M_p), steady-state value and settling time (t_s) decrease with the increase of the support stiffness (Table 5.14). When the shaft speed is increased to 15000 rpm (above the shaft critical speed) then the system is observed unstable for any value of the support stiffness. Table 5.15 shows the results

of the responses of the mid-span vertical deflection of the system, with an SVFB controller having the second set of weighting factors, for different support stiffness. The shaft speed is 4500 rpm. It is observed that the steady-state value is equal for the stiffness $K_e = 0.01K_f$ and $0.1K_f$ and the steady-state value decreases if the support stiffness $K_e \geq K_f$ (Table 5.15). The system exhibited this result for the disturbance applied vertically at the bearing housing. When a disturbance is applied at the mid-span the steady-state value of the mid-span deflection is $7.625(10^{-8})$m for $K_e \leq K_f$; the steady state value decreases with the increase of support stiffness when $K_e > K_f$. The values of t_d and t_r also changes with same trend as the value of the steady state. For $K_e > K_f$, t_d and t_r values are not effected by the location of the disturbance. The settling time t_s decreases with the increase of support stiffness for $K_e \leq K_f$ but the value of t_s is maximum at $K_e = 100K_f$ (Table 5.15).

Table 5.16 shows that for $K_e \leq 10K_f$ the steady-state value is zero, for $K_e = 100K_f$ the steady-state value is not zero. For $K_e \leq 10K_f$ the value of t_s increases with the increase of the stiffness when the disturbance is applied at the bearing housing. The position of the disturbance (either at the mid-span or at the bearing housing) does not effect the settling time, for $K_e \leq 0.1K_f$. For $k_f < k_e < 10k_f$, it takes less time to settle the vibration, when the disturbance is at mid-span (Table 5.16). The system with an LQS controller having the second set of weighting factors achieves a zero steady-state deflection except at $K_e = 0.01K_f$ and $K_e = 10K_f$ when the disturbance is applied vertically at mid-span and bearing housing respectively (Table 5.17). The

value of M_p increases from $6125(10^{-10})$m to $6569(10^{-10})$m when the stiffness increases from $0.01K_f$ to $0.1K_f$, the value of M_p decreases as the support stiffness increases if $K_e > 0.1K_f$. From Table 5.17 one finds that the largest peak value (M_p) is at $K_e = 0.1K_f$ and the minimum peak time (t_p) is at $K_e = K_f$; settling time (t_s) increases with the increase of the support stiffness. For any support stiffness the value of t_p is not affected by the position of the disturbance; the value of t_s varies on the location of the disturbance when $K_e \leq 0.1K_f$ and the location of disturbance does not affect t_s when $K_e \geq K_f$ (Table 5.17)

Table 5.18 shows the result of the system with the SVFB controller when shaft speed is taken as 15000 rpm (above the critical speed of the rotor). The controller is used with the second set of weighting factors. One observes that the maximum steady-state value is at $K_e = 0.01K_f$, the minimum value of steady-state deflection is at $K_e = 100K_f$. The delay time is maximum at $K_e = 0.1K_f$ and minimum at $K_e \geq 10K_f$ when disturbance is applied either at the bearing housing or at the mid-span. The maximum rise time is observed at $K_e = 0.01K_f$, the minimum rise time is obtained at $K_e \geq 10K_f$. The settling time is maximum at $K_e = 0.01K_f$ and minimum at $K_e = 100K_f$ when the disturbance is applied at the bearing housing and the mid-span. For any value of support stiffness, t_d, t_r, t_s is always less for the disturbance at mid-span as compared to the values when the disturbance is applied at the bearing housing, except at $K_e \geq 10K_f$ where the value of t_r is same irrespective of the location of the disturbance. The values of t_r, t_s and steady-state decrease when the value of K_e

increases (Table 5.18).

Table 5.19 shows the characteristic values of the response of the system with ISVFB controller having the second set of weighting factors. The shaft speed is 15000 rpm. One observes that for the disturbance applied at bearing housing, the peak value (M_p) slightly increases from $13.75(10^{-10})$m to $13.826(10^{-10})$m when the support stiffness increases from $0.01K_f$ to $0.1K_f$. The value of M_p then decreases with the increase of the support stiffness. When the disturbance is applied at mid-span the value of M_p decreases from $747.6(10^{-10})$m to $746.22(10^{-10})$m when the stiffness changes from $0.01K_f$ to $0.1K_f$, the value of M_p increases to $747.12(10^{-10})$m at $K_e = K_f$; the value of M_p then decreases with the increase of the support stiffness (Table 5.19). The delay time t_d decreases with the increase of support stiffness when the disturbance is applied vertically at bearing housing. When the disturbance is applied at the mid-span then the value of t_d decreases from $10.5(10^{-3})$s to $10(10^{-3})$s for the stiffness changes from $0.01K_f$ to $0.1K_f$, when the support stiffness $K_e > K_f$ the delay time has the value of $15(10^{-3})$s. When the disturbance applied at the bearing housing, the settling time t_s increases with the increase of support stiffness except for $K_e = 0.1K_f$ and K_f. The value of t_s is 6.161s for $K_e = 0.1K_f$ (see Table 5.19).

Table 5.20 shows the (M_p), t_d, t_r, t_s values of the response curves, when LQS controller with the second set of weighting factors is used in the rotor-bearing system, when the shaft speed is 15000 rpm. One observes that when the stiffness

of the supports is increased from $0.01K_f$ to $0.1K_f$ the peak value increases from $6523.8(10^{-10})$m to $6579.7(10^{-10})$m; the peak values goes on decreasing on further increasing the stiffness of the supports and it reduces to $10.042(10^{-10})$m at $K_e = 100K_f$ (the disturbance is applied at the bearing housing). Similar trend of variation of the peak value is observed when the disturbance is applied at the mid-span (see Table 5.20). The settling time t_s increases as the stiffness of the supports is increased. The minimum value of t_p is observed at $K_e = K_f$. The steady-state value at 15000 rpm is zero for all values of the support stiffness (Table 5.20).

5.6 Relative Suitability of different Controllers

The results presented in the previous sections show the response of the mid-span deflection of the rotor with the different controllers and under the different conditions. These results have been obtained by considering two sets of weighting factors as mentioned previously. These results are discussed here so that the performance of SVFB, ISVFB and LQS controllers can be compared. The system represented by model II is found to be stable at a low shaft speed of 500 rpm and at higher speeds (at and above 1500 rpm) the system becomes unstable (see Table 5.1). The results show a higher peak value (11×10^{-6}m for vertical deflection and 10^{-6}m for horizontal deflection) when a disturbance is applied at the mid-span as compared to the peak values (9.86×10^{-6}m for vertical deflection and 5.6×10^{-7}m for horizontal deflection)

obtained owing to a disturbance at the bearing housing (Figs. 5.1 and 5.2). The mid-span deflection of the system with a state variable feedback (SVFB) controller shows a better damped response than that of the system without a controller (Fig. 5.3 to 5.6). The steady state values of the mid-span vertical deflection of the system without a controller are $7.042(10^{-6})$ and $11(10^{-6})$m for the disturbance at the bearing housing and the mid span respectively. The speed of shaft in this case is 500 rpm. For an SVFB controller with the first set of weighting factors, at 500 rpm, the steady-state values are $2.9419(10^{-6})$m and $2.25(10^{-5})$m. When the second set of weighting factors are used at 500 rpm the steady state values reduce to $3.75(10^{-9})$m and $7.625(10^{-8})$m (see Figures 5.3(a-b) and 5.5(a-b)). The results show that the SVFB controller with the first set of weighting factors damps out the vibration but yields a finite value of the steady state deflection. The value of this steady-state deflection is greater than the value given by the system without a controller. Using the second set of weighting factors the steady state value is reduced to a level lower than the steady state value of the system without a controller. Thus an SVFB controller can be used to control the vibration of the system and with proper tuning of the controller a desired value of the steady state deflection can be obtained. However, a steady state value of zero can not be achieved by this controller.

An integral plus state variable feedback (ISVFB) controller with the first set of weighting factors responds quickly to a disturbance in that the mid-span deflection reaches a steady state deflection following the same trend as in the case of an SVFB

controller with the second set of weighting factors. When a disturbance is applied on the bearing housing, the steady state value decreases with the increase of shaft speed (Table 5.6). If a disturbance is applied on the mid-span, the steady state value at a shaft speed of 500 rpm is $8.312(10^{-8})$m and for all higher shaft speeds a constant steady-state value of $7.625(10^{-8})$m is observed (Table 5.7). These results show that the an ISVFB controller with the first set of weighting factors provide a better control than an SVFB controller. The system with an ISVFB controller with the second set of weighting factors achieves a zero-steady state deflection in 6.923s when the rotor runs below the critical speed; it takes 6.105s when the rotor runs at above critical speed (Tables 5.8 and 5.9).

When an LQS controller with the first set of weighting factors is employed in the system, the system exhibits oscillatory behavior before approaching the steady state condition as shown in Figures 5.13 and 5.14. The peak value (M_p) of the oscillation is $12.25(10^{-6})$m for all shaft speeds when a disturbance is applied at the bearing housing. On the other hand when the disturbance is applied at the mid-span the value of M_P is observed as $12.375(10^{-6})$m for a shaft speed in the range of 500 to 2500 rpm; the value of M_P changes to $12.25(10^{-6})$m at a shaft speed of 3000 rpm and above (Tables 5.10 and 5.11). The steady state value of the responses for all shaft speed is zero when a disturbance is applied at the bearing housing. On the other hand when the disturbance is applied at the mid-span the steady state value of the response is $-1.25(10^{-7})$m at a shaft speed of 3000 rpm and above. The settling

time (t_s) and the peak value (M_p) of the response of an LQS controller with the first set of weighting factors are of higher value than those of the response of an ISVFB controller with the second set of weighting factors (see Tables 5.9 to 5.12).

When an LQS controller with the second set of weighting factors is employed an improved disturbance rejection quality is observed(Figures 5.15 and 5.16). The peak value is lower compared to the previous case but still its magnitude is greater than the peak value of the response obtained by employing an ISVFB controller with the second set of weighting factors. The settling time (t_s) decreases to a value of 0.378s (at a speed of 500 rpm and it further decreases with the increase of shaft speed) in comparison to the value of t_s when ISVFB controller is employed(see Table 5.8, 5.10 and 5.12). Observation of the results reveals that an LQS controller with proper tuning controls the system against a disturbance and achieves a steady state value of zero in less time as compared to any other controller. The results of the response for different support stiffness (K_e) show that $K_e = 0.1K_f$ is not a suitable selection for the bearing supports. When the control system fails then the most favorable stiffness for the safety of the system is $K_e \geq K_f$.

It can be concluded that for a system that requires a quick control action in rejecting the external disturbance an LQS controller is preferable. While for a system that requires a smooth control of the disturbances as well as any desired level of steady-state deflection, an ISVFB controller is suitable. An SVFB controller can be employed in the system if a non-zero steady state deflection is acceptable.

Chapter 6

Conclusion

Two different models of rotor-bearing system are presented. The derivation of dynamic equations of each of the models are presented. Three different controllers (SVFB, ISVFB and LQS) are developed on the basis of modern control theory. The performance of each of the three controllers is simulated using a digital computer. An initial study is made on the most generic type of representative model of a single disk flexible rotor on rigid supports (model I). The performance of the controllers is studied by applying a unit-step disturbance at the mid-span of the rotor. The response is obtained by considering different shaft speeds. With the aid of these results one can observe the performance characteristics of the systems with and without a controller. The results of the system without a controller shows that the system which is stable at low speed (i.e., up to 4500 rpm) but the system becomes unstable at a higher rotor speed (i.e., at and above 10000 rpm). It implies that

at low speeds the cross-coupling effect of the oil-film is not so significant but at higher speeds the effect of cross-coupling is significant. When an SVFB controller is employed the disturbance is damped out smoothly without any oscillation. The steady state deflection of the rotor can be set to a desired level by proper tuning of the weighting matrices. The results of an ISVFB controller show that a versatile control strategy can be achieved by this controller. This type of controller can be tuned to get a zero steady state deflection as well as any level of steady state value. An LQS controller brings the system to a zero steady state at a faster rate than an ISVFB controller. However, the system with an LQS controller show an oscillation in the system before reaching the steady state; the system with an ISVFB controller show no oscillation in reaching the steady state.

The study has been directed towards a model comprising of single disk flexible rotor mounted on flexible supports (model II). The results show that the system becomes unstable when shaft runs at and above a speed of 1500 rpm. All the three controllers (SVFB, ISVFB and LQS) make the system stable and control it against an external disturbance. Specially an LQS controller exhibits a better performance in this model as compared to the previous model. In order to observe the safety provision in the case of failure of the active components of the control system, the effect of the stiffness of the supports on the performance of the system with and without a controller has also been studied. The results show that the system without a controller exhibits a stable response against the external disturbance when

the cross-coupling stiffness and damping coefficients of the oil-film are considered to be zero. When the cross-coupling terms are taken into consideration then the system is stable at low speeds of the rotor and becomes unstable at higher speed particularly above the critical speed. It can be concluded that it is not suitable to consider the cross-coupling terms negligible in the study of the vibration control of the rotor-bearing system.

It may thus be summarized that the optimal control theory provides a useful mathematical tool for the design of vibration control system. In the light of the above finding one can apply either a SVFB or ISVFB or LQS controller for safe-run of a rotor bearing system. This is only a specific example of practical implication of these control schemes. It would appear that these schemes can be applied to a complex rotor with multiple disks or to complex suspension systems.

6.1 Suggestions for Further Work

- This study may be expanded to include different types of inputs and other controllers.
- Other models of rotor-bearing system (which may include flexible supports, dampers, multiple disk rotor, etc.) of practical importance may be studied with these controllers.

- The performance of the controllers may be studied by applying inputs on the non-rotating part of the rotor-bearing system.

- In the present study an external disturbance of step-function is considered; the study may be expanded by applying other types of disturbance.

- An experimental set up may be designed so that the performance of the controllers may be studied experimentally.

Appendix A

Controllability and Observability test of the Models

Flexible Rotor in Flexible Bearings Mounted on Rigid Supports (Model-I)

Derivation of equations of motion in state variable form of this system is presented in Chapter 2. Denoting the non-zero elements by × the equation of the system in matrix form can be written as,

$$\begin{bmatrix} \dot{x}_1 \\ \dot{x}_2 \\ \dot{x}_1 \\ \dot{x}_4 \\ \dot{x}_5 \\ \dot{x}_6 \\ \dot{x}_7 \\ \dot{x}_8 \end{bmatrix} = \begin{bmatrix} 0 & \times & 0 & 0 & 0 & 0 & 0 & 0 \\ \times & \times & \times & 0 & \times & \times & 0 & 0 \\ 0 & 0 & 0 & \times & 0 & 0 & 0 & 0 \\ \times & 0 & \times & 0 & 0 & 0 & 0 & 0 \\ 0 & 0 & 0 & 0 & 0 & \times & 0 & 0 \\ \times & \times & 0 & 0 & \times & \times & \times & 0 \\ 0 & 0 & 0 & 0 & 0 & 0 & 0 & \times \\ 0 & 0 & 0 & 0 & \times & 0 & \times & 0 \end{bmatrix} \begin{bmatrix} x_1 \\ x_2 \\ x_3 \\ x_4 \\ x_5 \\ x_6 \\ x_7 \\ x_8 \end{bmatrix} + \begin{bmatrix} 0 & 0 & 0 & 0 \\ \times & 0 & 0 & 0 \\ 0 & 0 & 0 & 0 \\ 0 & \times & 0 & 0 \\ 0 & 0 & 0 & 0 \\ 0 & 0 & \times & 0 \\ 0 & 0 & 0 & 0 \\ 0 & 0 & 0 & \times \end{bmatrix} \begin{bmatrix} f_1 \\ f_2 \\ f_3 \\ f_4 \end{bmatrix} \tag{A.1}$$

Input is applied vertically at the mid-span, hence the input coefficient matrix reduces to the following form

$$\mathbf{b}_1 = \begin{bmatrix} 0 & 0 & 0 & \frac{1}{m_f} & 0 & 0 & 0 & 0 \end{bmatrix}^T \tag{A.2}$$

The structure of the matrix **A** is shown in Fig 2. and test for state accessibility can be done using the algorithm developed by Burrows and Sahinkaya [8].

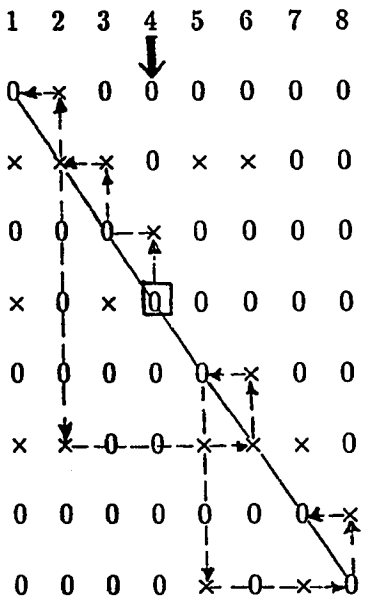

Fig. 2. Test for accessibility on matrix A.

The input is applied to state x_4 and this affects state x_3. Column 3 shows x_3 is connected to states x_2 and x_4. State x_2 is reached thrpugh the path from the location a_{33} to

a_{22}. Column 2 shows x_2 is connected to states x_1 and x_6. Again x_1 is reached through the pathfrom a_{22} to the location a_{11} which is a zero but this is admissible as it lies along the disgonal. Now clumn 1 shows that x_1 is connected to states x_2, x_4 and x_6. Return to column 2, then element a_{62} allows state x_6 to be reached(alternatively we could have used element a_{61} in column 1). State x_6 is connected to state x_5 through element a_{56}. State x_5 is connected to state x_8 through element a_{85}. Finally state x_7 is reached from state x_8 by the path through element a_{78}. Thus the system is checked to be accessible by the input applied at mid-span. To test for a dilation, that is the occurence of form II as described in chapter 3, the algorithm is applied in the following way,

$$\left(\mathbf{A} \vdots \mathbf{b}_1\right) = \begin{bmatrix} 0 & \times & 0 & 0 & 0 & 0 & 0 & 0 & 0 \\ \times & \times & \times & 0 & \times & \times & 0 & 0 & 0 \\ 0 & 0 & 0 & \times & 0 & 0 & 0 & 0 & 0 \\ \times & 0 & \times & 0 & 0 & 0 & 0 & 0 & \times \\ 0 & 0 & 0 & 0 & 0 & \times & 0 & 0 & 0 \\ \times & \times & 0 & 0 & \times & \times & \times & 0 & 0 \\ 0 & 0 & 0 & 0 & 0 & 0 & 0 & \times & 0 \\ 0 & 0 & 0 & 0 & \times & 0 & \times & 0 & 0 \end{bmatrix} \begin{matrix} 1 \\ 2 \\ 3 \\ 4 \\ 5 \\ 6 \\ 7 \\ 8 \end{matrix} \tag{A.3}$$

$$\left(\mathbf{A} \vdots \mathbf{b}_1\right)_2 = \begin{bmatrix} 0 & \times & 0 & 0 & 0 & 0 & 0 & 0 & 0 \\ 0 & 0 & 0 & \times & 0 & 0 & 0 & 0 & 0 \\ 0 & 0 & 0 & 0 & 0 & \times & 0 & 0 & 0 \\ 0 & 0 & 0 & 0 & 0 & 0 & 0 & \times & 0 \\ 0 & 0 & 0 & 0 & \times & 0 & \times & 0 & 0 \\ \times & 0 & \times & 0 & 0 & 0 & 0 & 0 & \times \\ \times & \times & \times & 0 & \times & \times & 0 & 0 & 0 \\ \times & \times & 0 & 0 & \times & \times & \times & 0 & 0 \end{bmatrix} \begin{matrix} 1 \\ 3 \\ 5 \\ 7 \\ 8 \\ 4 \\ 2 \\ 6 \end{matrix} \tag{A.4}$$

The rows of augmented matrix $(\mathbf{A}\vdots\mathbf{b}_1)$ are interchanged to form the new matrix $(\mathbf{A}\vdots\mathbf{b}_1)_2$ in which the rows are arranged in order according to the number of fixed(zero) elements that they contain. The rows 1,3,5 and 7 have one non-zero element and their order of priority in $(\mathbf{A}\vdots\mathbf{b}_1)_2$ is decided by their order of occurrence in $(\mathbf{A}\vdots\mathbf{b}_1)$. The procedure is described in chapter 3.

NAC1=(2) and NIC1=(2)×1

NAC2=(4) and NIC2=(2)×1; (4)×1

NAC3=(6) and NIC1=(2)×1; (4)×1;(6)×1

NAC4=(8) and NIC1=(2)×1; (4)×1;(6)×1;(8)×1

NAC5=(5,7) and NIC1=(2)×1; (4)×1;(6)×1;(8)×1;(5,7)×1

NAC6=(1,3,9) and NIC1=(2)×1; (4)×1;(6)×1;(8)×1;(5,7)×1;(1,3,9)×2

NAC7=(1,2,3,5,6) and NIC1=(1,2,3,5,6,7,9)×5; (4)×1;(8)×1

NAC8=(1,2,5,6,7) and NIC1=(1,2,3,5,6,7,9)×6; (4)×1;(8)×1

The results show that every row introduces a new independent column, therefore Form-II can not occur, hence there is no dilation in the independency of columns. Since it is found that all the states of the system are accessible by the applied input therefore, the system is structurally controllabe and hence completely controllable. Similarly the controllability of the system for the input applied to other location of the system can be checked.

Observability

The structural observability of the model-I can be checked by checking the structural controllability of the adjoint system of the model. The state variable coefficient matrix of adjoint system is the transpose ($\mathbf{A}^T$) of the coefficient matrix ($\mathbf{A}$) of the original system(see chappter-3), and bfA^T is shown in equation A.5. For the input at mid-span in the vertical direction, the inputs for the adjoint system would be such that they are applied at columns 3 and 4 simultaneously as shown in Fig.3.

$$\mathbf{A}^T = \begin{bmatrix} 0 & \times & 0 & \times & 0 & \times & 0 & 0 \\ \times & \times & 0 & 0 & 0 & \times & 0 & 0 \\ 0 & \times & 0 & \times & 0 & 0 & 0 & 0 \\ 0 & 0 & \times & 0 & 0 & 0 & 0 & 0 \\ 0 & \times & 0 & 0 & 0 & \times & 0 & \times \\ 0 & \times & 0 & 0 & \times & \times & 0 & 0 \\ 0 & 0 & 0 & 0 & 0 & \times & 0 & \times \\ 0 & 0 & 0 & 0 & 0 & 0 & \times & 0 \end{bmatrix} \tag{A.5}$$

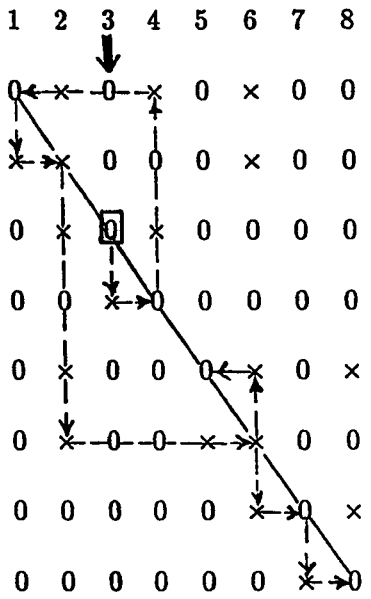

Fig. 3. Accessibility of the state coefficient matrix of adjoint system of Model-I.

Since input at position 3 accessed all the diagonal elements which implies that the sytem is structurally controllable by this input, so the input at position 7 is not required for accessibility test.

For dialation test of the independency of columns the augmented matrix of adjoint system can be written as,

$$\left(\mathbf{A}^* \;\vdots\; \mathbf{b}^*_1 \right) = \begin{bmatrix} 0 & \times & 0 & \times & 0 & \times & 0 & 0 & 0 \\ \times & \times & 0 & 0 & 0 & \times & 0 & 0 & 0 \\ 0 & \times & 0 & \times & 0 & 0 & 0 & 0 & \times \\ 0 & 0 & \times & 0 & 0 & 0 & 0 & 0 & 0 \\ 0 & \times & 0 & 0 & 0 & \times & 0 & \times & 0 \\ 0 & \times & 0 & 0 & \times & \times & 0 & 0 & 0 \\ 0 & 0 & 0 & 0 & 0 & \times & 0 & \times & 0 \\ 0 & 0 & 0 & 0 & 0 & 0 & \times & 0 & 0 \end{bmatrix} \begin{matrix} 1 \\ 2 \\ 3 \\ 4 \\ 5 \\ 6 \\ 7 \\ 8 \end{matrix} \tag{A.6}$$

$$\left(\mathbf{A}^* \;\vdots\; \mathbf{b}_1^* \right)_2 = \begin{bmatrix} 0 & 0 & \times & 0 & 0 & 0 & 0 & 0 & 0 \\ 0 & 0 & 0 & 0 & 0 & 0 & \times & 0 & 0 \\ 0 & 0 & 0 & 0 & 0 & \times & 0 & \times & 0 \\ 0 & \times & 0 & \times & 0 & \times & 0 & 0 & 0 \\ \times & \times & 0 & 0 & 0 & \times & 0 & 0 & 0 \\ 0 & \times & 0 & \times & 0 & 0 & 0 & 0 & \times \\ 0 & \times & 0 & 0 & \times & \times & 0 & 0 & 0 \\ 0 & \times & 0 & 0 & 0 & \times & 0 & \times & 0 \end{bmatrix} \begin{matrix} 4 \\ 8 \\ 7 \\ 2 \\ 1 \\ 3 \\ 6 \\ 5 \end{matrix} \qquad \text{(A.7)}$$

NAC1 = (3) and NIC1 = (3)×1
NAC2 = (7) and NIC1 = (3)×1; (7)×1
NAC3 = (6,8) and NIC1 = (3)×1; (7)×1; (6,8)×1
NAC4 = (1,2,6) and NIC1 = (3)×1; (7)×1; (1,2,6,8)×2
NAC5 = (2,4,6) and NIC1 = (3)×1; (7)×1; (1,2,4,6,8)×3
NAC6 = (2,4,9) and NIC1 = (3)×1; (7)×1; (1,2,4,6,8,9)×4
NAC7 = (2,5,6) and NIC1 = (3)×1; (7)×1; (1,2,4,5,6,8,9)×5
NAC8 = (2,6,8) and NIC1 = (3)×1; (7)×1; (1,2,4,5,6,8,9)×6

The results show that every row introduces a new column which implies that the system is free from dilation of columns. Hence adjoint of the system is controllable and in other words the system is observable with respect to the desired state variables. The same procedure can be followed to check the system's observability with respect to other state variables.

Following the same prosedure it can be shown that the model II of the rotor-bearing system is also controllable and observable [8].

Appendix B

Optimal Feedback Gain matrix

The objective of any feed back controller is to transfer a system from initial state $x(0) = x_o$ to the desired state x_e and in many cases the desired state is the equilibrium point of the system and same is the case for our system. Relative to the desired state x_e , the quantity (x(t) - x_e) can be taken as the instantaneous system error. If we transfer the system coordinates such that x_e becomes the origin then the new state x(t) is itself the error [44].

The itegral square error is,

$$J = \int_{t_o}^{t_1} [\sum_{i=1}^{n} (x_1(t))^2] dt = \int_{t_o}^{t_1} (\mathbf{X}^T(t).\mathbf{X}(t)) dt \tag{B.1}$$

is a reeasonable measure of the system transient response from time t_0 to t_1. To be more general,

$$J = \int_{t_o}^{t_1} [\mathbf{X}^T(t)\mathbf{Q}\mathbf{X}(t)] dt \tag{B.2}$$

with **Q** a real, symmetric, positive definite or positive semidefinite, constant matrix used as performance measure. The simplest form of **Q** that can be used is a diagonal matrix:

$$Q = \begin{bmatrix} q_1 & 0 & \cdots & 0 \\ 0 & q_2 & \cdots & 0 \\ \vdots & \vdots & \vdots & \vdots \\ 0 & 0 & \cdots & q_n \end{bmatrix} \tag{B.3}$$

To minimize the deviation of final state x(t_1) of the system from the desired state $x_e = 0$, a possible performance measure is

$$J = \mathbf{X}^T(t_1)\mathbf{H}\mathbf{X}(t_1) \tag{B.4}$$

where, **H** is a positive semidefinite, real, symmetric constant matrix. Hence, the performance index is modified to

$$J = \mathbf{X}^T(t_1)\mathbf{H}\mathbf{X}(t_1) + \int_{t_o}^{t_1} [\mathbf{X}^T(t)\mathbf{Q}\mathbf{X}(t)] dt \tag{B.5}$$

To get more realistic solution to the problem the performance index can be modified by adding an energy minimizing term for physical constraints on **u**.

$$J = \int_{t_o}^{t_1} [\mathbf{u}^T(t)\mathbf{R}\mathbf{u}(t)]dt \tag{B.6}$$

where, **R** is a positive definite, real, symmetric constant matrix.

For the state optimal controllers, a useful performance measure is therefore given by

$$J = 1/2[\mathbf{X}^T(t_1)\mathbf{H}\mathbf{X}(t_1)] + 1/2\int_{t_o}^{t_1} [\mathbf{X}^T(t)\mathbf{Q}\mathbf{X}(t) + \mathbf{u}^T(t)\mathbf{R}\mathbf{u}(t)]dt \tag{B.7}$$

If the terminal time is not constrained, i.e., $t_1 \rightarrow \infty$, and importance is given to approach the equilibrium state $x_e = 0$. So the terminal constraint in the performance index is not necessary. For infinite-time state controller, the performance index is

$$J = 1/2\int_{o}^{\infty} [\mathbf{X}^T(t)\mathbf{Q}\mathbf{X}(t) + \mathbf{u}^T(t)\mathbf{R}\mathbf{u}(t)]dt \tag{B.8}$$

The control law which minimizes (4.8) will be have the following form:

$$\mathbf{u} = -\mathbf{K}\mathbf{X} \tag{B.9}$$

Where, **K** is the state variable feedback and **K** is a constant matrix if **A**, **B**, **C**, **Q**, and **R** are constant matrices. Equation (4.1) then becomes

$$\dot{\mathbf{X}} = (\mathbf{A} - \mathbf{B}\mathbf{K})\mathbf{X} \tag{B.10}$$

Kalman [35] has shown that the closed-loop system

$$\dot{\mathbf{X}} = (\mathbf{A} - \mathbf{B}\mathbf{K})\mathbf{X} \tag{B.11}$$

is stable if **K** is computed as follows:

We assume that **K** is such that the system is stable. Assume the existance of a symmetric differentiable matrix **P**(t) such that $\mathbf{X}^T\mathbf{P}\mathbf{X}$ is a scalar. **P** is n×n matrix. Differentiating $\mathbf{X}^T\mathbf{P}\mathbf{X}$ with respect to time using Eq. (4.1) and adding and subtracting the integrand (4.8), we get,

$$d/dt(\mathbf{X}^T\mathbf{P}\mathbf{X}) = \dot{\mathbf{X}}^T\mathbf{P}\mathbf{X}+\mathbf{X}^T\dot{\mathbf{P}}\mathbf{X}+\mathbf{X}^T\mathbf{P}\dot{\mathbf{X}} = (\mathbf{A}\mathbf{X}+\mathbf{B}\mathbf{u})^T\mathbf{P}\mathbf{X}+\mathbf{X}^T\dot{\mathbf{P}}\mathbf{X}+\mathbf{X}^T\mathbf{P}(\mathbf{A}\mathbf{X}+\mathbf{B}\mathbf{u})$$

$$= \mathbf{X}^T(\mathbf{A}^T\mathbf{P}+\mathbf{P}\mathbf{A}+\dot{\mathbf{P}})\mathbf{X}+\mathbf{u}^T\mathbf{B}^T\mathbf{P}\mathbf{X}+\mathbf{X}^T\mathbf{P}\mathbf{B}\mathbf{u}$$

$$\Rightarrow 1/2\int_o^\infty d/dt(\mathbf{X}^T\mathbf{P}\mathbf{X})dt = 1/2\int_o^\infty [\mathbf{X}^T(\mathbf{A}^T\mathbf{P}+\mathbf{P}\mathbf{A}+\dot{\mathbf{P}})\mathbf{X}+\mathbf{u}^T\mathbf{B}^T\mathbf{P}\mathbf{X}+\mathbf{X}^T\mathbf{P}\mathbf{B}\mathbf{u}]dt+$$

$$1/2\int_o^\infty (\mathbf{X}^T\mathbf{Q}\mathbf{X}+\mathbf{u}^T\mathbf{R}\mathbf{u})dt - 1/2\int_o^\infty (\mathbf{X}^T\mathbf{Q}\mathbf{X}+\mathbf{u}^T\mathbf{R}\mathbf{u})dt$$

$$\Rightarrow 1/2(\mathbf{X}^T\mathbf{P}\mathbf{X})_0^\infty = 1/2\int_o^\infty [\mathbf{X}^T(\mathbf{A}^T\mathbf{P}+\mathbf{P}\mathbf{A}+\dot{\mathbf{P}}+\mathbf{Q})\mathbf{X}+\mathbf{u}^T\mathbf{B}^T\mathbf{P}\mathbf{X}+\mathbf{X}^T\mathbf{P}\mathbf{B}\mathbf{u}+\mathbf{u}^T\mathbf{R}\mathbf{u})]dt$$

$$-1/2\int_o^\infty (\mathbf{X}^T\mathbf{Q}\mathbf{X}+\mathbf{u}^T\mathbf{R}\mathbf{u})dt$$

$$\Rightarrow 1/2[\mathbf{X}^T(\infty)\mathbf{P}(\infty)\mathbf{X}(\infty) - \mathbf{X}^T(0)\mathbf{P}(0)\mathbf{X}(0)]$$

$$= 1/2\int_o^\infty [\mathbf{X}^T(\mathbf{A}^T\mathbf{P}+\mathbf{P}\mathbf{A}+\dot{\mathbf{P}}+\mathbf{Q})\mathbf{X}+\mathbf{X}^T\mathbf{P}\mathbf{B}\mathbf{u}+\mathbf{u}^T(\mathbf{B}^T\mathbf{P}\mathbf{X}+\mathbf{R}\mathbf{u})]dt \qquad \text{(B.12)}$$

If $\mathbf{P}(t)$ does not approach infinity as $t \rightarrow \infty$ then, $\mathbf{X}^T(\infty)\mathbf{P}(\infty)\mathbf{X}(\infty) = 0$, since $\mathbf{X}(\infty) \rightarrow 0$ from stability assumption. By considering

$$\mathbf{A}^T\mathbf{P}+\mathbf{P}\mathbf{A}+\dot{\mathbf{P}}+\mathbf{Q} = \mathbf{P}\mathbf{B}\mathbf{R}^{-1}\mathbf{B}^T\mathbf{P} \qquad \text{(B.13)}$$

Equation (B.12) becomes

$$-1/2(\mathbf{X}^T(0)\mathbf{P}(0)\mathbf{X}(0)) = 1/2\int_o^\infty [\mathbf{X}^T\mathbf{P}\mathbf{B}+\mathbf{u}^T\mathbf{R}]\mathbf{R}^{-1}[\mathbf{B}^T\mathbf{P}\mathbf{X}+\mathbf{R}\mathbf{u}]dt - J$$

$$\Rightarrow J = 1/2(\mathbf{X}^T(0)\mathbf{P}(0)\mathbf{X}(0)) + 1/2\int_o^\infty [\mathbf{X}^T\mathbf{P}\mathbf{B}+\mathbf{u}^T\mathbf{R}]\mathbf{R}^{-1}[\mathbf{B}^T\mathbf{P}\mathbf{X}+\mathbf{R}\mathbf{u}]dt \qquad \text{(B.14)}$$

But $\mathbf{X}(0)$ and $\mathbf{P}(0)$ are independent of the control input $\mathbf{u}$, which is to be chosen. Now, J can be minimized by considering only the integrand of Eq. (B.14). Again, J is non-negative and therefore has a minimum of zero. This minimum occurs at

$$\mathbf{B}^T\mathbf{P}\mathbf{X}+\mathbf{R}\mathbf{u} = 0 \Rightarrow \mathbf{u} = -\mathbf{R}^{-1}\mathbf{B}^T\mathbf{P}\mathbf{X} \qquad \text{(B.15)}$$

The time-invarient nature of the problem implies that $\mathbf{P}$ should be constant, therefore, $\dot{\mathbf{P}} = 0$ and hence, Eq. (4.13) becomes

$$\mathbf{A}^T\mathbf{P}+\mathbf{P}\mathbf{A}+\mathbf{Q}-\mathbf{P}\mathbf{B}\mathbf{R}^{-1}\mathbf{B}^T\mathbf{P} = 0 \qquad \text{(B.16)}$$

Hence, the control law that minimizes (4.9) is given by

$$\begin{aligned} &\mathbf{u} = -\mathbf{K}\mathbf{X} \\ &\mathbf{K} = \mathbf{R}^{-1}\mathbf{B}^T\mathbf{P} \\ &\mathbf{A}^T\mathbf{P}+\mathbf{P}\mathbf{A}+\mathbf{Q}-\mathbf{P}\mathbf{B}\mathbf{R}^{-1}\mathbf{B}^T\mathbf{P} = 0 \end{aligned} \qquad \text{(B.17)}$$

Appendix C

Coefficient and Controller Matrices for Mdel-I and Model-II

Model-I

State variable Feedback Controller

Coefficient matrices of the system are:

$$\mathbf{A} = \begin{bmatrix} 0 & 1.0 & 0 & 0 & 0 & 0 \\ -2.3931\times10^{8} & -2.9070\times10^{6} & 7.1000\times10^{7} & 0 & -9.9142\times10^{7} & -6.8081\times10^{5} \\ 0 & 0 & 0 & 1.0 & 0 & 0 \\ 1.1517\times10^{6} & 0 & -1.1517\times10^{6} & 0 & 0 & 0 \\ 0 & 0 & 0 & 0 & 0 & 1.0 \\ 1.2546\times10^{7} & -6.8081\times10^{5} & 0 & 0 & -1.0540\times10^{8} & -4.0102\times10^{5} \\ 0 & 0 & 0 & 0 & 0 & 0 \\ 0 & 0 & 0 & 0 & 1.1517\times10^{6} & 0 \end{bmatrix}$$

$$\begin{bmatrix} 0 & 0 \\ 0 & 0 \\ 0 & 0 \\ 0 & 0 \\ 0 & 0 \\ 7.1000\times10^{7} & 0 \\ 0 & 1.0 \\ -1.1517\times10^{6} & 0 \end{bmatrix}$$

123

$$\mathbf{B} = \begin{bmatrix} 0 & 0 & 0 & 0 \\ 5.0 & 0 & 0 & 0 \\ 0 & 0 & 0 & 0 \\ 0 & 8.1103\times10^{-2} & 0 & 0 \\ 0 & 0 & 0 & 0 \\ 0 & 0 & 5.0 & 0 \\ 0 & 0 & 0 & 0 \\ 0 & 0 & 0 & 8.1103\times10^{-2} \end{bmatrix}$$

The following weighting factors are used to compute the gain and control matrices:

- the first set of values of weighting factors are: $q_1=q_2=\cdots\cdots=q_8=1$; and $r_1=r_3=10^{-10}$, $r_2=r_4=10^{-8}$
- the second set of values of weighting factors are: $q_3=q_7=10^6$,$q_1=q_2=q_4=q_5=q_6=q_8=1$; and $r_1=r_3=10^{-10}$, $r_2=r_4=10^{-8}$

using the first set of weighting factors the following gain and control matrices are obtained:

$$\mathbf{K} = \begin{bmatrix} 2.196\times10^{7} & 1.149\times10^{4} & -2.237\times10^{7} & 2.855\times10^{3} & -9.315\times10^{6} & -1.345\times10^{4} \\ 9.637\times10^{5} & 4.631\times10^{-1} & -4.430\times10^{5} & 9.406\times10^{3} & -1.930\times10^{5} & -6.731\times10^{-1} \\ -4.667\times10^{6} & -1.345\times10^{4} & 9.658\times10^{6} & -4.150\times10^{3} & 5.556\times10^{7} & 6.099\times10^{4} \\ -3.726\times10^{5} & -8.446\times10^{-1} & 3.033\times10^{5} & 5.896\times10^{2} & 1.947\times10^{6} & 3.477 \end{bmatrix}$$

$$\begin{bmatrix} 8.079\times10^{6} & -5.207\times10^{3} \\ 4.128\times10^{5} & 5.896\times10^{2} \\ -5.338\times10^{7} & 2.143\times10^{4} \\ -1.664\times10^{6} & 7.332\times10^{3} \end{bmatrix}$$

$$\mathbf{A_c} = \begin{bmatrix} 0 & 1.0 & 0 & 0 & 0 & 0 \\ -3.491\times10^{8} & -2.965\times10^{6} & 1.829\times10^{8} & -1.427\times10^{4} & -5.257\times10^{7} & -6.136\times10^{5} \\ 0 & 0 & 0 & 1.0 & 0 & 0 \\ 1.074\times10^{6} & -3.756\times10^{-2} & -1.116\times10^{6} & -7.629\times10^{2} & 1.565\times10^{4} & 5.459\times10^{-2} \\ 0 & 0 & 0 & 0 & 0 & 1.0 \\ 3.588e\times10^{7} & -6.136\times10^{5} & -4.829\times10^{7} & 2.075\times10^{4} & -3.832\times10^{8} & -7.060\times10^{5} \\ 0 & 0 & 0 & 0 & 0 & 0 \\ 3.022\times10^{4} & 6.850\times10^{-2} & -2.460\times10^{4} & -4.782\times10^{1} & 9.938\times10^{5} & -2.820\times10^{-1} \end{bmatrix}$$

$$\begin{bmatrix} 0 & 0 \\ -4.040\times10^{7} & 2.604\times10^{4} \\ 0 & 0 \\ -3.348\times10^{4} & -4.782e\times10^{1} \\ 0 & 0 \\ 3.379\times10^{8} & -1.072\times10^{5} \\ 0 & 1.0 \\ -1.017\times10^{6} & -5.947\times10^{2} \end{bmatrix}$$

using the second set of weighting factors the following gain and control matrices are obtained:

$$\mathbf{K} = \begin{bmatrix} 6.404\times10^{7} & 1.150\times10^{4} & -2.010\times10^{7} & 1.118\times10^{4} & -7.864\times10^{6} & -1.346\times10^{4} \\ 4.263\times10^{6} & 1.8134 & 2.880\times10^{6} & 1.298\times10^{4} & -1.770\times10^{5} & -1.8225 \\ -5.102\times10^{6} & -1.346\times10^{4} & 4.180\times10^{6} & -1.124\times10^{4} & 9.012\times10^{7} & 6.105\times10^{4} \\ -2.472\times10^{5} & -1.8773 & 3.655\times10^{4} & 3.721\times10^{2} & 4.986\times10^{6} & 8.67172 \end{bmatrix}$$

$$\begin{bmatrix} 2.010\times10^{6} & -1.157\times10^{4} \\ 1.137\times10^{5} & 3.721\times10^{2} \\ -3.047\times10^{7} & 5.346\times10^{4} \\ 2.642\times10^{6} & 1.162\times10^{4} \end{bmatrix}$$

$$\mathbf{A_c} = \begin{bmatrix} 0 & 1.0 & 0 & 0 & 0 & 0 \\ -5.595\times10^{8} & -2.965\times10^{6} & 1.715\times10^{8} & -5.590\times10^{4} & -5.982\times10^{7} & -6.135\times10^{5} \\ 0 & 0 & 0 & 1.0 & 0 & 0 \\ 8.059\times10^{5} & -1.471\times10^{-1} & -1.385\times10^{6} & -1.052\times10^{3} & 1.436\times10^{4} & 1.478\times10^{-1} \\ 0 & 0 & 0 & 0 & 0 & 1.0 \\ 3.806\times10^{7} & -6.135\times10^{5} & -2.090\times10^{7} & 5.618\times10^{4} & -5.560\times10^{8} & -7.063\times10^{5} \\ 0 & 0 & 0 & 0 & 0 & 0 \\ 2.005\times10^{4} & 1.523\times10^{-1} & -2.964\times10^{3} & -3.018\times10^{1} & 7.473\times10^{5} & -7.033\times10^{-1} \end{bmatrix}$$

$$\begin{bmatrix} 0 & 0 \\ -1.005\times10^{7} & 5.787\times10^{4} \\ 0 & 0 \\ -9.217\times10^{3} & -3.018\times10^{1} \\ 0 & 0 \\ 2.233\times10^{8} & -2.673\times10^{5} \\ 0 & 1.0 \\ -1.366\times10^{6} & -9.427\times10^{2} \end{bmatrix}$$

Integral plus Satate variable Feedback controller

Augmented matrix $\mathbf{A}_a$ of the system is;

$$\mathbf{A}_a = \begin{bmatrix} 0 & 1.0 & 0 & 0 & 0 & 0 \\ -2.393\times10^{8} & -2.907\times10^{6} & 7.10\times10^{7} & 0 & -9.914\times10^{7} & -6.808\times10^{5} \\ 0 & 0 & 01.0 & 0 & 0 & \\ 1.152\times10^{6} & 0 & -1.152\times10^{6} & 0 & 0 & 0 \\ 0 & 0 & 0 & 0 & 0 & 1.0 \\ 1.255\times10^{7} & -6.808\times10^{5} & 0 & 0 & -1.054\times10^{8} & -4.010\times10^{5} \\ 0 & 0 & 0 & 0 & 0 & 0 \\ 0 & 0 & 0 & 0 & 1.152\times10^{6}0 & \\ 0 & 0 & 1.0 & 0 & 0 & 0 \\ 0 & 0 & 0 & 0 & 0 & 0 \end{bmatrix}$$

$$\begin{bmatrix} 0 & 0 & 0 & 0 \\ 0 & 0 & 0 & 0 \\ 0 & 0 & 0 & 0 \\ 0 & 0 & 0 & 0 \\ 0 & 0 & 0 & 0 \\ 7.10\times10^{7} & 0 & 0 & 0 \\ 0 & 1.0 & 0 & 0 \\ -1.152\times10^{6} & 0 & 0 & 0 \\ 0 & 0 & 0 & 0 \\ 1.0 & 0 & 0 & 0 \end{bmatrix}$$

Augmented matrix $\mathbf{B}_a$ of the system is;

$$B_a = \begin{bmatrix} 0 & 0 & 0 & 0 \\ 5.0 & 0 & 0 & 0 \\ 0 & 0 & 0 & 0 \\ 0 & 8.110\times10^{-2} & 0 & 0 \\ 0 & 0 & 0 & 0 \\ 0 & 0 & 5.0 & 0 \\ 0 & 0 & 0 & 0 \\ 0 & 0 & 0 & 8.11\times10^{-2} \\ 0 & 0 & 0 & 0 \\ 0 & 0 & 0 & 0 \end{bmatrix}$$

the following weighting factors are used to compute the gain and control matrices:

- the first set of values of weighting factors are: $q_3 = q_7 = 10^6$, $q_1 = q_2 = q_4 = q_5 = q_6 = q_8 = q_9 = q_{10} = 1$; and $r_1 = r_3 = 10^{-10}$, $r_2 = r_4 = 10^{-8}$ $q_9 = q_{10} = 1$ and 10^6
- the second set of values of weighting factors are: $q_3 = q_7 = q_9 = q_{10} = 10^6$, $q_1 = q_2 = q_4 = q_5 = q_6 = q_8 = 1$; and $r_1 = r_3 = 10^{-10}$, $r_2 = r_4 = 10^{-8}$

using the first set of weighting factors the following gain and control matrices are obtained:

$$A_c = \begin{bmatrix} 0 & 1.0 & 0 & 0 & 0 & 0 \\ -5.595\times10^{8} & -2.965\times10^{6} & 1.715\times10^{8} & -5.590\times10^{4} & -5.982\times10^{7} & -6.135\times10^{5} \\ 0 & 0 & 0 & 1.0 & 0 & 0 \\ 8.059\times10^{5} & -1.471\times10^{-1} & -1.385\times10^{6} & -1.052\times10^{3} & 1.436\times10^{4} & 1.478\times10^{-1} \\ 0 & 0 & 0 & 0 & 01.0 & \\ 3.806\times10^{7} & -6.135\times10^{5} & -2.090\times10^{7} & 5.618\times10^{4} & -5.560\times10^{8} & -7.063\times10^{5} \\ 0 & 0 & 0 & 0 & 0 & 0 \\ 2.005\times10^{4} & 1.523\times10^{-1} & -2.964\times10^{3} & -3.018\times10^{1} & 7.473\times10^{5} & -7.033\times10^{-1} \\ 0 & 0 & 1.0 & 0 & 0 & 0 \\ 0 & 0 & 0 & 0 & 0 & 0 \end{bmatrix}$$

$$\begin{bmatrix} 0 & 0 & 0 & 0 \\ -1.005\times10^{7} & 5.787\times10^{4} & -3.296\times10^{5} & -3.600\times10^{4} \\ 0 & 0 & 0 & 0 \\ -9.217\times10^{3} & -3.018\times10^{1} & -6.069\times10^{2} & -1.094\times10^{1} \\ 0 & 0 & 0 & 0 \\ 2.233\times10^{8} & -2.673\times10^{5} & 3.599\times10^{4} & -3.159\times10^{5} \\ 0 & 1.0 & 0 & 0 \\ -1.366\times10^{6} & -9.427\times10^{2} & 1.269\times10^{1} & -6.258\times10^{2} \\ 0 & 0 & 0 & 0 \\ 1.0 & 0 & 0 & 0 \end{bmatrix}$$

using the second set of weighting factors the following gain and control matrices are obtained:

$$\mathrm{K} = \begin{bmatrix} 6.429\times10^{7} & 1.151\times10^{4} & -2.004\times10^{7} & 1.124\times10^{4} & -7.815\times10^{6} & -1.346\times10^{4} \\ 4.290\times10^{6} & 1.823 & 2.887\times10^{6} & 1.298\times10^{4} & -1.720\times10^{5} & -1.824 \\ -5.060\times10^{6} & -1.346\times10^{4} & 4.170\times10^{6} & -1.124\times10^{4} & 9.018\times10^{7} & 6.105\times10^{4} \\ -2.394\times10^{5} & -1.877 & 3.606\times10^{4} & 3.719\times10^{2} & 4.993\times10^{6} & 8.681 \end{bmatrix}$$

$$\begin{bmatrix} 2.010\times10^{6} & -1.157\times10^{4} & 6.575\times10^{7} & 7.124\times10^{6} \\ 1.128\times10^{5} & 3.719\times10^{2} & 7.499\times10^{6} & 1.374\times10^{5} \\ -3.039\times10^{7} & 5.352\times10^{4} & -7.195\times10^{6} & 6.314\times10^{7} \\ 2.651\times10^{6} & 1.163\times10^{4} & -1.517\times10^{5} & 7.720\times10^{6} \end{bmatrix}$$

$$\mathrm{A}_c = \begin{bmatrix} 0 & 1.0 & 0 & 0 & 0 & 0 \\ -5.607\times10^{8} & -2.965\times10^{6} & 1.712\times10^{8} & -5.619\times10^{4} & -6.007\times10^{7} & -6.135\times10^{5} \\ 0 & 0 & 0 & 1.0 & 0 & 0 \\ 8.037\times10^{5} & -1.478\times10^{-1} & -1.386\times10^{6} & -1.053\times10^{3} & 1.395\times10^{4} & 1.479\times10^{-1} \\ 0 & 0 & 0 & 0 & 0 & 1.0 \\ 3.785e\times10^{7} & -6.135\times10^{5} & -2.085\times10^{7} & 5.621\times10^{4} & -5.563\times10^{8} & -7.063\times10^{5} \\ 0 & 0 & 0 & 0 & 00 & \\ 1.942\times10^{4} & 1.522\times10^{-1} & -2.925\times10^{3} & -3.016\times10^{1} & 7.467\times10^{5} & -7.041\times10^{-1} \\ 0 & 0 & 1.0 & 0 & 0 & 0 \\ 0 & 0 & 0 & 0 & 0 & 0 \end{bmatrix}$$

$$\begin{bmatrix} 0 & 0 & 0 & 0 \\ -1.005\times10^{7} & 5.785\times10^{4} & -3.287\times10^{8} & -3.562\times10^{7} \\ 0 & 0 & 0 & 0 \\ -9.150\times10^{3} & -3.016\times10^{1} & -6.082\times10^{5} & -1.114\times10^{4} \\ 0 & 0 & 0 & 0 \\ 2.230\times10^{8} & -2.676\times10^{5} & 3.598\times10^{7} & -3.157\times10^{8} \\ 0 & 1.0 & 0 & 0 \\ -1.367\times10^{6} & -9.432\times10^{2} & 1.230\times10^{4} & -6.262\times10^{5} \\ 0 & 0 & 0 & 0 \\ 1.0 & 0 & 0 & 0 \end{bmatrix}$$

Linear Quadratic Servo controller

Augmented matrix $\mathbf{A}_a$ of the system is;

$$\mathbf{A}_a = \begin{bmatrix} 0 & 0 & 0 & 0 & 1.0 & 0 \\ 0 & 0 & 0 & 0 & 0 & 0 \\ 0 & 0 & 0 & 1.0 & 0 & 0 \\ 0 & 0 & -2.393\times10^{8} & -2.907\times10^{6} & 7.100\times10^{7} & 0 \\ 0 & 0 & 0 & 0 & 0 & 1.0 \\ 0 & 0 & 1.152\times10^{6} & 0 & -1.152\times10^{6} & 0 \\ 0 & 0 & 0 & 0 & 0 & 0 \\ 0 & 0 & 1.255\times10^{7} & -6.808\times10^{5} & 0 & 0 \\ 0 & 0 & 0 & 0 & 0 & 0 \\ 0 & 0 & 0 & 0 & 0 & 0 \end{bmatrix}$$

$$\begin{bmatrix} 0 & 0 & 0 & 0 \\ 0 & 0 & 1.0 & 0 \\ 0 & 0 & 0 & 0 \\ -9.914\times10^{7} & -6.808\times10^{5} & 0 & 0 \\ 0 & 0 & 0 & 0 \\ 0 & 0 & 0 & 0 \\ 0 & 1.0 & 0 & 0 \\ -1.054\times10^{8} & -4.010\times10^{5} & 7.100\times10^{7} & 0 \\ 0 & 0 & 0 & 1.0 \\ 1.152\times10^{6} & 0 & -1.152\times10^{6} & 0 \end{bmatrix}$$

Augmented matrix $\mathbf{B}_a$ of the system is;

$$\mathbf{B_a} = \begin{bmatrix} 0 & 0 & 0 & 0 \\ 0 & 0 & 0 & 0 \\ 0 & 0 & 0 & 0 \\ 5.0 & 0 & 0 & 0 \\ 0 & 0 & 0 & 0 \\ 0 & 8.110\times10^{-2} & 0 & 0 \\ 0 & 0 & 0 & 0 \\ 0 & 0 & 5.0 & 0 \\ 0 & 0 & 0 & 0 \\ 0 & 0 & 0 & 8.110\times10^{-2} \end{bmatrix} \mathbf{outputcoefficientmatrixis}$$

$$\mathbf{C} = \begin{bmatrix} 0 & 0 & 1 & 0 & 0 & 0 & 0 & 0 \\ 0 & 0 & 0 & 0 & 0 & 0 & 1 & 0 \end{bmatrix}$$

the following sets of weighting factors,

- the first set of values of weighting factors are: $q_9 = q_{10} = 1$; and r_1=$r_3 = 10^{-10}$, r_2=r_4= 10^{-8}
- the second set of values of weighting factors are: $q_9 = q_{10} = 10^6$, and r_1=$r_3 = 10^{-10}$, r2= r_4= 10^{-8}

using the first set of weighting factors the following gain and control matrices are obtained:

$$\mathbf{K} = \begin{bmatrix} 8.2445\times10^{4} & 4.504\times10^{4} & 1.349\times10^{3} & 4.836\times10^{-4} & -2.669\times10^{-4} & 1.014\times10^{-1} \\ 2.865\times10^{3} & 1.366\times10^{3} & 4.258\times10^{1} & 1.645\times10^{-5} & 9.421\times10^{-6} & 3.502\times10^{-3} \\ -4.861\times10^{4} & 8.614\times10^{4} & 1.625\times10^{3} & -8.423\times10^{-5} & 3.188\times10^{-4} & -4.740\times10^{-2} \\ 4.297\times10^{2} & 1.908\times10^{3} & 4.295\times10^{1} & 5.502\times10^{-6} & 2.270\times10^{-6} & 7.123\times10^{-4} \end{bmatrix}$$

$$\begin{bmatrix} 2.955\times10^{2} & -8.423\times10^{-5} & -3.998\times10^{-4} & 3.392\times10^{-2} \\ 8.115 & -7.689\times10^{-6} & -6.704\times10^{-6} & 7.123\times10^{-4} \\ 1.044\times10^{3} & 2.747\times10^{-3} & 8.838\times10^{-4} & 2.441\times10^{-1} \\ 1.963\times10^{1} & 3.960\times10^{-5} & 2.555\times10^{-5} & 4.098\times10^{-3} \end{bmatrix}$$

$$\mathbf{A_c} = \begin{bmatrix} 0 & 0 & 0 & 0 & 1.0 & 0 \\ 0 & 0 & 0 & 0 & 0 & 0 \\ 0 & 0 & 0 & 1.0 & 0 & 0 \\ -4.123\times10^{5} & -2.252\times10^{5} & -2.393\times10^{8} & -2.907\times10^{6} & 7.100\times10^{7} & -5.070\times10^{-1} \\ 0 & 0 & 0 & 0 & 0 & 1.0 \\ -2.324\times10^{2} & -1.108\times10^{2} & 1.152\times10^{6} & -1.334\times10^{-6} & -1.152\times10^{6} & -2.840\times10^{-4} \\ 0 & 0 & 0 & 0 & 0 & 0 \\ 2.431\times10^{5} & -4.307\times10^{5} & 1.254\times10^{7} & -6.808\times10^{5} & -1.594\times10^{-3} & 2.370\times10^{-1} \\ 0 & 0 & 0 & 0 & 0 & 0 \\ -3.485\times10^{1} & -1.547\times10^{2} & -3.484 & -4.462\times10^{-7} & -1.841\times10^{-7} & -5.777\times10^{-5} \end{bmatrix}$$

$$\begin{bmatrix} 0 & 0 & 0 & 0 \\ 0 & 0 & 1.0 & 0 \\ 0 & 0 & 0 & 0 \\ -9.914\times10^{7} & -6.808\times10^{5} & 1.999\times10^{-3} & -1.696\times10^{-1} \\ 0 & 0 & 0 & 0 \\ -6.582\times10^{-1} & 6.236\times10^{-7} & 5.437\times10^{-7} & -5.777\times10^{-5} \\ 0 & 1.0 & 0 & 0 \\ -1.054\times10^{8} & -4.010\times10^{5} & 7.100\times10^{7} & -1.221 \\ 0 & 0 & 0 & 1.0 \\ 1.152\times10^{6} & -3.212\times10^{-6} & -1.152\times10^{6} & -3.324\times10^{-4} \end{bmatrix}$$

using the second set of weighting factors the following gain and control matrices are obtained:

$$\mathbf{K} = \begin{bmatrix} 8.423\times10^{7} & 4.088\times10^{7} & 1.318\times10^{6} & 4.984\times10^{-1} & -2.558\times10^{2} & 1.039\times10^{2} \\ 2.964\times10^{6} & 1.355\times10^{6} & 4.339\times10^{4} & 1.686\times10^{-2} & 6.012 & 3.739 \\ -4.474\times10^{7} & 8.811\times10^{7} & 1.366\times10^{6} & -1.925\times10^{-1} & 1.977\times10^{2} & -5.080\times10^{1} \\ 4.983\times10^{5} & 1.952\times10^{6} & 3.886\times10^{4} & 3.820\times10^{-3} & -2.696\times10^{-1} & 6.967\times10^{-1} \end{bmatrix}$$

$$\begin{bmatrix} 2.621\times10^{5} & -1.925\times10^{-1} & -3.960\times10^{2} & 2.355\times10^{1} \\ 8.171\times10^{3} & -8.240\times10^{-3} & -7.648 & 6.967\times10^{-1} \\ 1.003\times10^{6} & 2.829 & 9.658\times10^{2} & 2.513\times10^{2} \\ 1.895\times10^{4} & 4.076\times10^{-2} & 2.658\times10^{1} & 4.231 \end{bmatrix}$$

$$\mathbf{A_c} = \begin{bmatrix} 0 & 0 & 0 & 0 & 1.0 & 0 \\ 0 & 0 & 0 & 0 & 0 & 0 \\ 0 & 0 & 0 & 1.0 & 0 & 0 \\ -4.212\times10^{8} & -2.044\times10^{8} & -2.459\times10^{8} & -2.907\times10^{6} & 7.100\times10^{7} & -5.196\times10^{2} \\ 0 & 0 & 0 & 0 & 0 & 1.0 \\ -2.404\times10^{5} & -1.099\times10^{5} & 1.148\times10^{6} & -1.367\times10^{-3} & -1.152\times10^{6} & -3.033\times10^{-1} \\ 0 & 0 & 0 & 0 & 0 & 0 \\ 2.237\times10^{8} & -4.406\times10^{8} & 5.716\times10^{6} & -6.808\times10^{5} & -9.884\times10^{2} & 2.540\times10^{2} \\ 0 & 0 & 0 & 0 & 0 & 0 \\ -4.041\times10^{4} & -1.583\times10^{5} & -3.151\times10^{3} & -3.098\times10^{-4} & 2.187\times10^{-2} & -5.650\times10^{-2} \end{bmatrix}$$

$$\begin{bmatrix} 0 & 0 & 0 & 0 \\ 0 & 0 & 1.0 & 0 \\ 0 & 0 & 0 & 0 \\ -1.005\times10^{8} & -6.808\times10^{5} & 1.980\times10^{3} & -1.178\times10^{2} \\ 0 & 0 & 0 & 0 \\ -6.627\times10^{2} & 6.683\times10^{-4} & 6.203\times10^{-1} & -5.650\times10^{-2} \\ 0 & 1.0 & 0 & 0 \\ -1.104\times10^{8} & -4.010\times10^{5} & 7.100\times10^{7} & -1.256\times10^{3} \\ 0 & 0 & 0 & 1.0 \\ 1.150\times10^{6} & -3.306\times10^{-3} & -1.152\times10^{6} & -3.431\times10^{-1} \end{bmatrix}$$

Model-II

State variable Feedback Controller

Coefficient matrices of the system are:

$$\mathbf{A} = \begin{bmatrix} 0 & 1.0 & 0 & 0 & 0 & 0 \\ -3.9770\times10^{7} & -6.8401\times10^{5} & 3.9603\times10^{7} & 6.8401\times10^{5} & 0 & 0 \\ 0 & 0 & 0 & 1.0 & 0 & 0 \\ 1.6831e+008 & 2.9070\times10^{6} & -2.3931\times10^{8} & -2.9070\times10^{6} & 7.1000\times10^{7} & 0 \\ 0 & 0 & 0 & 0 & 0 & 1.0 \\ 0 & 0 & 1.1517\times10^{6} & 0 & -1.1517\times10^{6} & 0 \\ 0 & 0 & 0 & 0 & 0 & 0 \\ 2.9521\times10^{6} & -1.6019\times10^{5} & -2.9521\times10^{6} & 1.6019\times10^{5} & 0 & 0 \\ 0 & 0 & 0 & 0 & 0 & 0 \\ -1.2546\times10^{7} & 6.8081\times10^{5} & 1.2546\times10^{7} & -6.8081\times10^{5} & 0 & 0 \\ 0 & 0 & 0 & 0 & 0 & 0 \\ 0 & 0 & 0 & 0 & 0 & 0 \end{bmatrix}$$

$$\begin{bmatrix}
0 & 0 & 0 & 0 & 0 & 0 \\
-2.3328\times10^{7} & -1.6019\times10^{5} & 2.3328\times10^{7} & 1.6019\times10^{5} & 0 & 0 \\
0 & 0 & 0 & 0 & 0 & 0 \\
9.9142\times10^{7} & 6.8081\times10^{5} & -9.9142\times10^{7} & -6.8081\times10^{5} & 0 & 0 \\
0 & 0 & 0 & 0 & 0 & 0 \\
0 & 0 & 0 & 0 & 0 & 0 \\
0 & 1.0 & 0 & 0 & 0 & 0 \\
-8.2612\times10^{6} & -9.4358\times10^{4} & 8.0941\times10^{6} & 9.4358\times10^{4} & 0 & 0 \\
0 & 0 & 0 & 1.0 & 0 & 0 \\
3.4400\times10^{7} & 4.0102\times10^{5} & -1.0540\times10^{8} & -4.0102\times10^{5} & 7.1000\times10^{7} & 0 \\
0 & 0 & 0 & 0 & 0 & 1.0 \\
0 & 0 & 1.1517\times10^{6} & 0 & -1.1517\times10^{6} & 0
\end{bmatrix}$$

$$\mathbf{B} = \begin{bmatrix}
0 & 0 & 0 & 0 & 0 & 0 \\
1.1765 & 0 & 0 & 0 & 0 & 0 \\
0 & 0 & 0 & 0 & 0 & 0 \\
0 & 5.0 & 0 & 0 & 0 & 0 \\
0 & 0 & 0 & 0 & 0 & 0 \\
0 & 0 & 8.1103\times10^{-2} & 0 & 0 & 0 \\
0 & 0 & 0 & 0 & 0 & 0 \\
0 & 0 & 0 & 1.1765 & 0 & 0 \\
0 & 0 & 0 & 0 & 0 & 0 \\
0 & 0 & 0 & 0 & 5.0 & 0 \\
0 & 0 & 0 & 0 & 0 & 0 \\
0 & 0 & 0 & 0 & 0 & 8.1103\times10^{-2}
\end{bmatrix}$$

the following weighting factors are used to compute the gain and control matrices:

- the first set of weighting factors are: $q_1=q_2=q_3=\cdots\cdots=q_{12}=1$ and $r_3=r_6=10^{-8}$, $r_1=r_2=\cdots\cdots=10^{-10}$
- the second set of weighting factors are $q_5=q_{11}=10^6$, $q_1=q_2=q_3=\cdots\cdots=q_{12}=1$ and $r_3=r_6=10^{-8}$, $r_1=r_2=\cdots\cdots=10^{-10}$

using the first set of weighting factors the following gain and control matrices are obtained:

$$\mathbf{K} = \begin{bmatrix}
2.654\times10^{6} & 7.681\times10^{4} & 2.712\times10^{7} & 1.806\times10^{4} & -2.971\times10^{7} & 7.305\times10^{3} \\
2.942\times10^{6} & 7.674\times10^{4} & 4.088\times10^{7} & 2.841\times10^{4} & -4.375\times10^{7} & 1.107\times10^{4} \\
-1.839\times10^{5} & 5.036 & 1.730\times10^{6} & 1.796 & -1.538\times10^{6} & 7.760\times10^{3} \\
2.996\times10^{5} & 8.674\times10^{2} & 8.701\times10^{6} & 1.868\times10^{3} & -8.993\times10^{6} & 1.797\times10^{3} \\
-4.581\times10^{6} & 7.932\times10^{3} & 1.291\times10^{6} & -1.013\times10^{4} & 3.275\times10^{6} & -2.163\times10^{3} \\
1.737\times10^{5} & 1.696 & -2.220\times10^{5} & -3.934\times10^{-1} & 4.866\times10^{4} & 1.347\times10^{2}
\end{bmatrix}$$

$$\begin{bmatrix}
7.060\times10^{5} & 8.674\times10^{2} & 7.660\times10^{6} & 1.866\times10^{3} & -8.367\times10^{6} & 2.460\times10^{3} \\
1.533\times10^{6} & 7.941\times10^{3} & -4.303\times10^{6} & -1.013\times10^{4} & 2.763\times10^{6} & -2.425\times10^{3} \\
-5.112\times10^{4} & 1.239 & -2.102\times10^{4} & -3.508\times10^{-1} & 7.279\times10^{4} & 1.347\times10^{2} \\
2.102\times10^{6} & 7.363\times10^{4} & -3.757\times10^{6} & 1.118\times10^{4} & 1.698\times10^{6} & -9.576\times10^{2} \\
4.133\times10^{5} & 4.752\times10^{4} & 5.451\times10^{7} & 6.568\times10^{4} & -5.482\times10^{7} & 1.954\times10^{4} \\
-1.135\times10^{5} & 7-6.601\times10^{-1} & 1.861\times10^{6} & 3.170 & -1.742\times10^{6} & 7.286\times10^{3}
\end{bmatrix}$$

$$\mathbf{A_c} = \begin{bmatrix}
0 & 1.0 & 0 & 0 & 0 & 0 \\
-4.289\times10^{7} & -7.744\times10^{5} & 7.704\times10^{6} & 6.628\times10^{5} & 3.496\times10^{7} & -8.594\times10^{3} \\
0 & 0 & 0 & 1.0 & 0 & 0 \\
1.536\times10^{8} & 2.523\times10^{6} & -4.437\times10^{8} & -3.049\times10^{6} & 2.898\times10^{8} & -5.536\times10^{4} \\
0 & 0 & 0 & 0 & 0 & 1.0 \\
1.492\times10^{4} & -4.084\times10^{-1} & 1.011\times10^{6} & -1.457\times10^{-1} & -1.027\times10^{6} & -6.293\times10^{2} \\
0 & 0 & 0 & 0 & 0 & 0 \\
2.600\times10^{6} & -1.612\times10^{5} & -1.319\times10^{7} & 1.580\times10^{5} & 1.058\times10^{7} & -2.114\times10^{3} \\
0 & 0 & 0 & 0 & 0 & 0 \\
1.036\times10^{7} & 6.412\times10^{5} & 6.081\times10^{6} & -6.302\times10^{5} & -1.638\times10^{7} & 1.081\times10^{4} \\
0 & 0 & 0 & 0 & 0 & 0 \\
-1.409\times10^{4} & -1.375\times10^{-1} & 1.800\times10^{4} & 3.190\times10^{-2} & -3.947\times10^{3} & -1.092\times10^{1}
\end{bmatrix}$$

$$\begin{bmatrix}
0 & 0 & 0 & 0 & 0 & 0 \\
-2.416\times10^{7} & -1.612\times10^{5} & 1.432\times10^{7} & 1.580\times10^{5} & 9.843\times10^{6} & -2.894\times10^{3} \\
0 & 0 & 0 & 0 & 0 & 0 \\
9.148\times10^{7} & 6.411\times10^{5} & -7.763\times10^{7} & -6.302\times10^{5} & -1.381\times10^{7} & 1.213\times10^{4} \\
0 & 0 & 0 & 0 & 0 & 0 \\
4.146\times10^{3} & -1.005\times10^{-1} & 1.705\times10^{3} & 2.845\times10^{-2} & -5.903\times10^{3} & -1.092\times10^{1} \\
0 & 1.0 & 0 & 0 & 0 & 0 \\
-1.073\times10^{7} & -1.810\times10^{5} & 1.252\times10^{7} & 8.120\times10^{4} & -1.998\times10^{6} & 1.127\times10^{3} \\
0 & 0 & 0 & 1.0 & 0 & 0 \\
3.233\times10^{7} & 1.634\times10^{5} & -3.780\times10^{8} & -7.294\times10^{5} & 3.451\times10^{8} & -9.772\times10^{4} \\
0 & 0 & 0 & 0 & 0 & 1.09.204\times10^{3} \\
5.354\times10^{-2} & 1.001\times10^{6} & -2.571\times10^{-1} & -1.010\times10^{6} & -5.909\times10^{2} &
\end{bmatrix}$$

using the second set of weighting factors the following gain and control matrices are obtained:

$$\mathbf{K} = \begin{bmatrix}
4.527\times10^{6} & 7.690\times10^{4} & 5.110\times10^{7} & 1.809\times10^{4} & -1.820\times10^{7} & 2.517\times10^{4} \\
5.688\times10^{6} & 7.686\times10^{4} & 7.308\times10^{7} & 2.845\times10^{4} & -2.771\times10^{7} & 3.585\times10^{4} \\
-3.807\times10^{3} & 1.735\times10^{1} & 5.067\times10^{6} & 5.814 & 2.605\times10^{6} & 1.202\times10^{4} \\
-1.343\times10^{4} & 8.925\times10^{2} & 1.560\times10^{7} & 1.876\times10^{3} & -6.091\times10^{6} & 6.343\times10^{3} \\
-8.009\times10^{6} & 7.955\times10^{3} & 3.311\times10^{6} & -1.013\times10^{4} & 1.079\times10^{6} & -4.722\times10^{3} \\
-1.482\times10^{4} & 4.386 & 2.157\times10^{4} & -7.615-1 & -1.196\times10^{4} & 1.015\times10^{2}
\end{bmatrix}$$

$$\begin{bmatrix} 1.305\times10^{6} & 8.925\times10^{2} & 1.261\times10^{7} & 1.872\times10^{3} & -6.027\times10^{6} & 6.362\times10^{3} \\ 2.174\times10^{6} & 7.971\times10^{3} & -5.517\times10^{6} & -1.013\times10^{4} & 6.481\times10^{5} & -4.695\times10^{3} \\ -3.987\times10^{3} & 4.372 & 7.704\times10^{3} & -7.660\times10^{-1} & 5.174\times10^{3} & 1.015\times10^{2} \\ 3.200\times10^{6} & 7.364\times10^{4} & 1.280\times10^{5} & 1.119\times10^{4} & 3.693\times10^{6} & 1.705\times10^{3} \\ 2.387\times10^{6} & 4.755\times10^{4} & 9.184\times10^{7} & 6.575\times10^{4} & -3.085\times10^{7} & 5.319\times10^{4} \\ -2.166\times10^{3} & 1.175 & 5.041\times10^{6} & 8.627 & 2.618\times10^{6} & 1.165\times10^{4} \end{bmatrix}$$

$$A_c = \begin{bmatrix} 0 & 1.0 & 0 & 0 & 0 & 0 \\ -4.501\times10^{7} & -7.745\times10^{5} & -2.051\times10^{7} & 6.627\times10^{5} & 2.141\times10^{7} & -2.961\times10^{4} \\ 0 & 0 & 0 & 1.0 & 0 & 0 \\ 1.399\times10^{8} & 2.523\times10^{6} & -6.047\times10^{8} & -3.049\times10^{6} & 2.096\times10^{8} & -1.792\times10^{5} \\ 0 & 0 & 0 & 0 & 0 & 1.0 \\ 3.087\times10^{2} & -1.407 & 7.407\times10^{5} & -4.716\times10^{-1} & -1.363\times10^{6} & -9.746\times10^{2} \\ 0 & 0 & 0 & 0 & 0 & 0 \\ 2.968\times10^{6} & -1.612\times10^{5} & -2.130\times10^{7} & 1.580\times10^{5} & 7.166\times10^{6} & -7.462\times10^{3} \\ 0 & 0 & 0 & 0 & 0 & 0 \\ 2.750\times10^{7} & 6.410\times10^{5} & -4.006\times10^{6} & -6.302\times10^{5} & -5.393\times10^{6} & 2.361\times10^{4} \\ 0 & 0 & 0 & 0 & 0 & 0 \\ 1.202\times10^{3} & -3.557\times10^{-1} & -1.749\times10^{3} & 6.176\times10^{-2} & 9.703\times10^{2} & -8.230 \end{bmatrix}$$

$$\begin{bmatrix} 0 & 0 & 0 & 0 & 0 & 0 \\ -2.486\times10^{7} & -1.612\times10^{5} & 8.497\times10^{6} & 1.580\times10^{5} & 7.090\times10^{6} & -7.485\times10^{3} \\ 0 & 0 & 0 & 0 & 0 & 0 \\ 8.827\times10^{7} & 6.410\times10^{5} & -7.156\times10^{7} & -6.302\times10^{5} & -3.241\times10^{6} & 2.347\times10^{4} \\ 0 & 0 & 0 & 0 & 0 & 0 \\ 3.233\times10^{2} & -3.546\times10^{-1} & -6.248\times10^{2} & 6.212-2 & -4.196\times10^{2} & -8.230 \\ 0 & 1.0 & 0 & 0 & 0 & 0 \\ -1.203\times10^{7} & -1.810\times10^{5} & 7.944\times10^{6} & 8.120\times10^{4} & -4.344\times10^{6} & -2.005\times10^{3} \\ 0 & 0 & 0 & 1.0 & 0 & 0 \\ 2.247\times10^{7} & 1.633\times10^{5} & -5.646\times10^{8} & -7.298\times10^{5} & 2.252\times10^{8} & -2.659\times10^{5} \\ 0 & 0 & 0 & 0 & 0 & 1.0 \\ 1.757\times10^{2} & -9.530\times10^{-2} & 7.429\times10^{5} & -6.997\times10^{-1} & -1.364\times10^{6} & -9.445\times10^{2} \end{bmatrix}$$

Integral plus State variable Feedback controller

Augmented matrix A_a of the system is;

$$A_a = \begin{bmatrix}
0 & 1.0 & 0 & 0 & 0 & 0 \\
-3.977\times10^{7} & -6.840\times10^{5} & 3.960\times10^{7} & 6.840\times10^{5} & 0 & 0 \\
0 & 0 & 0 & 1.0 & 0 & 0 \\
1.683\times10^{8} & 2.907\times10^{6} & -2.393\times10^{8} & -2.9070\times10^{6} & 7.1000\times10^{7} & 0 \\
0 & 0 & 0 & 0 & 0 & 1.0 \\
0 & 0 & 1.152\times10^{6} & 0 & -1.152\times10^{6} & 0 \\
0 & 0 & 0 & 0 & 0 & 0 \\
2.952\times10^{6} & -1.602\times10^{5} & -2.952\times10^{6} & 1.602\times10^{5} & 0 & 0 \\
0 & 0 & 0 & 0 & 0 & 0 \\
-1.255\times10^{7} & 6.808\times10^{5} & 1.255\times10^{7} & -6.808\times10^{5} & 0 & 0 \\
0 & 0 & 0 & 0 & 0 & 0 \\
0 & 0 & 0 & 0 & 0 & 0 \\
0 & 0 & 0 & 0 & 1.0 & 0 \\
0 & 0 & 0 & 0 & 0 & 0
\end{bmatrix}$$

$$\begin{bmatrix}
0 & 0 & 0 & 0 & 0 & 0 \\
-2.333\times10^{7} & -1.602\times10^{5} & 2.333\times10^{7} & 1.602\times10^{5} & 0 & 0 \\
0 & 0 & 0 & 0 & 0 & 0 \\
9.914\times10^{7} & 6.808\times10^{5} & -9.914\times10^{7} & -6.808\times10^{5} & 0 & 0 \\
0 & 0 & 0 & 0 & 0 & 0 \\
0 & 0 & 0 & 0 & 0 & 0 \\
0 & 1.0 & 0 & 0 & 0 & 0 \\
-8.261\times10^{6} & -9.436\times10^{4} & 8.094\times10^{6} & 9.436\times10^{4} & 0 & 0 \\
0 & 0 & 0 & 1.0 & 0 & 0 \\
3.440\times10^{7} & 4.010\times10^{5} & -1.054\times10^{8} & -4.010\times10^{5} & 7.100\times10^{7} & 0 \\
0 & 0 & 0 & 0 & 0 & 1.0 \\
0 & 0 & 1.1517\times10^{6} & 0 & -1.1517\times10^{6} & 0 \\
0 & 0 & 0 & 0 & 0 & 0 \\
0 & 0 & 0 & 0 & 1.0 & 0
\end{bmatrix}$$

$$\begin{bmatrix} 0 & 0 \\ 0 & 0 \\ 0 & 0 \\ 0 & 0 \\ 0 & 0 \\ 0 & 0 \\ 0 & 0 \\ 0 & 0 \\ 0 & 0 \\ 0 & 0 \\ 0 & 0 \\ 0 & 0 \\ 0 & 0 \end{bmatrix}$$

output coefficient matrix of the system:

$$C = \begin{bmatrix} 0 & 0 & 0 & 0 & 1 & 0 & 0 & 0 & 0 & 0 & 0 & 0 \\ 0 & 0 & 0 & 0 & 0 & 0 & 0 & 0 & 0 & 0 & 1 & 0 \end{bmatrix}$$

The response of mid-span deflection is simulated by considering the following set of weighting factors:

- the first set of weighting factors are: $q_5=q_{11}=10^6$, $q_1=q_2=q_3=\cdots\cdots=q_{12}=q_{13}=q_{14}=1$ and $r_3=r_6=10^{-8}$, $r_1=r_2=\cdots\cdots=10^{-10}$
- the second set of weighting factors are $q_5=q_{11}=q_{13}=q_{14}=10^6$, $q_1=q_2=q_3=\cdots\cdots=q_{12}=1$ and $r_3=r_6=10^{-8}$, $r_1=r_2=\cdots\cdots=10^{-10}$

using the first set of weighting factors the following gain and control matrices are obtained:

$$K = \begin{bmatrix} 4.527\times10^6 & 7.690\times10^4 & 5.110\times10^7 & 1.809\times10^4 & -1.820\times10^7 & 2.517\times10^4 \\ 5.688\times10^6 & 7.686\times10^4 & 7.308\times10^7 & 2.845\times10^4 & -2.771\times10^7 & 3.585\times10^4 \\ -3.806\times10^3 & 1.735\times10^1 & 5.067\times10^6 & 5.814 & 2.605\times10^6 & 1.202\times10^4 \\ -1.343\times10^4 & 8.925\times10^2 & 1.560\times10^7 & 1.876\times10^3 & -6.091\times10^6 & 6.343\times10^3 \\ -8.009\times10^6 & 7.955\times10^3 & 3.311\times10^6 & -1.013\times10^4 & 1.079\times10^6 & -4.722\times10^3 \\ -1.482\times10^4 & 4.386 & 2.157\times10^4 & -7.615\times10^{-1} & -1.196\times10^4 & 1.015\times10^2 \end{bmatrix}$$

$$\begin{bmatrix} 1.305\times10^6 & 8.925\times10^2 & 1.261\times10^7 & 1.872\times10^3 & -6.027\times10^6 & 6.362\times10^3 \\ 2.174\times10^6 & 7.971\times10^3 & -5.517\times10^6 & -1.013\times10^4 & 6.481\times10^5 & -4.695\times10^3 \\ -3.987\times10^3 & 4.372 & 7.704\times10^3 & -7.660\times10^{-1} & 5.174\times10^3 & 1.015\times10^2 \\ 3.200\times10^6 & 7.364\times10^4 & 1.280\times10^5 & 1.119\times10^4 & 3.693\times10^6 & 1.705\times10^3 \\ 2.387\times10^6 & 4.755\times10^4 & 9.184\times10^7 & 6.575\times10^4 & -3.085\times10^7 & 5.319\times10^4 \\ -2.166\times10^3 & 1.175 & 5.041\times10^6 & 8.627 & 2.618\times10^6 & 1.165\times10^4 \end{bmatrix}$$

$$\begin{bmatrix} 3.748\times10^{4} & 7.895\times10^{3} \\ 5.111\times10^{4} & -2.684\times10^{3} \\ 7.668\times10^{3} & 8.909 \\ 9.490\times10^{3} & 7.062\times10^{3} \\ -3.607\times10^{3} & 6.338\times10^{4} \\ -5.187 & 7.657\times10^{3} \end{bmatrix}$$

$$\mathbf{A}_c = \begin{bmatrix} 0 & 1.0 & 0 & 0 & 0 & 0 \\ -4.510\times10^{7} & -7.745\times10^{5} & -2.051\times10^{7} & 6.627\times10^{5} & 2.141\times10^{7} & -2.961\times10^{4} \\ 0 & 0 & 0 & 1.0 & 0 & 0 \\ 1.399\times10^{8} & 2.523\times10^{6} & -6.047\times10^{8} & -3.049\times10^{6} & 2.096\times10^{8} & -1.792\times10^{5} \\ 0 & 0 & 0 & 0 & 0 & 1.0 \\ 3.087\times10^{2} & -1.407 & 7.407\times10^{5} & -4.716\times10^{-1} & -1.363\times10^{6} & -9.746\times10^{2} \\ 0 & 0 & 0 & 0 & 0 & 0 \\ 2.968\times10^{6} & -1.612\times10^{5} & -2.130\times10^{7} & 1.580\times10^{5} & 7.166\times10^{6} & -7.462\times10^{3} \\ 0 & 0 & 0 & 0 & 0 & 0 \\ 2.750\times10^{7} & 6.410\times10^{5} & -4.006\times10^{6} & -6.302\times10^{5} & -5.393\times10^{6} & 2.361\times10^{4} \\ 0 & 0 & 0 & 0 & 0 & 0 \\ 1.202\times10^{3} & -3.557\times10^{-1} & -1.749\times10^{3} & 6.176\times10^{-2} & 9.703\times10^{2} & -8.230 \\ 0 & 0 & 0 & 0 & 1.00 & \\ 0 & 0 & 0 & 0 & 0 & 0 \end{bmatrix}$$

$$\begin{bmatrix} 0 & 0 & 0 & 0 & 0 & 0 \\ -2.486\times10^{7} & -1.612\times10^{5} & 8.497\times10^{6} & 1.580\times10^{5} & 7.090\times10^{6} & -7.485\times10^{3} \\ 0 & 0 & 0 & 0 & 0 & 0 \\ 8.827\times10^{7} & 6.410\times10^{5} & -7.156\times10^{7} & -6.302\times10^{5} & -3.241\times10^{6} & 2.347\times10^{4} \\ 0 & 0 & 0 & 0 & 0 & 0 \\ 3.233\times10^{2} & -3.546\times10^{-1} & -6.248\times10^{2} & 6.212\times10^{-2} & -4.196\times10^{2} & -8.230 \\ 0 & 1.0 & 0 & 0 & 0 & 0 \\ -1.203\times10^{7} & -1.810\times10^{5} & 7.944\times10^{6} & 8.120\times10^{4} & -4.344\times10^{6} & -2.005\times10^{3} \\ 0 & 0 & 0 & 1.0 & 0 & 0 \\ 2.247\times10^{7} & 1.633\times10^{5} & -5.646\times10^{8} & -7.298\times10^{5} & 2.252\times10^{8} & -2.659\times10^{5} \\ 0 & 0 & 0 & 0 & 0 & 1.0 \\ 1.757\times10^{2} & -9.530\times10^{-2} & 7.429\times10^{5} & -6.997\times10^{-1} & -1.364\times10^{6} & -9.445\times10^{2} \\ 0 & 0 & 0 & 0 & 0 & 0 \\ 0 & 0 & 0 & 0 & 1.0 & 0 \end{bmatrix}$$

$$\begin{bmatrix} 0 & 0 \\ -4.410\times10^{4} & -9.288\times10^{3} \\ 0 & 0 \\ -2.555\times10^{5} & 1.342\times10^{4} \\ 0 & 0 \\ -6.219\times10^{2} & -7.225\times10^{-1} \\ 0 & 0 \\ -1.116\times10^{4} & -8.308\times10^{3} \\ 0 & 0 \\ 1.804\times10^{4} & -3.169\times10^{5} \\ 0 & 0 \\ 4.207\times10^{-1} & -6.210\times10^{2} \\ 0 & 0 \\ 0 & 0 \end{bmatrix}$$

using the second set of weighting factors the following gain and control matrices are obtained:

$$\mathbf{K} = \begin{bmatrix} 4.529\times10^{6} & 7.690\times10^{4} & 5.113\times10^{7} & 1.809\times10^{4} & -1.815\times10^{7} & 2.521\times10^{4} \\ 5.691\times10^{6} & 7.686\times10^{4} & 7.312\times10^{7} & 2.845\times10^{4} & -2.765\times10^{7} & 3.589\times10^{4} \\ -3.304\times10^{3} & 1.738\times10^{1} & 5.073\times10^{6} & 5.822 & 2.614\times10^{6} & 1.202\times10^{4} \\ -1.323\times10^{4} & 8.925\times10^{2} & 1.560\times10^{7} & 1.876\times10^{3} & -6.079\times10^{6} & 6.352\times10^{3} \\ -8.013\times10^{6} & 7.955\times10^{3} & 3.314\times10^{6} & -1.013\times10^{4} & 1.074\times10^{6} & -4.726\times10^{3} \\ -1.528\times10^{4} & 4.391 & 2.230\times10^{4} & -7.619\times10^{-1} & -1.202\times10^{4} & 1.015\times10^{2} \end{bmatrix}$$

$$\begin{bmatrix} 1.306\times10^{6} & 8.925\times10^{2} & 1.261\times10^{7} & 1.872\times10^{3} & -6.017\times10^{6} & 6.369\times10^{3} \\ 2.175\times10^{6} & 7.972\times10^{3} & -5.518\times10^{6} & -1.013\times10^{4} & 6.443\times10^{5} & -4.697\times10^{3} \\ -3.858\times10^{3} & 4.379 & 7.884\times10^{3} & -7.665\times10^{-1} & 5.104\times10^{3} & 1.015\times10^{2} \\ 3.201\times10^{6} & 7.364\times10^{4} & 1.334\times10^{5} & 1.119\times10^{4} & 3.701\times10^{6} & 1.711\times10^{3} \\ 2.390\times10^{6} & 4.755\times10^{4} & 9.188\times10^{7} & 6.575\times10^{4} & -3.077\times10^{7} & 5.325\times10^{4} \\ -1.833\times10^{3} & 1.180 & 5.046\times10^{6} & 8.637 & 2.628\times10^{6} & 1.165\times10^{4} \end{bmatrix}$$

$$\begin{bmatrix} 3.744\times10^{7} & 7.903\times10^{6} \\ 5.108\times10^{7} & -2.682 \\ 7.672\times10^{6} & 9.043\times10^{3} \\ 9.500\times10^{6} & 6.991\times10^{6} \\ -3.606\times10^{6} & 6.334\times10^{7} \\ -5.080\times10^{3} & 7.661\times10^{6} \end{bmatrix}$$

$$
\mathbf{A}_c = \begin{bmatrix}
0 & 1.0 & 0 & 0 & 0 & 0 \\
-4.510\times10^{7} & -7.745\times10^{5} & -2.055\times10^{7} & 6.627\times10^{5} & 2.136\times10^{7} & -2.965\times10^{4} \\
0 & 0 & 0 & 1.0 & 0 & 0 \\
1.399\times10^{8} & 2.523\times10^{6} & -6.049\times10^{8} & -3.049\times10^{6} & 2.093\times10^{8} & -1.795\times10^{5} \\
0 & 0 & 0 & 0 & 0 & 1.0 \\
2.680\times10^{2} & -1.409 & 7.4021\times10^{5} & -4.722\times10^{-1} & -1.364\times10^{6} & -9.752\times10^{2} \\
0 & 0 & 0 & 0 & 0 & 0 \\
2.968\times10^{6} & -1.612\times10^{5} & -2.131\times10^{7} & 1.580\times10^{5} & 7.152\times10^{6} & -7.472\times10^{3} \\
0 & 0 & 0 & 0 & 0 & 0 \\
2.752\times10^{7} & 6.410\times10^{5} & -4.022\times10^{6} & -6.302\times10^{5} & -5.370\times10^{6} & 2.363\times10^{4} \\
0 & 0 & 0 & 0 & 0 & 0 \\
1.239\times10^{3} & -3.561\times10^{-1} & -1.808\times10^{3} & 6.179\times10^{-2} & 9.747\times10^{2} & -8.231 \\
0 & 0 & 0 & 0 & 1.0 & 0 \\
0 & 0 & 0 & 0 & 0 & 0
\end{bmatrix}
$$

$$
\begin{bmatrix}
0 & 0 & 0 & 0 & 0 & 0 \\
-2.486\times10^{7} & -1.612\times10^{5} & 8.490\times10^{6} & 1.580\times10^{5} & 7.079\times10^{6} & -7.493\times10^{3} \\
0 & 0 & 0 & 0 & 0 & 0 \\
8.827\times10^{7} & 6.410\times10^{5} & -7.155\times10^{7} & -6.302\times10^{5} & -3.221\times10^{6} & 2.349\times10^{4} \\
0 & 0 & 0 & 0 & 0 & 0 \\
3.129\times10^{2} & -3.551\times10^{-1} & -6.394\times10^{2} & 6.217\times10^{-2} & -4.139\times10^{2} & -8.231 \\
0 & 1.0 & 0 & 0 & 0 & 0 \\
-1.203\times10^{7} & -1.810\times10^{5} & 7.937\times10^{6} & 8.120\times10^{4} & -4.354\times10^{6} & -2.013\times10^{3} \\
0 & 0 & 0 & 1.0 & 0 & 0 \\
2.245\times10^{7} & 1.633\times10^{5} & -5.648\times10^{8} & -7.298\times10^{5} & 2.249\times10^{8} & -2.662\times10^{5} \\
0 & 0 & 0 & 0 & 0 & 1.0 \\
1.487\times10^{2} & -9.567\times10^{-2} & 7.424\times10^{5} & -7.005\times10^{-1} & -1.365\times10^{6} & -9.451\times10^{2} \\
0 & 0 & 0 & 0 & 0 & 0 \\
0 & 0 & 0 & 0 & 1.0 & 0
\end{bmatrix}
$$

$$\begin{bmatrix} 0 & 0 \\ -4.405\times10^{7} & -9.297\times10^{6} \\ 0 & 0 \\ -2.554\times10^{8} & 1.341\times10^{7} \\ 0 & 0 \\ -6.222\times10^{5} & -7.334\times10^{2} \\ 0 & 0 \\ -1.118\times10^{\times}10^{7} & -8.225\times10^{6} \\ 0 & 0 \\ 1.803\times10^{7} & -3.167\times10^{8} \\ 0 & 0 \\ 4.120\times10^{2} & -6.213\times10^{5} \\ 0 & 0 \\ 0 & 0 \end{bmatrix}$$

Linear Quadratic Servo controller

Augmented matrix $\mathbf{A}_a$ of the system is;

$$\mathbf{A}_a = \begin{bmatrix} 0 & 0 & 0 & 0 & 0 & 0 \\ 0 & 0 & 0 & 0 & 0 & 0 \\ 0 & 0 & 0 & 1.0 & 0 & 0 \\ 0 & 0 & -3.9770\times10^{7} & -6.8401\times10^{5} & 3.9603\times10^{7} & 6.8401\times10^{5} \\ 0 & 0 & 0 & 0 & 0 & 1.0 \\ 0 & 0 & 1.6831\times10^{8} & 2.9070\times10^{6} & -2.3931\times10^{8} & -2.9070\times10^{6} \\ 0 & 0 & 0 & 0 & 0 & 0 \\ 0 & 0 & 0 & 0 & 1.1517\times10^{6}0 & \\ 0 & 0 & 0 & 0 & 0 & 0 \\ 0 & 0 & 2.9521\times10^{6} & -1.6019\times10^{5} & -2.9521\times10^{6} & 1.6019\times10^{5} \\ 0 & 0 & 0 & 0 & 0 & 0 \\ 0 & 0 & -1.2546\times10^{7} & 6.8081\times10^{5} & 1.2546\times10^{7} & -6.8081\times10^{5} \\ 0 & 0 & 0 & 0 & 0 & 0 \\ 0 & 0 & 0 & 0 & 0 & 0 \end{bmatrix}$$

$$
\begin{bmatrix}
1.0 & 0 & 0 & 0 & 0 & 0 \\
0 & 0 & 0 & 0 & 0 & 0 \\
0 & 0 & 0 & 0 & 0 & 0 \\
0 & 0 & -2.3328\times10^{7} & -1.6019\times10^{5} & 2.3328\times10^{7} & 1.6019\times10^{5} \\
0 & 0 & 0 & 0 & 0 & 0 \\
7.1000\times10^{7} & 0 & 9.9142\times10^{7} & 6.8081\times10^{5} & -9.9142\times10^{7} & -6.8081\times10^{5} \\
0 & 1.0 & 0 & 0 & 0 & 0 \\
-1.1517\times10^{6} & 0 & 0 & 0 & 0 & 0 \\
0 & 0 & 0 & 1.0 & 0 & 0 \\
0 & 0 & -8.2612\times10^{6} & -9.4358\times10^{4} & 8.0941\times10^{6} & 9.4358\times10^{4} \\
0 & 0 & 0 & 0 & 0 & 1.0 \\
0 & 0 & 3.4400\times10^{7} & 4.0102\times10^{5} & -1.0540\times10^{8} & -4.0102\times10^{5} \\
0 & 0 & 0 & 0 & 0 & 0 \\
0 & 0 & 0 & 0 & 1.1517\times10^{6} & 0
\end{bmatrix}
$$

$$
\begin{bmatrix}
0 & 0 \\
1.0 & 0 \\
0 & 0 \\
0 & 0 \\
0 & 0 \\
0 & 0 \\
0 & 0 \\
0 & 0 \\
0 & 0 \\
0 & 0 \\
0 & 0 \\
7.1000\times10^{7} & 0 \\
0 & 1.0 \\
-1.1517\times10^{6} & 0
\end{bmatrix}
$$

Augmented matrix B_a of the system is;

$$B_a = \begin{bmatrix} 0 & 0 & 0 & 0 & 0 & 0 \\ 0 & 0 & 0 & 0 & 0 & 0 \\ 0 & 0 & 0 & 0 & 0 & 0 \\ 1.1765 & 0 & 0 & 0 & 0 & 0 \\ 0 & 0 & 0 & 0 & 0 & 0 \\ 0 & 5.0 & 0 & 0 & 0 & 0 \\ 0 & 0 & 0 & 0 & 0 & 0 \\ 0 & 0 & 8.1103\times10^{-2} & 0 & 0 & 0 \\ 0 & 0 & 0 & 0 & 0 & 0 \\ 0 & 0 & 0 & 1.1765 & 0 & 0 \\ 0 & 0 & 0 & 0 & 0 & 0 \\ 0 & 0 & 0 & 0 & 5.0 & 0 \\ 0 & 0 & 0 & 0 & 0 & 0 \\ 0 & 0 & 0 & 0 & 0 & 8.1103\times10^{-2} \end{bmatrix}$$

The response of mid-span deflection is simulated by considering the following sets of weighting factors:

- the first set of weighting factors are: $q_{13}=q_{14}=1$ and $r_3=r_6=10^{-8}$, $r_1=r_2=\cdots\cdots=10^{-10}$
- the second set of weighting factors are: $q_{13}=q_{14}=10^6$, and $r_3=r_6=10^{-8}$, $r_1=r_2=\cdots\cdots=10^{-10}$

using the first set of weighting factors the following gain and control matrices are obtained:

$$K = \begin{bmatrix} 7.041\times10^4 & 1.787\times10^2 & -6.333\times10^2 & 7.644\times10^{-1} & 6.341\times10^2 & 1.803\times10^{-1} \\ 7.065\times10^4 & 2.613\times10^2 & -6.377\times10^2 & 7.664\times10^{-1} & 6.385\times10^2 & 1.808\times10^{-1} \\ 7.135\times10^2 & 2.630 & -6.438 & 7.738\times10^{-3} & 6.446 & 1.826\times10^{-3} \\ 1.314\times10^2 & 6.993\times10^4 & -1.548\times10^3 & 6.535\times10^{-2} & 1.546\times10^3 & 1.534\times10^{-2} \\ -5.627\times10^2 & 7.112\times10^4 & -1.572\times10^3 & 6.076\times10^{-2} & 1.571\times10^3 & 1.426\times10^{-2} \\ -5.613 & 7.182\times10^2 & -1.588\times10^1 & 6.137\times10^{-4} & 1.586\times10^1 & 1.440\times10^{-4} \end{bmatrix}$$

$$\begin{bmatrix}
1.125\times10^{1} & 1.122\times10^{1} & 1.137\times10^{2} & 6.535\times10^{-2} & -1.117\times10^{2} & 1.430\times10^{-2} \\
1.023\times10^{1} & 1.125\times10^{1} & 1.139\times10^{2} & 6.522\times10^{-2} & -1.119\times10^{2} & 1.426\times10^{-2} \\
1.034\times10^{-1} & 1.136\times10^{-1} & 1.151 & 6.582\times10^{-4} & -1.130 & 1.439\times10^{-4} \\
-2.145\times10^{1} & 9.547\times10^{-1} & -9.429\times10^{2} & 6.150\times10^{-1} & 9.435\times10^{2} & 1.471\times10^{-1} \\
-1.981\times10^{1} & 8.873\times10^{-1} & -9.627\times10^{2} & 6.252\times10^{-1} & 9.631\times10^{2} & 1.496\times10^{-1} \\
-2.001\times10^{-1} & 8.961\times10^{-3} & -9.720 & 6.312\times10^{-3} & 9.724 & 1.510\times10^{-3}
\end{bmatrix}$$

$$\begin{bmatrix}
2.317\times10^{1} & 8.903\times10^{-1} \\
2.280\times10^{1} & 8.880\times10^{-1} \\
2.301\times10^{-1} & 8.962\times10^{-3} \\
9.373 & 9.156 \\
6.922 & 9.309 \\
7.014\times10^{-2} & 9.398\times10^{-2}
\end{bmatrix}$$

$$\mathbf{A}_c = \begin{bmatrix}
0 & 0 & 0 & 0 & 0 & 0 \\
0 & 0 & 0 & 0 & 0 & 0 \\
0 & 0 & 0 & 1.0 & 0 & 0 \\
-8.283\times10^{4} & -2.102\times10^{2} & -3.977\times10^{7} & -6.840\times10^{5} & 3.960\times10^{7} & 6.840\times10^{5} \\
0 & 0 & 0 & 0 & 0 & 1.0 \\
-3.533\times10^{5} & -1.306\times10^{3} & 1.683\times10^{8} & 2.907\times10^{6} & -2.393\times10^{8} & -2.907\times10^{6} \\
0 & 0 & 0 & 0 & 0 & 0 \\
-5.787\times10^{1} & -2.133\times10^{-1} & 5.221\times10^{-1} & -6.276\times10^{-4} & 1.152\times10^{6} & -1.481\times10^{-4} \\
0 & 0 & 0 & 0 & 0 & 0 \\
-1.546\times10^{2} & -8.227\times10^{4} & 2.954\times10^{6} & -1.602\times10^{5} & -2.954\times10^{6} & 1.602\times10^{5} \\
0 & 0 & 0 & 0 & 0 & 0 \\
2.813\times10^{3} & -3.556\times10^{5} & -1.254\times10^{7} & 6.808\times10^{5} & 1.254\times10^{7} & -6.808\times10^{5} \\
0 & 0 & 0 & 0 & 0 & 0 \\
4.553\times10^{-1} & -5.825\times10^{1} & 1.288 & -4.977\times10^{-5} & -1.286 & -1.168\times10^{-5}
\end{bmatrix}$$

$$\begin{bmatrix}
1.0 & 0 & 0 & 0 & 0 & 0 \\
0 & 0 & 0 & 0 & 0 & 0 \\
0 & 0 & 0 & 0 & 0 & 0 \\
-1.323\times10^{1} & -1.321\times10^{1} & -2.333\times10^{7} & -1.602\times10^{5} & 2.333\times10^{7} & 1.602\times10^{5} \\
0 & 0 & 0 & 0 & 0 & 0 \\
7.100\times10^{7} & -5.627\times10^{1} & 9.914\times10^{7} & 6.808\times10^{5} & -9.914\times10^{7} & -6.808\times10^{5} \\
0 & 1.0 & 0 & 0 & 0 & 0 \\
-1.152\times10^{6} & -9.215\times10^{-3} & -9.332\times10^{-2} & -5.338\times10^{-5} & 9.165\times10^{-2} & -1.167\times10^{-5} \\
0 & 0 & 0 & 1.0 & 0 & 0 \\
2.523\times10^{1} & -1.123 & -8.260\times10^{6} & -9.436\times10^{4} & 8.093\times10^{6} & 9.436\times10^{4} \\
0 & 0 & 0 & 0 & 0 & 1.0 \\
9.905\times10^{1} & -4.436 & 3.441\times10^{7} & 4.010\times10^{5} & -1.054\times10^{8} & -4.010\times10^{5} \\
0 & 0 & 0 & 0 & 0 & 0 \\
1.623\times10^{-2} & -7.267\times10^{-4} & 7.883\times10^{-1} & -5.119\times10^{-4} & 1.152\times10^{6} & -1.225\times10^{-4}
\end{bmatrix}$$

$$\begin{bmatrix}
0 & 0 \\
1.0 & 0 \\
0 & 0 \\
-2.726\times10^{1} & -1.047 \\
0 & 0 \\
-1.140\times10^{2} & -4.440 \\
0 & 0 \\
-1.867\times10^{-2} & -7.268\times10^{-4} \\
0 & 0 \\
-1.103\times10^{1} & -1.077\times10^{1} \\
0 & 0 \\
7.100\times10^{7} & -4.655\times10^{1} \\
0 & 1.0 \\
-1.152\times10^{6} & -7.622\times10^{-3}
\end{bmatrix}$$

using the second set of weighting factors the following gain and control matrices are obtained:

$$\mathbf{K} = \begin{bmatrix}
7.049\times10^{7} & 4.534\times10^{4} & -4.935\times10^{4} & 1.716\times10^{2} & 9.241\times10^{4} & 4.042\times10^{1} \\
7.057\times10^{7} & -6.882\times10^{4} & -4.949\times10^{4} & 1.718\times10^{2} & 9.259\times10^{4} & 4.047\times10^{1} \\
7.170\times10^{5} & -6.789\times10^{2} & -4.996\times10^{2} & 1.7369 & 9.362\times10^{2} & 4.092\times10^{-1} \\
8.436\times10^{4} & 7.025\times10^{7} & -3.649\times10^{4} & 4.265\times10^{-1} & 3.658\times10^{4} & 3.029\times10^{-2} \\
-5.899\times10^{4} & 7.080\times10^{7} & -3.713\times10^{4} & 1.330\times10^{-2} & 3.716\times10^{4} & -6.783\times10^{-2} \\
-5.723\times10^{2} & 7.193\times10^{5} & -3.751\times10^{2} & 1.673\times10^{-4} & 3.754\times10^{2} & -6.779\times10^{-4}
\end{bmatrix}$$

$$\begin{bmatrix}
5.110\times10^{5} & 2.520\times10^{3} & 3.887\times10^{3} & 4.265\times10^{-1} & -3.769\times10^{3} & 3.128\times10^{-3} \\
5.115\times10^{5} & 2.523\times10^{3} & 4.007\times10^{3} & 1.287\times10^{-1} & -3.956\times10^{3} & -6.783\times10^{-2} \\
5.181\times10^{3} & 2.551\times10^{1} & 4.047\times10^{1} & 1.317\times10^{-3} & -3.995\times10^{1} & -6.819\times10^{-4} \\
2.307\times10^{2} & 1.910 & -5.933\times10^{4} & 1.700\times10^{2} & 1.020\times10^{5} & 4.036\times10^{1} \\
-5.066\times10^{2} & -4.204 & -6.0372\times10^{4} & 1.715\times10^{2} & 1.034\times10^{5} & 4.072\times10^{1} \\
-5.005 & -4.174\times10^{-2} & -6.094\times10^{2} & 1.734 & 1.045\times10^{3} & 4.117\times10^{-1}
\end{bmatrix}$$

$$\begin{bmatrix}
5.137 & 2.427\times10^{-1} \\
-7.994\times10^{2} & -4.179 \\
-7.979 & -4.174\times10^{-2} \\
5.106\times10^{5} & 2.516\times10^{3} \\
5.139\times10^{5} & 2.538\times10^{3} \\
5.205\times10^{3} & 2.566\times10^{1}
\end{bmatrix}$$

$$\mathbf{A}_c = \begin{bmatrix}
0 & 0 & 0 & 0 & 0 & 0 \\
0 & 0 & 0 & 0 & 0 & 0 \\
0 & 0 & 0 & 1.0 & 0 & 0 \\
-8.293\times10^{7} & -5.335\times10^{4} & -3.971\times10^{7} & -6.842\times10^{5} & 3.950\times10^{7} & 6.840\times10^{5} \\
0 & 0 & 0 & 0 & 0 & 1.0 \\
-3.528\times10^{8} & 3.441\times10^{5} & 1.686\times10^{8} & 2.906\times10^{6} & -2.398\times10^{8} & -2.907\times10^{6} \\
0 & 0 & 0 & 0 & 0 & 0 \\
-5.815\times10^{4} & 5.506\times10^{1} & 4.052\times10^{\times}10^{1} & -1.409\times10^{-1} & 1.152\times10^{6} & -3.319\times10^{-2} \\
0 & 0 & 0 & 0 & 0 & 0 \\
-9.924\times10^{4} & -8.265\times10^{7} & 2.995\times10^{6} & -1.602\times10^{5} & -2.995\times10^{6} & 1.602\times10^{5} \\
0 & 0 & 0 & 0 & 0 & 0 \\
2.949\times10^{5} & -3.540\times10^{8} & -1.236\times10^{7} & 6.808\times10^{5} & 1.236\times10^{7} & -6.808\times10^{5} \\
0 & 0 & 0 & 0 & 0 & 0 \\
4.642\times10^{1} & -5.834\times10^{4} & 3.043\times10^{1} & -1.357\times10^{-5} & -3.045\times10^{1} & 5.498\times10^{-5}
\end{bmatrix}$$

$$
\begin{array}{cccccc}
1.0 & 0 & 0 & 0 & 0 & 0 \\
0 & 0 & 0 & 0 & 0 & 0 \\
0 & 0 & 0 & 0 & 0 & 0 \\
-6.012\times10^{5} & -2.964\times10^{3} & -2.333\times10^{7} & -1.602\times10^{5} & 2.333\times10^{7} & 1.602\times10^{5} \\
0 & 0 & 0 & 0 & 0 & 0 \\
6.844\times10^{7} & -1.261\times10^{4} & 9.912\times10^{7} & 6.808\times10^{5} & -9.912\times10^{7} & -6.808\times10^{5} \\
0 & 1.0 & 0 & 0 & 0 & 0 \\
-1.152\times10^{6} & -2.069 & -3.283 & -1.068\times10^{-4} & 3.2402 & 5.530\times10^{-5} \\
0 & 0 & 0 & 1.0 & 0 & 0 \\
-2.714\times10^{2} & -2.247 & -8.191\times10^{6} & -9.456\times10^{4} & 7.974\times10^{6} & 9.431\times10^{4} \\
0 & 0 & 0 & 0 & 0 & 1.0 \\
2.533\times10^{3} & 2.102\times10^{1} & 3.470\times10^{7} & 4.002\times10^{5}n & -1.059\times10^{8} & -4.012\times10^{5} \\
0 & 0 & 0 & 0 & 0 & 0 \\
4.059\times10^{-1} & 3.385\times10^{-3} & 4.943\times10^{1} & -1.407\times10^{-1} & 1.152\times10^{6} & -3.339\times10^{-2}
\end{array}
$$

$$
\left[\begin{array}{cc}
0 & 0 \\
1.0 & 0 \\
0 & 0 \\
-6.043 & -2.856\times10^{-1} \\
0 & 0 \\
3.997\times10^{3} & 2.090\times10^{1} \\
0 & 0 \\
6.471\times10^{-1} & 3.385\times10^{-3} \\
0 & 0 \\
-6.007\times10^{5} & -2.960\times10^{3} \\
0 & 0 \\
6.843\times10^{7} & -1.269\times10^{4} \\
0 & 1.0 \\
-1.152\times10^{6} & -2.081
\end{array}\right]
$$

Nomenclature

$\mathbf{A}$	:	coefficient matrix
A_{11}, etc.	:	components of $\mathbf{A}$
$\mathbf{B}$	:	input transducer matrix
B_{11}, etc.	:	components of $\mathbf{B}$
$\mathbf{C}$	:	output transducer matrix
C_{xx}, etc	:	oil-film damping coefficients (Ns/m)
c_{xx}, etc	:	non-dimensional oil-film damping coefficients
f	:	frequency of vibration (Hz)
$f_1, \cdots, f_6$	:	elements of input vector
$\mathbf{K}$	:	feedback gain matrix
J	:	performance index
K_{xx}, etc	:	oil-film stiffness coefficients (N/m)
k_{xx}, etc	:	non-dimensional oil-film stiffness coefficients
k_e	:	support stiffness per bearing (N/m)
k_f	:	rotor stiffness per bearing (N/m)
m_b	:	journal mass per bearing (Kg)
m_e	:	bearing housing mass per bearing (Kg)
m_f	:	mid-span mass per bearing (Kg)

M_p : peak value of vibration (m)

N : shaft speed (rpm)

t_A, t_B : time of amplitude of vibration (s)

t_d : delay time (s)

t_r : rise time (s)

t_s : settling time (s)

$\mathbf{u}$: input vector

$\mathbf{u}_h$, $\mathbf{u}_v$: components of $\mathbf{u}$

$\mathbf{v}$: adjoint input vector

$\mathbf{W}$: load per bearing (N)

$\mathbf{X}$: state vector

$\mathbf{x}_h$, $\mathbf{x}_v$: components of $\mathbf{X}$

$x_1, \cdots x_{12}$: elements of state vector

$\hat{\mathbf{X}}$: adjoint state vector for ISVFB controller

x_A, x_B : amplitude of vibration (m)

$\mathbf{y}$: output vector

$\hat{\mathbf{Z}}$: adjoint state vector for LQS controller

Greek Symbols

ϵ_o : eccentricity ratio

ζ : damping ratio

ω : shaft speed (rad/s)

References

[1] Reiger, N.F., 'underline Flexible Rotor-Bearing system dynamics. Part 3: Unbalance Response and Balancing of flexible rotors in Bearings,' *Published by ASME.*, NewYork, 1973.

[2] Gunter, E.J., Barrett, L.E., and Allaire, P.E., 'Stabilization of Turbomachinery with Squeeze film dampers- Theory and applications,' *Institution of Mechanical Engineers Conference on Vibration in Rotating Machinery*, Cambridge, 1976, Paper # C233/76, pp. 291-300.

[3] Cunningham, R.E., 'Steady-state unbalance response of a three disk flexible rotor on flexible, damped support,' *Journal of Mechanical Design, Transaction of ASME.*, Vol. 100, July 1978, pp. 563-573.

[4] Nikolajsen, J.L., and Holmes, R., 'Investigation of Squeeze-film Isolators for the Vibration Control of a Flexible rotor,' *Journal of Mechanical Engineering Science.*, Vol. 21, No. 4, 1979, pp. 247-252.

[5] Mu, C., Darling, J., and Burrows, C.R., 'An appraisal of a proposed active squeeze-film damper,' *Journal of Tribology, ASME Trans.*, 90-Trib-68, 1990, pp. 1-5.

[6] Gondhalekar, V.M., Nikolajsen, J., and Jayawant, B.V., 'Electromagnetic control of flexible transmission shaft vibration,' *Proc. IEEE*, vol. 126, No. 10, 1979. pp. 1008-1010.

[7] Schweitzer, G., and Lange, R., 'Characteristics for a Magnetic rotor- bearing for Active vibration control,' *Institution of Mechanical Engineers Conference on Vibration in Rotating Machinery,* Cambridge, 1976, Paper# 239/76, pp. 301-306.

[8] Stanway,R., Burrows, C.R., 'Active vibration control of a flexible Rotor on flexibly-mounted Journal Bearings,' *Journal of Dynamic systems, Measurements, and Control.*, Vol. 103, 1981., pp. 383-388.

[9] Katsuhiko Ogata, '*Modern Control Engineering,*' Prentice-Hall, Inc., Englewood cliffs, N.J., USA, 1970.

[10] Yu Lie, Xi You-Bai, Zhu Jun, and Qiu Damou, ' Vibration Control for Rotor-Bearing system and Calculation of the Optimum control forces,' *Journal of Vibration, Acoustics, Stress, and Reliability in Design.*, Vol. 111, October 1989, pp. 366-369.

[11] Shapiro, W., and Rumbarger, J.H., 'Bearing influence and representation in Rotor dynamic analysis,' *Flexible Rotor-Bearing System Dynamics., ASME,* 1972.

[12] Adams, M.L., and Rashidi, M., 'On the use of rotor-bearing instability thresholds to accurately measure bearing rotor-dynamic properties,' *Journal of Vibration, Acoustics, Stress, and Reliability in design.*, Vol. 107, October 1985, pp. 404-409.

[13] Strenlicht, B., 'Elastic and Damping properties of Cylindrical Journal bearings,' *ASME Journal of Basic Engineering.*, Vol. 81, 1959. pp 101-108

[14] Morton, P.G., 'Measurement of Dynamic characteristics of a large sleeve bearing,' *ASME Journal of Lubrication Technology.,* Vol. 93, 1971, pp. 143-150.

[15] Emerson, W., and Walter, D.P., 'The estimation of parameters in a Linear Rotor-Bearing system model,' *ASME Design conference,* Chicago, 1978, pp. 157-169.

[16] Burrows, C.R., and Stanway, R., 'Identification of Journal bearing characteristics,' *ASME Journal of Dynamic systems, Measurements, and Control.*, Vol. 99, 1977, pp. 167-173.

[17] Morton. P.G., 'Dynamic characteristics of bearings, Measurements under operating conditions,' *GEC Journal of Science and Technology.*, Vol. 42 No. 1, 1975, pp. 37-47.

[18] Stanway, R., Burrows, C.R., and Holmes, R., 'Parametric estimation of a squeeze-film bearing,' *5th IFAC Symposium* 1979, pp. 1271-1278.

[19] Vance, J.M., '*Rotor-dynamics of Turbomachinery,*' John Willey and Sons., NewYork, 1988.

[20] Burrows, C.R., and Stanway, R., 'A coherent strategy for estimating linearized oil-film coefficients,' *Proc. R. Soc. Lond.* A-370, 1980, pp. 89-105.

[21] Burrows, C.R., Kucuk, N.C., Sahinkaya, M.N., and Stanway, R., 'Linearized squeeze-film dynamics: Model structure and interpretation of experimentally derived parameters,' *Journal of Mechanical Engineering Science.*, Part C:, Vol. 204, 1990, pp. 263-272.

[22] Goodwin, M.J., '*Dynamics of Rotor-Bearing systems,*' Published by Unwin Hyman Ltd., London, 1989.

[23] Reddi, M.M., and Trumpler, P.R., 'Stability of the High-speed Journal bearing under steady load, Part 1: The incompressible film,' *Journal of Engineering for industry. Trans. of ASME.*, August 1962, pp. 351-358.

[24] Rao, J.S., '*Rotor-Dynamics,*' John Willey and Sons., NewYork, 1983.

[25] Burrows, C. R., Sahinkaya, M. N., and Turkey, O. S., 'An Adaptive Squeeze-Film Bearing,' *Journal of Tribology., ASME Transetion,* Vol. 106, Jan. 1984, pp. 145-151.

[26] Palazzolo,A.B., Lin, R.R., Alexander, R.M., Kascak, A.F., and and Montague, J., 'Test and Theory for Piezoelectric Actuator - Active Vibration Control of Rotating Machinery,' *Journal of Vibration and Acoustics.*, Vol. 113, April 1991, pp. 167-175.

[27] Elmadany, M.M., 'Integral and State Variable Feed-Back Controllers for Improved Performance in Automotive Vehicles,' *Computers and Structures,* vol.42, pp.237-242, 1992.

[28] Surgenor, B.W., and Hesketh, T., 'Multivariable control of a Furnace: Optimal LQS versus Model based GMC,' *American control conference,* June 21-23, Pittsburgh, Pennsylvania, 1989, pp. 1491-1496.

[29] Kalman, R.E. 'Contributions to the Theory of Optimal Control,' *Bol. Soc. Mat. Mex.*, Vol. 5, 1960, pp. 102-119.

[30] Ching-Tai Lin , 'Structural Controllability,' *IEEE Transactions on Automatic Control.*, Vol. AC-19, No. 3, 1974, pp. 201-208.

[31] Sheilds, R.W., and Boyd Pearson, J., 'Structural Controllability of Multi-input Linear Systems,' *IEEE Trans. on Automatic Control,* Vol. AC-21, No. 2 April 1976, pp. 203-212.

[32] Burrows, C.R., and Sahinkaya M.N., 'A new Algorithm for Determining Structural Controllability,' *Int. J. Control,* vol. 33, No. 2, 1981, pp. 379-392.

[33] Pillou, c., and Rech, c., 'Simple Algebraic Algorithm for Determination of the Generic-rank of Structured Systems,' *Int. J. Control,* vol. 50, No. 4, 1989, pp. 1533-1539.

[34] Kalman, R.E., 'On the General Theory of Control System,' *Proc. First Intern. Congress, IFAC,* Moscow, 1960, pp. 481-492.

[35] David G. Luenberger,'An Introduction to Observers,' *IEEE Trans. on Automatic Control.,* Vol. AC-16, No. 6, 1971, pp. 596-602.

[36] Kalman, R.E., 'When is a Linear Control System Optimal?,' *Trans. ASME, J. Basic Engg,* Vol. 86, 1964, pp. 51-60.

[37] Ferguson J.D., and Rekasius, Z.V., 'Optimal Linear Control Systems with Incomplete State Measurements,' *IEEE Trans. on Automatic Control.,* Vol. AC-14, No. 2, April, 1969, pp. 135-140.

[38] S. Zaman, 'The effect of Control Actuator Position on the Performance of Ground Vehicle Suspension,' *M.S. Thesis,* June 1988, Dept. of Mehc. Engg. King Fahad University of Petroleum and Minerals, Dhahran, Saudi Arabia.

[39] Gopal, M., '*Modern control system theory.*' Willey eastern limited, New Delhi, India, 1989.

[40] Ogata, K., '*State space analysis of control systems.*' Prentice-Hall Inc., Englewood cliffs, N.J., 1967.

[41] Shigley, J. E., and Mischke, C. E., '*Mechanical Engineering Design.*' Fifht edition, Mcgraw-Hill Publishing company, Newyork, 1989.

[42] Kamal A. F. Moustafa and Asfar, A., 'Identification of Journal Bearing Modal Parameters,' *The International Journal of Analytical and Experimental Analysis,* vol. 5, Oct. 1990, pp. 213-221.

[43] Burrows, C. R., and Sahinkaya,M. N., 'Frequency domain estimation of Linearized Oil-Coefficients,' *Journal of Lubrication Technology,* Vol. 104, April 1982, pp. 210-215.

[44] '*PC-MATLAB,' for MS-DOS persional Computers,* version 3.2, The Math Works, Inc. Portolavalley, CA,94025., 1987.

[45] Palm, W. J. '*Modeling, Analysis, and Control of Dynamic systems,*' John Willey and Sons, Inc. Newyork, USA., 1983.

[46] I. J. Nagrath and M. Gopal, '*Control System Engineering* 2nd edition.', Willey Eastern Limited, New Delhi, India, 1992

[47] Kuo,B.C., '*Automatic Control Systems,*' 5th ed. Prentice-Hall Inc. Englewood Cliffs, N.J. 07632, 1987.

[48] Nikolajsen, J. L. and Hoque, M. S. ' An Electroviscous Damper for Rotor Applications,' *Journal of Vibration and Acoustics, Transaction of the ASME,* vol. 112, October 1990, pp. 440-441.

[49] Cher, H. M. and Darlow, M. S. ' Magnetic Bearing with Rotating force Control,' *Journal of Tribology, Transaction of the ASME,* vol. 110, January 1988, pp. 100-105.

[50] Palazzol, A. B., Lin, R. R., Alexander, R. M., Kascak, A. F., and Montague, J., 'Test and Theory for Piezoelectric Actuator-Active Vibration Control of Rotating Machinery,' *Jurnal of Vibration and Acoustics, Transaction of the ASME,* vol. 113, April 1991, pp. 167-175.

Vita

- Neaz Ahmed
- Born at Comilla, East Pakistan in June 1959.
- Finished high school studies from Adamjee Govt. Science College, Karachi, Pakistan in 1977.
- Graduated with a degree in B.E. (Mechanical Engineering) from N.E.D University of Engineering and Technology, Karachi, Pakistan in February 1984.
- Had been Working in Karachi Shipyard and Engineering Works Ltd., as a Design Engineer, before arriving at King Fahd University of Petroleum and Minerals, Dhahran, Saudi Arabia to pursue M.S. in Mechanical Engineering in December 1989.